10/9/76

"D_3 CHROMOPHORES -
geometric distortion in trigonal-dihedral transition metal chromophores and its relevance to optical circular dichroism."

a thesis submitted for the
Degree of Doctor of Philosophy
at the University of Adelaide
in May, 1973.

by KEITH RAYMOND BUTLER, B.Sc. (Hons.)

Department of Physical and Inorganic Chemistry.

CONTENTS

Page.

SUMMARY i

DECLARATION iii

ACKNOWLEDGEMENTS iv

INTRODUCTION 1

RELEVANT TERMINOLOGY 7

(1) Crystal Structure Refinement 7

(2) Optical Rotatory Dispersion and Circular Dichroism 10

(3) Ligand Abbreviations and Structural Formulae 17

PART I. EXPERIMENTAL

CHAPTER 1. THE STRUCTURE OF SODIUM $(+)_{546}$-BIS(MALONATO)-ETHYLENEDIAMINE COBALTATE(III) DIHYDRATE. 22

1.1 STRUCTURE ABSTRACT 22

1.2 EXPERIMENTAL 22

1.3 STRUCTURE SOLUTION AND REFINEMENT 24

1.4 STRUCTURE FIGURES AND TABLES 28

1.5 DESCRIPTION OF STRUCTURE AND DISCUSSION 44

CHAPTER 2. THE STRUCTURE OF $(-)_{589}$-TRIS($(-)_{589}$ 1,2-DIAMINOPROPANE)COBALT(III) $(+)_{589}$-TRIS(MALONATO)-CHROMATE(III) TRIHYDRATE. 49

2.1 STRUCTURE ABSTRACT 49

2.2 EXPERIMENTAL 49

2.3 STRUCTURE SOLUTION AND REFINEMENT 53

Page

2.4 STRUCTURE FIGURES AND TABLES 60

2.5 DESCRIPTION OF STRUCTURE AND DISCUSSION 60

CHAPTER 3. THE STRUCTURE OF POTASSIUM CALCIUM $(+)_{589}$-TRIS-(DITHIO-OXALATO)COBALTATE(III) TETRAHYDRATE. 78

3.1 STRUCTURE ABSTRACT 78

3.2 EXPERIMENTAL 78

3.3 STRUCTURE SOLUTION AND REFINEMENT 81

3.4 STRUCTURE FIGURES AND TABLES 88

3.5 DESCRIPTION OF STRUCTURE AND DISCUSSION 105

CHAPTER 4. THE ABSOLUTE CONFIGURATION OF POTASSIUM $(+)_{589}$-TRIS(1,10-PHENANTHROLINE)-NICKEL(II) $(-)_{589}$-TRIS(OXALATO)COBALTATE(III) DIHYDRATE. 110

4.1 INTRODUCTION 110

4.2 DETERMINATION OF THE CONFIGURATION 110

CHAPTER 5. ABSOLUTE CONFIGURATIONS BY CORRELATION. 115

5.1 INTRODUCTION 115

5.2 EXPERIMENTAL 119

(1) MO_6 Chromophores. 119

(2) MN_6 Chromophores. 122

(3) Phenanthrolines, Dipyridyls. 125

(4) Technical Details. 126

Page

5.3 DISCUSSION 127

5.3.1 ORD and CD curves. 127

5.3.2 Absolute Configurations: Literature References. 143

PART II. ANALYSIS OF STRUCTURAL DATA

CHAPTER 6. ML_6 TRANSITION METAL CHROMOPHORES: SPECTRAL THEORY. 150

6.1 INTRODUCTORY REMARKS 150

6.2 ABSORPTION SPECTRA 151

6.2.1 Octahedral Symmetry (O_h). 151

6.2.2 Distortion from O_h Symmetry. 155

6.3 OPTICAL ACTIVITY 162

6.3.1 Configurational Activity. 162

6.3.2 Vicinal, Conformational and Environmental Effects. 168

CHAPTER 7. MODELS FOR CORRELATING THE SIGNED ROTATORY STRENGTHS OF D_3 TRANSITION METAL CHROMOPHORES. 172

7.1 SUMMARY OF RELEVANT MODELS 172

7.2 DEVELOPMENT OF THE TRIGONAL-DISTORTION MODEL 184

7.3 THE TRIGONAL-DISTORTION PROGRAM: AZIMUTH 201

CHAPTER 8. ANALYSIS OF ML_6-CORE GEOMETRY OF D_3 COMPLEXES. 215

8.1 THE STRUCTURAL DATA 215

8.2 GEOMETRY OF TRIS-BIDENTATE COMPLEXES 238

Page

8.2.1 Critique of Stiefel and Brown's Analysis. 239

8.2.2 Repulsive Potential of the ML_6-Core. 245

8.3 ASSESSMENT OF THE VALIDITY OF THE PK TRIGONAL-DISTORTION MODEL 277

8.3.1 Co(III), Cr(III) N_6 Chromophores. 278

8.3.2 Co(III), Cr(III) O_6 Chromophores. 306

8.3.3 MS_6 Chromophores. 323

8.3.4 Miscellaneous Chromophores. 331

8.4 CONCLUDING REMARKS 336

APPENDICES

APPENDIX I. COMPUTER PROGRAMS USED IN CRYSTAL STRUCTURE ANALYSES. 340

APPENDIX II. REDUCTION OF THE PHOTOGRAPHIC DATA. 342

APPENDIX III. DIFFRACTOMETER DATA COLLECTION AND REDUCTION. 347

APPENDIX IV. MISCELLANEOUS NOTES ON THE CRYSTAL STRUCTURES. 353

APPENDIX V. PROGRAM OCTANT. 355

APPENDIX VI. PROGRAM NHANGLE. 360

BIBLIOGRAPHY 363

SUMMARY

The crystal structures of the inorganic salts, sodium $(+)_{546}$-bis(malonato)1,2-diaminoethane cobaltate(III) dihydrate, Na $(+)_{546}[Co(C_3H_2O_4)_2(C_2H_8N_2)].2H_2O$, $(-)_{589}$-tris($(-)_{589}$1,2-diaminopropane)cobalt(III) $(+)_{589}$-tris(malonato)chromate(III) trihydrate, $(-)_{589}[Co(-)_{589}(C_3H_{10}N_2)_3](+)_{589}[Cr(C_3H_2O_4)_3].3H_2O$, and potassium calcium $(+)_{589}$-tris(dithiooxalato)cobaltate(III) tetrahydrate, K.Ca $(+)_{589}[Co(C_2O_2S_2)_3].4H_2O$, have been determined and refined by a full-matrix least-squares procedure with conventional *R* factors at convergence of 0.050, 0.073 and 0.062 respectively. The absolute configurations of the complex anions in the respective structures were assigned as Δ,Λ and Λ.

The absolute configurations of the complex ions in the previously determined structure, potassium $(+)_{589}$-tris(1,10-phenanthroline)nickel(II) $(-)_{589}$-tris(oxalato)cobaltate(III) dihydrate, $K(+)_{589}[Ni(C_{12}H_8N_2)_3](-)_{589}[Co(C_2O_4)_3].2H_2O$, have both been determined as Λ using the technique of X-ray anomalous dispersion. The complex ions $(+)_{589}$-tris(oxalato)chromate(III), $(+)_{589}[Cr(C_2O_4)_3]^{3-}$, $(-)_{600}$-tris(malonato)cobaltate(III), $(-)_{600}[Co(C_3H_2O_4)_3]^{3-}$, $(-)_{400}$-tris(1,3-diaminopropane)chromium(III), $(-)_{400}[Cr(C_3H_{10}N_2)_3]^{3+}$ and $(+)_{589}$-tris(1,10-phenanthroline)ruthenium(II), $(+)_{589}[Ru(C_{12}H_8N_2)_3]^{2+}$, have all been assigned a Λ absolute configuration on the basis of X-ray powder diffraction patterns of the relevant least-soluble diastereoisomers.

Angular distortion parameters of the ML_6 coordination polyhedra in several inorganic structures of pseudo-D_3 symmetry have been computed from the crystal coordinates; the distortion of this core from O_h symmetry in tris-bidentate complexes has been correlated with the size of the ligand bite angle, α, on the basis of a repulsive electrostatic potential operative between the six ligand donor atoms. This theoretical model predicts a distortion towards trigonal-prismatic geometry for tris-complexes containing bidentate ligands which subtend angles, α, less than 90° at the coordinated metal atom; for $\alpha > 90^o$ the model predicts a geometry more flattened relative to the three-fold axis than that in which the three bidentate ligands are orthogonal.

The computed ML_6-core distortions of relevant tris-bidentate transition metal complexes have been considered in assessing the validity of a limited crystal-field trigonal distortion model proposed by Piper and Karipides for correlating the absolute configuration of a chiral trigonal-dihedral (D_3) chromophore with the sign of the observed rotatory strength. It is concluded that this model does not adequately explain the observed Cotton effects for all pseudo-D_3 transition metal complexes.

DECLARATION

This thesis is an account of research conducted by the candidate in the Department of Physical and Inorganic Chemistry at The University of Adelaide, the School of Physical Sciences at The Flinders University of South Australia and through the agency of my supervisor, Dr. M.R. Snow, in the Department of Chemistry at Northwestern University, Illinois, U.S.A.

The thesis contains no work previously presented by the candidate for the award of any other degree and to the best of the author's knowledge includes no material written by another person, except where due reference is made in the text of the thesis.

Responsibility for any factual or typographical errors present in the text rests solely with the author.

Keith Butler,
May, 1973.

ACKNOWLEDGEMENTS

I express sincere thanks to my supervisor, Dr. M.R. Snow, for his interest and encouragement throughout the duration of this research and particularly for his willingness to determine numerous circular dichroism spectra on my behalf while on study leave.

Special thanks are due to Dr. M.R. Taylor of Flinders University for making available the diffractometer facilities used in one crystal data collection and together with Miss L. Srinivasan for helpful discussions on the refinement and absorption correction of counter data; to Dr. M. Dwyer for discussions on structure solution and refinement; to Dr. S.F. Lincoln for assistance in understanding the implications of several relevant nmr studies and to Dr. G.H. Searle for many informative discussions on optical activity. I also thank Drs. B.F. Hoskins and K. Matsumoto, and Professors W.D. Horrocks, Jr., and Y. Saito for crystal structure coordinates in advance of publication.

In particular thanks are due to some fellow students; to Mr. P.F. Crossing and Mr. R.J. Geue for providing the coordinates from the energy minimization studies of the tris-diamine and bis-triamine complexes and to Messrs. F.R. Keene, T.R. Norman and G.J. Sparrow for help with optical rotatory dispersion and spectral measurements. Messrs. A. Bowers, G. Duthie and B. Weste gave much assistance in the design and modification of an automatic low temperature device for use with the Weissenberg camera.

I thank Professors D.O. Jordan and D.R. Stranks for allowing me to undertake this research in the Department of Physical and Inorganic Chemistry and the Department of Education and Science for granting me a Commonwealth Postgraduate Award for the duration of this study. Finally I wish to acknowledge use of the facilities of the University of Adelaide's Computing Centre.

UNIVERSITY OF ADELAIDE LIBRARY

INTRODUCTION

At present the only definitive ways of assigning the absolute configurations of metal complexes are chemical relation to a compound of known chirality (*Gk.* χε*i*ρ ≡ *chir* - ≡ hand), e.g. complexes of (-)pn[†1] derivatives,[1-3] and X-ray structure solution employing the property of X-ray anomalous dispersion,[4-6] the latter being the only "direct" method. Earlier in the study of optical activity in transition metal complexes it was thought[7] that their absolute configurations could be deduced from the sign of the rotation of plane polarized light at a fixed reference wavelength. However, it had previously been observed that the optical rotatory dispersion (ORD) curves for chiral molecules exhibited an inflexion point and generally changed sign under an absorption band,[8,9] making predictions based on the sign of the optical rotation at fixed wavelength doubtful. It was subsequently shown theoretically that the sign of the observed Cotton effect (see terminology section, part (2)) for an isolated optically active transition was determined by the chromophore absolute configuration.[10,11] The finite extension of the rotatory dispersion beyond the limits of the absorption band envelope leads to a complicated ORD curve which is not readily resolvable into separate dispersions for chromophores having several optically active transitions in a narrow wavelength range.

It is currently held that the absolute configurations of chiral chromophores should most readily correlate with the features of the circular dichroism (CD) spectra, since for an isolated transition the CD peak is confined within the envelope of the absorption band, although a small shift to low energy relative to the frequency of the absorption maximum is predicted.[12,13] Transitions which give overlapping ORD curves should be more clearly resolved in the corresponding CD spectrum.

[†1] ligand abbreviations and structural formulae are given in the terminology section, part (3), immediately following this introduction.

Despite the fact that the Cotton effect in CD was first observed for an inorganic system,[14-17] the development of widely applicable theoretical models lags behind the theoretical interpretation of the phenomenon in organic chemistry.[18-20] This is partly a consequence of the differences in the electronic transitions being studied, and in the inorganic sphere theory best describes the experimental facts for the $\pi \rightarrow \pi^*$ transitions of unsaturated ligands such as 1,10-phenanthroline and 2,2'-dipyridyl when chelated to transition metal ions.[21-24] Analogous $n \rightarrow \pi^*$ and $\pi \rightarrow \pi^*$ transitions are the most studied in organic compounds containing, for example, the carbonyl chromophore. For transition metal complexes containing saturated ligands, such as the aliphatic diamines, the transitions most studied have been the low intensity, spin-allowed *d-d* transitions centred on the metal ion and generally observable in the visible spectral region. The theoretical treatment applicable to the $\pi \rightarrow \pi^*$ ligand transitions of phen and dipy complexes cannot be used in these cases.

The precise details of the ORD and CD spectra of a transition metal complex are related to its symmetry, the spectroscopic interpretation being least complex for ions of high symmetry. The highest symmetry transition metal complexes capable of existing in two non-superimposable mirror image forms (enantiomers) have trigonal-dihedral (D_3) symmetry, e.g. $Co(en)_3{}^{3+}$, $Co(ox)_3{}^{3-}$, $Ni(phen)_3{}^{2+}$, and it is these which have been studied most extensively theoretically.[25] Aware of the relevance of D_3 complex ions to the empirical CD correlations we had, in 1968, initiated determination of the crystal structure of $K(+)_{589}[Ni\ phen_3](-)_{589}[Co\ ox_3].2H_2O$ by X-ray diffraction, work which fulfilled the experimental requirements of the author's Honours Degree for that year. Assignment of the absolute configuration was completed in 1969 and when published (K.R. Butler and M.R. Snow, J. Chem. Soc. (A), 565 (1971)) constituted the first publication of a structure determination of the absolute configuration of a tris(oxalate) ion and the second of a tris(phenanthroline) complex, an earlier publication[26] of the structure of $\Lambda\ (-)_{589}[Fe\ phen_3](+)\ Sb_2(C_4H_2O_6).8H_2O$ being in abstract form only.

Our interest in conformational analysis of inorganic molecules prompted consideration of complexes containing six-membered chelate rings and the tris(malonate) ion presented itself as a logical extension of the tris(oxalate) study, particularly since some anomalies seemed to exist in the published CD[27,28] and spectral assignments.[29] As a complement to the proposed tris(malonate) study, solution of the crystal structure of $Na\ (+)_{546}[Co\ mal_2en].2H_2O$ was undertaken in 1969; crystals of this complex were readily available, the CD spectrum had been published[30] and the complex ion offered a link in the chain of an empirical correlation of the absolute configurations of the tris(~~ox~~ en) and tris(mal) ions. In addition, no X-ray studies of coordinated malonate ions had been reported and although nmr spectra of $Co(mal)_2(en)^-$ had previously been studied in detail[31,32] the conformations of the malonate rings could not be determined.

Crystallization and subsequent resolution of $K_3[Cr\ mal_3]$ proved difficult and delayed data collection for $(-)_{589}[Co\ (-)pn_3](+)_{589}[Cr\ mal_3]\text{-}.3H_2O$ until mid 1970. It was about this time that the crystal structure[33] of $(+)_{546}\ Co[TRI_2]I_3$ came to our notice; the optical activity of this bis-tridentate complex ion was attributed[33] to a chiral twist of the nitrogen donor atoms comprising the first coordination sphere, after a model proposed by Piper and Karipides.[34,35] The tris(malonate) complex promised a further test of this theoretical model. A published reassignment[36] of the components in the CD spectrum of $Co(tn)_3^{3+}$ which appeared shortly after was also claimed to support the Piper-Karipides trigonal-distortion model and increased our interest in the detailed theory. We subsequently published an interpretation of the experimental $[Co\ tn_3]^{3+}$ data available at that time (K.R. Butler and M.R. Snow, Inorg. Chem., 10, 1838 (1971)).

An accurate structure determination of the geometry of the $[Co\ tn_3]^{3+}$ complex ion in the crystal environment used for the experimental CD measurements was clearly required but rapid deterioration[37] of the crystals made this impossible by photographic techniques. Preparation of the related tris-(2,4-diaminopentanediamine)Co(III) complexes was begun with a view to determining the absolute configurations and detailed geometries of these conformationally rigid ions, only to find in a publication[38] some months later that the complexes had been resolved and X-ray structure determinations were in progress.[39,40]

Reversal of CD component energies under the long wavelength absorption band in the published spectra[27] of $[Co\ ox_3]^{3-}$ and $[Co\ thiox_3]^{3-}$ pointed to a probable axial elongation of the CoS_6 core in the latter complex ion relative to that of the CoO_6 core in the $[Co\ ox_3]^{3-}$. A less than satisfactory conclusion to the refinement of the $(-)[Co(-)pn_3](+)[Cr\ mal_3].3H_2O$ structure prompted the collection of extensive diffractometer data for the $K.Ca\ (+)_{589}[Co\ thiox_3].4H_2O$ structure. Richardson's theoretical paper[41] extending the original trigonal distortion model of Piper and Karipides to second order appeared in mid-1971; this paper suggested a further variation of the crystal field model which the tris(thiox) ion seemed eminently suited to test. A preliminary communication of the structure has been published (K.R. Butler and M.R. Snow, Inorg. Nucl. Chem. Letters, 8, 541 (1972)) as has a brief account of the two malonate complex ion structures (K.R. Butler and M.R. Snow, Chem. Comm., 550 (1971)).

However, the absolute configurations determined during the course of the present research do not constitute a sufficiently broad base for testing the model proposed by Piper and Karipides. It has therefore been necessary to abstract other relevant structures from the published literature and, since the parameters defining the deviation of the ML_6 first coordination sphere from regular O_h symmetry are seldom listed in structure reports of tris-bidentate complexes, a program was written to derive the required parameters from the crystal coordinates. Development of this program facilitated the evaluation of the ML_6-core distortion parameters for numerous trigonal-dihedral (D_3) structures which, although not all of immediate relevance to an evaluation of the trigonal distortion model, are of considerable structural and in some cases spectral interest.

This accumulation of structural data for a variety of tris-bidentates revealed a tendency for the three chelate-rings in many such complexes to adopt an orientation more nearly parallel to the pseudo three-fold axis than is the case for an orthogonal arrangement of the ligands. The observed distortion has been interpreted in terms of an electrostatic repulsion potential operative between the donor atoms of the ML_6-core, and its implications with respect to the trigonal twist inversion mechanism proposed for the intramolecular racemization of C_3 symmetric complexes discussed. Kepert[42] has recently published a similar analysis of the distortion of the ML_6-core in tris-bidentate complexes; the predictions of his independent treatment are in complete accord with those of the present work.

In presenting this research it has proved expedient to nominally divide the thesis into two parts. These introductory remarks are followed by a brief section of terminology used in the text of the thesis. Then — PART I, comprising the experimental sections: Chapters 1-5.

While the bulk of the experimental work undertaken during this research has been the solution of three crystal structures, some relevant rotatory dispersion and circular dichroism measurements have been made, these being summarised in Chapter 5.

PART II, comprising the analysis of chromophore geometries: Chapters 6-8.

Chapter 6 reviews the interpretation of the spectral theory of transition metal complexes adopted throughout this thesis. The trigonal distortion model is elaborated in Chapter 7. The derived geometrical parameters of several pseudo trigonal-dihedral (D_3) transition metal complexes are presented and discussed in the concluding chapter.

RELEVANT TERMINOLOGY

(1) Crystal Structure Refinement

The method of least-squares was used to refine the initial parameters, p_i, approximating the structure solution. The function minimized by program FUORFLS (see Appendix I) is

$$D = \sum_{hkl} w_{hkl} \Delta^2 \quad \textit{where } \Delta = ||F_o| - |F_c||$$

and w is the weight assigned to the observed structure factor amplitude $|F_o|$ (Appendices II, III); $|F_c|$ is the scaled calculated structure factor amplitude of reflection hkl.

Since the "normal equations"

$$\sum_{hkl} w_{hkl} \Delta \frac{\partial F_c}{\partial p_i} = 0 \qquad i = 1,\ldots m$$

are non-linear, minimization of D is an iterative procedure, each cycle resulting in improved values of the variables, p_i, which must be reintroduced to subsequent refinement cycles. The refineable variables are the scale factor, an extinction parameter (not refined in the structures reported here), the atomic positional coordinates x_i, y_i, z_i, an atomic occupancy factor (multiplier) and temperature factor(s): the multiplier and temperature factor(s) of a given atom may not be refined during the same least-squares cycle. For an anisotropically vibrating atom the isotropic temperature factor coefficient, B_i ($\mathring{A}^2$), is replaced by the six coefficients

$$\beta_{11} = a^{*2}.B/4, \quad \beta_{22} = b^{*2}.B/4, \quad \beta_{33} = c^{*2}.B/4$$

$$\beta_{12} = a^*b^*\cos\gamma^*.B/4, \quad \beta_{13} = a^*c^*\cos\beta^*.B/4, \quad \beta_{23} = b^*c^*\cos\alpha^*.B/4$$

and the atomic scattering factor is given by

$$f = f_o\exp\{-(h^2\beta_{11} + k^2\beta_{22} + l^2\beta_{33} + 2hk\beta_{12} + 2hl\beta_{13} + 2kl\beta_{23})\},$$

f_o being the scattering factor for the atom at rest. There are precise relationships restricting the independence of the six anisotropic temperature coefficients for an atom occupying a crystallographic special position.[54]

$$B_i = 8\pi^2 \overline{\mu^2}$$

where $\overline{\mu^2}$ is the mean-square amplitude of vibration.

After a least-squares cycle the temperature factor coefficients for each atom are tested for positive-definite form; non "positive-definiteness" signifies a physically unreal thermal ellipsoid.

Improvement in the reflection-by-reflection agreement between

$|F_o|$ and $|F_c|$ with successive least-squares cycles is indicated by the residual index

$$R_1 = \Sigma|\Delta|/\Sigma|F_o|.$$

Meaningful changes in R_1 as a result of altering the model can be distinguished[55] by a comparison of the values of the weighted residual, R_2, before and after the current cycle;

$$R_2 = (\Sigma w\Delta^2/\Sigma|F_o|^2)^{\frac{1}{2}}.$$

A further indicator of the refinement progress is the standard error, G, of an observation of unit weight; this is ideally unity for a properly weighted model (i.e. where $w_{hkl} = 1/\sigma_{F_o}{}^2$ on an absolute scale) if random experimental errors only are significant:[44a]

$$G = (D/(m - n))^{\frac{1}{2}}$$

where $(m - n)$ is the excess of independent reflections over variable parameters.

The estimated standard deviation (esd), σ_{p_i}, associated with a refined parameter is output, thus permitting a meaningful evaluation of the shift magnitudes of the variable parameters;

$$\sigma_{p_i} = G.\sqrt{b_{ii}}$$

where b_{ii} is the ith diagonal element of the inverse matrix used in solving the normal equations. σ_{p_i} is inversely proportional to the square root of the number of reflections included in the least-squares cycle and directly proportional to their standard deviations, σ_{F_o}.

In addition to outputting the above parameters and refinement indicators program FUORFLS lists R_1 and R_2 in ranges of $(\sin\theta)/\lambda$ and average $w\Delta^2$ ($\equiv$ *Av.* $w\Delta^2$) against max. $|F_o|$ for the data in specified intensity ranges. These distributions serve to indicate intensity outliers and the suitability of the chosen weighting scheme, which is important in deriving the correct standard deviations of the variable parameters.[44a] For correctly weighted data *Av.* $w\Delta^2$ should be constant in ranges of fifty or more reflections against both max. $|F_o|$ and $(\sin\theta)/\lambda$ provided the model is complete; neglect of hydrogen atoms or incomplete anisotropic refinement can disturb the distribution.[44a]

Finally, in comparing structural parameters derived by full-matrix least-squares refinement of X-ray crystallographic data it should be remembered that the derived standard deviations have been shown[52,56] to be too optimistic by a factor of about two.

primary references for this section

ORFLS and ORFFE manuals (see Appendix I).

ref. 45, 46, 50.

(2) Optical Rotatory Dispersion and Circular Dichroism

The electromagnetic radiation known as visible light spans a wavelength (λ) range of ca. 330-780 nm, corresponding to a frequency (ν) distribution of ca. 30,000-13,000 cm^{-1}. In monochromatic light the electric field ($\underset{\sim}{E}$) oscillates with fixed frequency perpendicular to the direction of propagation; the magnetic field vector ($\underset{\sim}{H}$) oscillates orthogonal to both $\underset{\sim}{E}$ and the direction of propagation.

The electric vector of monochromatic light can be viewed as the resultant of an orthogonal x and y component oscillating perpendicular to the axis of propagation; for a phase difference of $n\pi$ (n integral) | unclear the resultant is a straight line and the light is said to be linearly (or plane) polarized. When the orthogonal vibrations are out of phase the electric field vector traces an ellipse, i.e. the light is elliptically polarized. In the special case of equal components having phase difference $\pi/2$ the light is circularly polarized; plane polarized light can be physically separated into a right- and left-circularly polarized beam (phase difference + or − $\pi/2$).

A chromophore, i.e. colour centre having a transition in the wavelength range of interest, absorbs the monochromatic radiation of frequency corresponding to the transition energy. For an electric-dipole allowed one-electron transition $a \rightarrow b$[†1] the magnetic-dipole and electric-quadrupole intensity is sufficiently small to be neglected and to a good approximation the transition strength is given by

$$D_{ba} = |(a|\mu_e|b)|^2 = \rho^2$$

where μ_e is the electric-dipole moment operator

and ρ the electric-dipole moment.

[†1] Throughout this work absorption transitions are written $a \rightarrow b$ from ground state a to excited state b; the more usual representation is $b \leftarrow a$.

The dipole strength, D_{ba}, of the transition can be empirically determined[57] from the area of the unpolarized absorption band as

$$D_{ba} = \frac{3hc}{8\pi^3 N_1} \int_0^\infty \frac{\varepsilon}{\nu}\, d\nu \qquad c.g.s.\ units$$

where h = Planck's constant,

c = the velocity of light,

N_1 = the number of molecules per cm^3,

and ε is the decadic molar extinction coefficient.

The spin-allowed transitions of metal complexes give absorption bands of finite width (rather than the sharp lines of atomic spectra) due to the vibrational modes of the chromophore.

Chromophores lacking a rotary inversion axis[58,59] can exist in two non-superimposable mirror image forms; they are termed *chiral*. Where racemization is not too rapid chiral molecules can be separated into two enantiomers (or antipodes) which have identical chemical and physical properties apart from their interaction with other chiral molecules or polarized light. Because of their ability to rotate the plane of polarization of plane polarized light they are said to be *optically active*. The specific rotatory power, $[\alpha]_{\lambda}^{t}$, of a compound in a specified environment is constant for a fixed wavelength, being positive for one enantiomer and negative for the other (or zero for both); the enantiomers referenced in this work are designated (+) or (-), being dextro- or laevo-rotatory at the Na_D line (λ = 589 nm) unless an alternative reference wavelength is specified.

unclear

The variation of $[\alpha]_{\lambda}^{t}$ with wavelength is termed *optical rotatory dispersion*, ORD. The observed rotation, α, results from the different refractive indices (η_l, η_r) for left- and right-circularly polarized light in a chiral chromophore and the variation of $[\alpha]$ follows the dispersion of refractive index with wavelength;[9]

$$\alpha = \pi(\eta_l - \eta_r)/\lambda$$

For an isolated optically active transition $[\alpha]$ changes sign at the wavelength of the absorption maximum (λ_{max}) tailing asymptotically to zero outside of the absorption band envelope,[11,17] as represented by Drude's equation;[8]

$$[\alpha] = \frac{A}{(\lambda^2 - \lambda^2_{max})}$$

where A is a constant for a particular system.

In some practical cases an inflexion only is observed without sign change, e.g. $[\text{Co tn}_3]^{3+}$, (ref. 60).

Optically active molecules absorb left- and right- circularly polarized light to different extents; the difference $(\varepsilon_l - \varepsilon_r)$, where ε_l ε_r are the decadic molar extinction coefficients for left and right circularly polarized light, is called *optical circular dichroism*, CD. The ORD curve is the differential of the CD spectrum with respect to frequency; together they comprise the *Cotton Effect.*[17,61] A positive Cotton effect is defined as one in which the ORD passes through a maximum and then a minimum as the frequency increases; this corresponds to a positive CD peak $(\varepsilon_l > \varepsilon_r)$ centred at the absorption maximum (see

Figure A.1). If the (+)enantiomer exhibits a positive Cotton effect that of the (-)enantiomer is identical in form but negative.[62]

Potentially ORD and CD curves provide the same information about the absolute configuration of the enantiomer but the finite extension of the former outside of the absorption band envelope means that for systems having several optically active transitions of similar energy the ORD spectrum is often considerably more complicated than the CD. Transitions which are magnetic-dipole allowed will make the greatest contribution to the observed rotatory power, the magnitude of the contribution depending on the transition rotatory strength[63,64]

$$R_{ba} = Im\{(a|\mu_e|b).(b|\mu_m|a)\} = \rho\mu\cos\phi$$

where $Im\{\ \}$ denotes *imaginary part of*,

μ_m is the magnetic-dipole operator,

μ is the magnetic-dipole moment

and ϕ is the angle between the directions of ρ and μ.

Thus, transitions which are electric-dipole allowed but magnetic-dipole forbidden will make only a small contribution to the optical rotatory power. R_{ba} is maximal for transitions having parallel electric- and magnetic-dipole vectors, i.e. $\phi = 0^o$. Moffitt[25,65] Luhl? indicated that only the "electronically allowed" (as opposed to "vibronic" - see Chapter 6) part of the electric-dipole oscillator strength, μ_e, contributes to the rotatory strength.

The rotational strength of a transition may be determined[12] from the area under a CD peak as

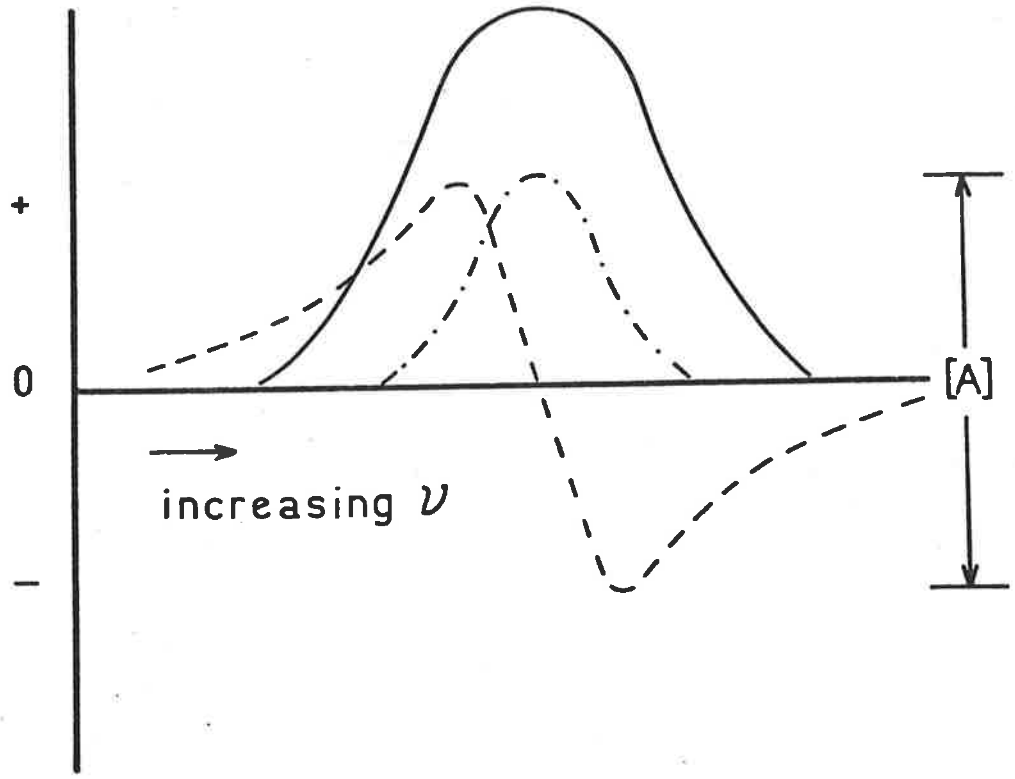

FIGURE A.1: POSITIVE COTTON EFFECT FOR AN ISOLATED TRANSITION.
—— Absorption, ε.
---- Molecular rotation, [M].
-.-. Optical circular dichroism ($\varepsilon_l - \varepsilon_r$) or ellipticity, ψ.

$$R_{ba} = \frac{3hc}{8\pi^3 N_1} \int_0^\infty \frac{(ellipticity)}{\nu}\, d\nu \qquad c.g.s.\ units$$

where *ellipticity* (in degrees) is a measure of the circular dichroism such that the molecular ellipticity

$$[\theta]_\lambda^t = 3300\ (\varepsilon_l - \varepsilon_r)\ \text{(degrees) cm}^{-1}\ \text{mole}^{-1}\ \text{litre.}$$

The measured ellipticity, ψ, is related to the molecular ellipticity in the same way that the measured optical rotation, α, relates to the molecular rotation $[M]_\lambda^t$, i.e.

$$\text{Specific ellipticity } [\psi]_\lambda^t = \psi/ldp$$

where l = path length in decimetres,

d = density of the solution,

p = grams of solute per 100 grams of solution,

t = temperature,

λ = wavelength

and $[\theta]_\lambda^t = [\psi]_\lambda^t M_w/100$ is the molecular ellipticity in degrees

where M_w is the molecular weight.

The amplitude $[A]$, (see Figure A.1), of the dispersion of molecular rotation, $[M]$, is related to the maximum circular dichroism of an isolated transition as

$$[A] = 4028\ (\varepsilon_l - \varepsilon_r)_{max}.$$

primary references for this section: refs. 66-71.

(3) Ligand Abbreviations and Structural Formulae

	Chemical and/or trivial name	*Structural formula*
acac	acetylacetonate	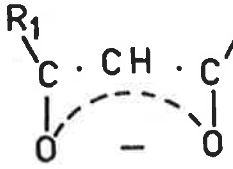 $R_1 = R_2 = Me$
atc	3-acetylcamphorate	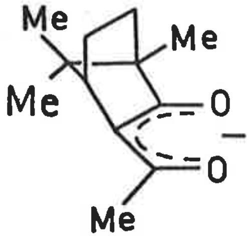
bdtc	di-*n*-butyldithiocarbamate	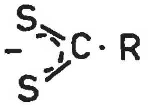 $R = N(C_4H_9)_2$
bgH	biguanide	$NH_2C(NH)NHC(NH)NH_2$
btxan	*tert*-butylthioxanthate	see bdtc, $R = S.C(Me)_3$
bzac	benzoylacetonate	see acac, $R_1 = Ph$
cat	catecholate anion of 1,2-dihydroxy benzene	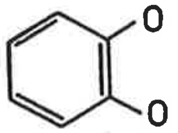 2−
chxn	1,2-diaminocyclohexane	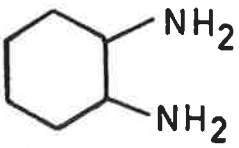
cptn	1,2-diaminocyclopentane	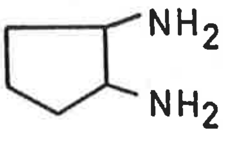

	Chemical and/or trivial name	*Structural formula*
dipy	2,2'-dipyridyl	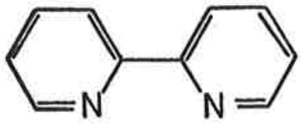
dpd	*cis*-1,2-diphenylethene-1,2-dithiolene(I) or -1,2-dithiolate(II)	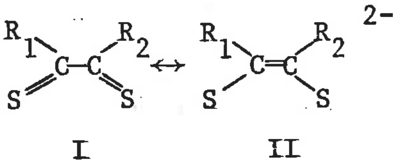 $R_1 = R_2 = Ph$
dtc	N,N-diethyldithiocarbamate	see bdtc, $R = N(Et)_2$
dtg	dithioglyoxal = 1,2-dithioethene	see dpd, $R_1 = R_2 = H$
dtpa	dithiophenylacetate	see bdtc, $R = CH_2Ph$
en	1,2-diaminoethane	$NH_2CH_2CH_2NH_2$
etp	0,0'-diethyldithiophosphate	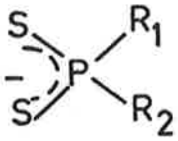 $R_1 = R_2 = O.Et$
exan	o-ethylxanthate	see bdtc, R = O.Et
gly	glycinate	$NH_2CH_2CO_2^-$
hfac	hexafluoro-acetylacetonate	see acac, $R_1 = R_2 = CF_3$
mal	malonate	$O_2C.CH_2.CO_2^{2-}$
mdtc	N-methyl-N-phenyldithiocarbamate	see bdtc, $R = N(Ph)CH_3$

	Chemical and/or trivial name	*Structural formula*
mnt	maleonitriledithiolate	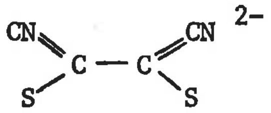
mtp	0,0'-dimethyldithiophosphate	see etp, $R_1 = R_2 = O.Me$
nph	N-nitroso-phenylhydroxylamine ion	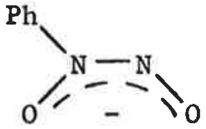
OMPA	octamethylpyrophosphoramide	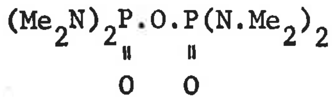 $(Me_2N)_2\underset{\overset{\|}{O}}{P}.O.\underset{\overset{\|}{O}}{P}(N.Me_2)_2$
ox	oxalate	$O_2C.CO_2{}^{2-}$
oxd	oxydiacetate	$O_2C.CH_2.O.CH_2.CO_2{}^{2-}$
pdtc	1-pyrrolidinecarbodithioate	see bdtc, R = 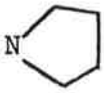
phen	1,10-phenanthroline	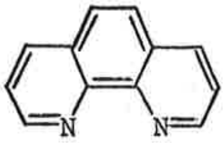
pn	1,2-diaminopropane	$CH_3CH(NH_2)CH_2NH_2$
ptn	2,4-diaminopentane	$CH_3CH(NH_2)CH_2CH(NH_2)CH_3$

	Chemical and/or trivial name	*Structural formula*
pyd	pyridine-2,6-dicarboxylate (dipicolinate)	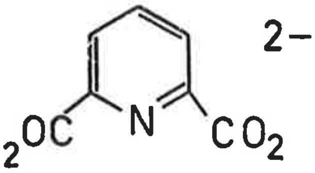
sacsac	dithio-acetylacetonate	see acac, both oxygen donors replaced by sulphur.
succ	succinate	${}_2OC.CH_2CH_2.CO_2{}^{2-}$
tame	tris-aminomethylethane	$CH_3C(CH_2NH_2)_3$
tfd	*cis*-1,2-bis(trifluoromethyl)ethylene-1,2-dithiolene	see dpd, $R_1 = R_2 = CF_3$
tfs	*cis*-1,2-bis(trifluoromethyl)ethylene-1,2-diselenolene	as for tfd but with both sulphur donors replaced by selenium.
thd	anion of 2,2,6,6-tetramethylheptane-3,5-dione	see acac, $R_1 = R_2 = C(CH_3)_3$
thiox	dithio-oxalate	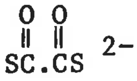 $S\overset{O}{\overset{\parallel}{C}}.\overset{O}{\overset{\parallel}{C}}S^{2-}$
tn	1,3-diaminopropane	$NH_2CH_2CH_2CH_2NH_2$
TRI	tribenzo(b,f,j)(1,5,9)triazacyclo-duodecine	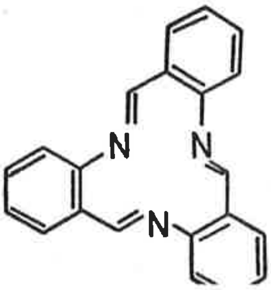

	Chemical and/or trivial name	*Structural formula*
trop	tropolonate	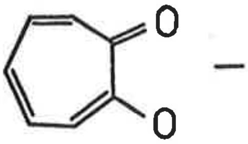
xan	ethylxanthate	see bdtc, R = S.Et

Et = ethyl, Me = methyl, Ph = phenyl

PART I

EXPERIMENTAL

CHAPTER 1 THE STRUCTURE OF SODIUM $(+)_{546}$-BIS(MALONATO)-ETHYLENEDIAMINECOBALTATE(III) DIHYDRATE.

$\mathrm{Na}\ (+)_{546}[\mathrm{Co\ mal_2\ en}].2\mathrm{H_2O}$, NADCOMALEN.[†1]

1.1 STRUCTURE ABSTRACT

The structure of the sodium salt of $(+)_{546}$-bis(malonato)ethylenediaminecobaltate(III), $\mathrm{Na}\ (+)_{546}[\mathrm{Co(CH_2(CO_2)_2)_2(C_2H_8N_2)}].2\mathrm{H_2O}$, has been solved and refined by full-matrix least-squares to $R_1 = 0.050$ using 838 integrated $MoK\alpha$ photographic intensities. The lattice is orthorhombic, space group $P2_12_12_1$ (No. 19), $a = 13.46\ (2)$, $b = 14.24\ (2)$, $c = 7.344\ (10)$ Å, $U = 1408\ (5)$ Å^3, $Z = 4$, $D_m = 1.78\ (2)$ g. cm^{-3}, $D_c = 1.80$. The trigonal-bidentate complex ion exhibits approximate two-fold symmetry with the two malonate ligands adopting boat conformations and folding toward each other while the ethylenediamine ligand is dissymmetrically skewed oblique to the pseudo- C_3 axis of the anion. The absolute configuration of the complex ion is Δ, in agreement with correlations from circular dichroism experiments.

1.2 EXPERIMENTAL

Racemic $\mathrm{Na[Co\ mal_2\ en]}.x\mathrm{H_2O}$ was prepared by the published method[72] but attempted resolution was unsuccessful due to low activity of the resolving agent. Recrystallization from aqueous solution of a sample of $\mathrm{Na}\ (+)_{546}[\mathrm{Co\ mal_2\ en}].2\mathrm{H_2O}$ supplied by Dr. A.M. Sargeson gave red-violet rectangular prisms, the majority of which exhibited

---

[†1] ten digit structure identifier.

$\{1,1,1; \bar{1},\bar{1},1\}$ bevels at one end of the needle axis and were badly twinned; the faces parallel to the needle axis were of the form $\{1,1,0\}$. The space group and unit cell parameters were determined from zero and upper level precession and Weissenberg films recorded with *MoKα/Zrf* radiation ($\lambda = 0.7107$ Å). The errors in the unit cell dimensions were estimated from multiple determinations of the constants for several crystals. Systematic absences of the form $\{h00\}$, $h = 2n + 1$, occurred.

Crystal Data - as in structure abstract.

$Na[Co(C_3H_2O_4)_2(C_2H_8N_2)].2H_2O$; $M = 3821$;

$\mu_{MoK\alpha} = 13.3\ cm^{-1}$.

D_m by flotation in carbon tetrachloride/1,3-diaminopropane at 22°C.

Integrated photographic intensities were recorded for reciprocal layers *h0l-h2l* and *0kl-2kl* using a Supper Buerger precession camera, three films per layer, exposure times 96, 36, 12 hours, *MoKα/Zrf*. Layers *hk0-hk7* were photographically recorded on triple film packs using a Nonius Weissenberg equi-inclination camera, exposure time increasing from 47 hours for *hk0* to 94 hours for *hk7*. 0.0013 (1) inch thick brass shims were placed between films one and two and two and three of the multifilm pack to increase the recording range with *Mo* radiation and a dummy film was placed in front of the first intensity recording film in an attempt to reduce the background film intensity due to the long wavelength scatter.

The crystal used for the intensity data collection was a rectangular prism 0.10 x 0.10 x 0.40 mm. mounted along the needle axis, *c*. This crystal was also used to generate a non-integrated *hkl* layer, using *CuKα/Nif* radiation, for subsequent determination of the absolute configuration of the anion. A microscope examination of the crystal following this period of data collection revealed signs of surface powdering but the diffraction spots remained sharp suggesting the powdering was probably only due to dehydration of the surface layers.

The *Cu* data were estimated visually against a calibrated intensity strip and the integrated intensities were measured with a Nonius II Microdensitometer, excluding systematic absences from the list and including unreliable reflections (e.g. on the white radiation streak of another reflection, spot distortion) and very weak reflections with markers (*E* and *U* respectively in the structure factor tables) which facilitated their special handling in the data reduction steps (AUFAC, AULAC) and permitted their exclusion from the least-squares refinement cycles (FUORFLS) while continuing to calculate their structure factors.

1.3 STRUCTURE SOLUTION AND REFINEMENT

The data reduction procedure used in scaling the raw photographic intensities and deriving the standard deviation of the scaled intensity for each unique reflection is summarised in Appendix II. Absorption corrections were not applied. All data were initially fitted to an

AUFAC weighting scheme having $a = 0.0023$, $b = 0.0098$, $c = 0$, $d = 0$. Reflections showing poor agreement were checked on all films on which they occurred. Because there were no precession data with $l = 6$ or 7, Weissenberg layers *hk6* and *hk7* were excluded from the inter-layer scaling sequence and the initial stages of structure refinement; they were subsequently introduced with scale factors determined from the other Weissenberg layers in proportion to exposure times.

The initial data set (excluding *hk6* and *hk7* data) comprised 889 unique reflections of which 181 were unobserved (*U*) and 24 unreliable (*E*). A Patterson synthesis using this data set yielded starting coordinates for the Co atom and the positions of all non-hydrogen atoms, other than the water oxygens, were obtained from a Fourier map phased by Co. Two cycles of least-squares refinement (684 data included) of the sixty positional parameters for the above atoms lowered R_1 from 0.350 to 0.155. Both water oxygen atoms (expected from density measurements) were located in Fourier and difference maps computed at this stage. The difference map also indicated some thermal anisotropy of the metal atoms. The water oxygens were included in the atoms list and after a further two cycles refining positional parameters and isotropic temperature factors of all atoms except Co and Na, which were refined anisotropically, the refinement converged with $R_1 = 0.069$ and $R_2 = 0.058$ for the 684 reflections. G, the error in an observation of unit weight, was 3.827. Examination of the low $\sin\theta$ data at this point showed no systematic deviations attributable to extinction and an extinction parameter was not refined in the subsequent treatment. The sources for the atomic scattering factors are indicated in Appendix IV.

Hydrogen atom positional coordinates (other than for the water molecules) were calculated using PLANEH such that C-H = 1.02 Å, N-H = 0.95 Å with tetrahedral angles at C and N. The twelve hydrogens were introduced to the atoms list with fixed isotropic thermal parameters; the scaled *hk6* and *hk7* Weissenberg data were added to the data set increasing the total number of unique reflections to 1060 of which 838 were included in subsequent refinement cycles. R_1 and R_2 became 0.066 and 0.063 respectively, dropping to 0.059 and 0.051 after one cycle of positional and isotropic temperature factor refinement; Co and Na were refined anisotropically and the hydrogens were kept fixed (number of variable parameters, $n = 98$). $G = 3.292$.

Calculation of the structure factors for the 38 pairs of *CuKα/Nif* Weissenberg data $(h \pm kl)$ ($\Delta f''_{Co_{Cu}} = 3.90$) indicated that the absolute configuration of the $(+)_{546}$-anion was Δ and not Λ as had been chosen (37 pairs agreed with the choice of Δ while only the weakest pair of reflections contradicted such an assignment). Moreover, analogous calculations on the *MoKα/Zrf* data with $\Delta f''_{Co_{Mo}} = 1.10$ gave $R_1 = 0.058$, $R_2 = 0.050$ for the Δ configuration as opposed to values of 0.063 and 0.056 for Λ.

Although the structure seemed chemically reasonable at this stage, the increasing trend of *Av.* $w\Delta^2$ with increasing $|F_o|$ indicated incorrect weighting of the intensity data. Re-examination of the AUFAC inter-film scaling sequence of the *Mo* data (see parameters above and Appendix II) showed that the more intense data had been assigned standard deviations of the same order as the weaker reflections, i.e. the intense data carried weights which were relatively too large in the least-squares refinement cycles. The large standard deviations of the isotropic thermal parameters of the light atoms were also symptomatic of the inadequacy of this weighting scheme. To overcome this situation the data were fitted to a Cruickshank weighting scheme[44a,46] of the form

$$\sigma_{F_o} = (a + F_o + bF_o^{\,2})^{\frac{1}{2}}$$

where $a = 1.35$, $b = 0.016$ and F_o is the square root of the observed unscaled intensity; $w = 1/\sigma_{F_o}^{\,2}$. A least-squares cycle using this weighting scheme and calculated for the Δ absolute configuration with Co anomalous scattering terms included gave $R_1 = 0.050$, $R_2 = 0.066$ and $G = 0.236$; the distribution of $Av.\ w\Delta^2$ versus F_o flattened and the weighted R_2 factor in all $(\sin\theta)/\lambda$ ranges containing more than 30 reflections averaged 0.072 (± 0.015). Estimated standard deviations of all refined parameters (positional and thermal) showed improvements ranging 30-50%.

The positions of the hydrogen atoms were recalculated and included in a final least-squares cycle refining positional and isotropic thermal parameters of all light atoms other than hydrogen; Co and Na were refined anisotropically. There was no change in the agreement factors and the positional coordinates and estimated standard deviations which resulted were used in calculating the distance and angle parameters and their estimated standard deviations (given in parentheses) tabulated in the following section. Full-matrix anisotropic refinement of all non-hydrogen atoms (n = 201) was not attempted for this structure because of prohibitive computing time requirements. A block refinement analogous to that used for anisotropic refinement of CADCOTHIOX (Chapter 3) could have been used.

Observed and calculated structure factors from the final least-squares cycle are listed in Table 1.1A and the *CuKα* Friedel (or Bijvoet) pairs are given in Table 1.1B: for both tables F_o, $F_c \times 10$; the meaning of U and E is given in the text.

1.4 STRUCTURE FIGURES AND TABLES

The figures and tables of structural parameters are collected together in this section preliminary to the discussion of section 1.5. The captions and table headings are, for the most part, self-explanatory; a few brief notes relevant to all three structures have been relegated to Appendix IV. Unit cell diagrams were not drawn for any of the structures presented in this work.

TABLE 1.1A FINAL $|F_o|$ AND $|F_c|$ FOR Na (+)$_{546}$[Co mal$_2$ en].2H$_2$O.

	H	K	FOBS	FCAL	
	**L =		0****		U
	0	2	729	754	U
E	0	4	1554	1795	U
E	0	6	1216	1369	U
E	0	8	692	730	
E	0	10	359	372	
	0	12	779	811	U
E	0	14	278	182	
E	1	1	295	983	U
	1	2	994	1002	U
	1	3	1033	1068	U
	1	4	873	912	
U	1	5	85	108	
	1	6	192	152	U
	1	7	847	902	U
	1	8	1169	1196	
E	1	9	640	521	
U	1	10	114	237	U
U	1	11	120	32	
U	1	12	126	187	
	1	13	354	331	U
U	1	14	139	121	
	1	15	314	242	
	2	0	352	397	
	2	1	871	913	
	2	2	231	211	
	2	3	597	556	
	2	4	901	882	U
	2	5	830	845	
	2	6	306	327	U
	2	7	640	670	
	2	8	219	180	
	2	9	312	330	
U	2	10	116	16	
	2	11	221	222	U
	3	1	191	151	U
U	3	2	78	99	U
E	3	3	121	170	
U	3	4	85	132	U
	3	5	301	350	
	3	6	382	348	U
	3	7	295	263	U
	3	8	235	266	U
	3	9	683	710	
U	3	10	118	67	U
	3	11	383	435	
U	3	12	129	81	U
	3	13	339	331	
U	3	14	142	92	
	3	15	551	637	U
E	4	0	629	650	U
	4	1	670	667	U
	4	2	737	779	
U	4	3	87	16	
	4	4	249	260	U
	4	5	279	243	
	4	6	1015	1030	U
	4	7	552	563	
	4	8	826	842	
U	4	9	115	54	
U	4	10	122	207	
	4	11	424	433	
	4	12	422	441	
	4	13	512	511	E
	4	14	323	287	
	5	1	224	213	
	5	2	628	641	

H	K	FOBS	FCAL	
5	3	94	55	
5	4	96	57	E
5	5	101	95	U
5	6	104	38	
5	7	356	315	
5	8	468	424	
5	9	120	75	
5	10	408	407	
5	11	129	273	
5	12	136	73	
5	13	142	163	
5	14	534	549	E
6	0	515	520	
6	1	95	54	
6	2	97	133	
6	3	468	466	U
6	4	424	437	U
6	5	104	83	U
6	6	643	646	
6	7	486	559	
6	8	118	18	
6	9	400	407	
6	10	552	540	
7	1	708	672	
7	2	793	777	
7	3	684	656	
7	4	383	388	
7	5	111	156	
7	6	232	225	
7	7	122	104	
7	8	666	674	
7	9	562	575	
8	0	518	469	
8	1	1120	1155	U
8	2	110	223	U
8	3	115	175	
8	4	115	110	E
8	5	819	868	
8	6	121	107	
8	7	862	878	
9	1	129	173	
9	2	116	52	
9	3	119	118	
9	4	666	663	
9	5	124	100	
9	6	366	385	
9	7	130	28	
9	8	564	602	
10	0	492	508	
10	1	123	179	
10	2	124	17	
10	3	128	113	
10	4	363	334	
10	5	243	225	
11	1	130	150	
11	2	271	222	
12	0	137	31	U
12	1	371	358	
15	2	420	421	
16	0	416	420	
**L =		1****		U
0	1	996	1172	
0	2	683	733	
0	3	125	100	
0	4	641	607	
0	5	482	514	
0	6	489	478	

H	K	FOBS	FCAL	
0	7	718	742	
0	8	446	367	
0	9	100	50	
0	11	314	335	U
1	0	1214	1347	E
1	1	548	453	
1	2	704	640	
1	3	666	630	
1	4	328	279	
1	5	513	483	
1	6	865	885	
1	7	603	464	U
1	8	482	459	U
1	9	469	475	U
1	10	314	287	
1	11	113	113	
1	12	119	169	
1	13	126	223	
1	14	362	397	
1	15	269	299	
2	0	751	788	
2	1	741	676	
2	2	677	629	
2	3	486	471	
2	4	348	304	
2	5	603	580	U
2	6	1068	1162	
2	7	434	409	U
2	8	412	381	
2	9	478	484	
2	10	393	427	
2	11	269	266	
2	12	268	245	
2	13	126	111	
2	14	131	136	
2	15	261	281	
3	0	167	156	
3	1	417	416	
3	2	1246	1240	
3	3	487	442	
3	4	162	179	
3	5	224	224	
3	6	728	705	
3	7	221	209	
3	8	691	727	
3	9	219	229	
3	10	422	411	U
3	11	190	156	
3	12	284	285	
3	13	240	216	
3	14	371	399	
4	0	1242	1254	
4	1	773	753	U
4	2	532	486	
4	3	599	554	U
4	4	534	532	
4	5	94	107	U
4	6	351	351	
4	7	196	156	U
4	8	192	211	
4	9	117	119	
4	10	267	274	
4	11	242	249	
4	12	218	217	U
4	13	260	210	U
4	14	277	225	
5	0	441	460	

H	K	FOBS	FCAL	
5	1	208	193	
5	2	384	382	
5	3	510	523	
5	4	94	167	
5	5	338	323	U
5	6	294	295	
5	7	643	674	
5	8	241	214	U
5	9	491	485	
5	10	378	405	
5	11	172	147	E
5	12	137	182	
5	13	142	160	U
5	14	148	90	
5	15	348	341	
6	0	579	536	
6	1	960	950	U
6	2	772	772	
6	3	756	755	E
6	4	312	288	
6	5	573	591	
6	6	267	261	U
6	7	575	570	U
6	8	296	290	
6	9	483	456	U
6	10	129	173	
6	11	364	402	
6	12	141	39	
6	13	302	297	
6	14	286	250	
7	0	476	423	
7	1	664	639	
7	2	573	562	
7	3	353	333	E
7	4	330	305	
7	5	380	341	
7	6	285	258	U
7	7	508	466	U
7	8	427	431	
7	9	364	355	U
7	10	376	366	U
7	11	264	252	U
7	12	218	243	
7	13	253	238	
7	14	315	288	
8	0	570	572	E
8	1	108	146	U
8	2	391	381	
8	3	228	227	
8	4	229	232	
8	5	292	315	
8	6	578	597	
8	7	123	80	
8	8	329	339	U
8	9	133	199	
8	10	289	276	
8	11	142	89	U
8	12	299	292	U
9	0	115	111	
9	1	412	401	
9	2	364	347	
9	3	232	213	
9	4	300	314	
9	5	122	176	
9	6	125	201	
9	7	339	321	
9	8	248	259	

H	K	FOBS	FCAL	
9	9	326	316	
10	0	360	372	
10	1	400	386	
10	2	336	358	
10	3	123	114	
10	4	382	404	
10	5	348	332	
10	6	131	170	
10	7	407	406	
10	8	388	351	
11	0	213	187	U
11	1	382	361	
11	2	128	156	
11	3	293	285	
11	4	213	205	
11	5	316	299	
11	6	137	136	U
11	9	286	256	
12	0	230	256	
12	6	302	310	
12	8	265	250	
13	0	142	159	
13	1	141	178	
13	2	269	297	U
13	3	144	64	
13	4	377	369	
13	8	316	341	
14	0	410	385	
14	1	355	339	
14	4	272	308	
15	3	393	407	
**L =		2****		
0	1	613	603	
0	2	133	113	
0	3	455	435	U
0	4	493	489	
0	5	71	82	
0	6	77	70	
0	7	288	288	
0	8	90	143	
0	9	96	101	U
0	10	102	75	
0	11	306	295	
0	15	348	354	
1	0	722	709	
1	1	179	329	
1	2	47	69	
1	3	597	587	
1	4	264	275	
1	5	389	381	
1	6	314	331	
1	7	653	675	
1	8	348	352	U
1	9	97	155	U
1	10	237	242	
1	11	276	268	
1	12	113	154	
1	13	119	122	
1	14	261	270	
2	0	824	833	
2	1	893	953	U
2	2	740	732	
2	3	207	191	
2	4	318	312	U
2	5	698	749	
2	6	174	159	U
2	7	615	609	U

H	K	FOBS	FCAL	
2	8	718	745	
2	9	211	223	
2	10	295	318	U
2	11	356	344	
2	14	352	318	
3	0	785	810	
3	1	523	466	
3	2	323	309	
3	3	200	132	U
3	4	494	442	U
3	5	77	116	
3	6	358	335	U
3	7	215	216	
3	8	486	523	
3	9	341	337	
3	10	378	371	
3	11	111	241	
3	12	300	342	
4	0	204	195	
4	1	264	196	
4	2	253	292	
4	3	244	224	
4	4	371	387	
4	5	81	118	U
4	6	376	381	
4	7	403	389	
4	8	405	415	
4	9	416	447	
5	0	237	212	
5	1	676	654	U
5	2	254	259	
5	3	718	699	U
5	4	335	320	
5	5	487	461	
5	6	90	146	U
5	7	326	330	U
5	8	352	317	
5	9	241	256	
5	10	293	280	
5	11	256	237	
5	12	120	130	
5	13	322	332	
6	0	914	949	
6	1	432	421	
6	2	408	391	
6	3	746	752	U
6	4	567	583	
6	5	379	392	
6	6	480	471	
6	7	324	305	
6	8	301	255	
6	9	541	548	E
6	10	113	171	
6	11	118	119	
6	12	309	314	
7	0	591	573	U
7	1	446	435	U
7	2	396	396	U
7	3	355	386	
7	4	281	314	U
7	5	96	125	
7	6	474	471	U
7	7	498	494	U
7	8	108	135	U
7	9	251	252	
7	10	117	189	U
7	11	122	171	

H	K	FOBS	FCAL	
7	12	275	252	
7	13	327	315	
8	0	93	19	
8	1	441	415	
8	2	569	575	
8	3	218	201	
8	4	545	576	
8	5	247	253	
8	6	104	91	
8	7	108	102	
8	8	452	463	
8	9	116	229	
8	10	320	321	
9	0	518	544	
9	1	368	366	
9	2	395	382	
9	3	436	419	
9	4	205	205	
9	5	429	435	U
9	6	379	395	
9	7	432	442	U
9	8	330	353	
9	9	285	286	
9	10	124	118	
10	0	558	553	U
10	1	508	504	U
10	2	336	345	U
10	3	490	486	
10	4	306	290	
10	5	112	177	
10	6	357	402	
10	7	118	191	
10	8	265	284	
10	9	345	381	
10	10	129	158	U
11	0	112	21	
11	1	264	288	U
11	5	249	288	
11	7	321	353	
12	4	350	360	
13	0	384	376	
13	2	309	324	U
13	3	416	391	
13	6	384	398	
13	9	333	307	
14	0	131	197	
14	2	424	427	
14	3	331	345	
14	5	330	331	U
15	1	340	353	
**L =		3****		
0	1	270	315	
0	2	734	813	
0	3	360	351	
0	4	675	705	
0	5	66	61	
0	6	73	17	
0	7	79	34	
0	8	765	777	
0	9	90	56	U
0	10	477	438	
0	11	102	99	
0	12	106	126	
0	13	112	32	U
0	14	452	450	
0	15	124	101	
0	16	360	363	U

H	K	FOBS	FCAL
1	0	626	648
1	1	959	996
1	2	610	568
1	3	300	304
1	4	177	190
1	5	482	458
1	6	406	418
1	7	365	364
1	8	178	171
1	9	240	224
1	10	294	300
1	11	243	260
1	12	200	224
1	13	290	318
2	0	216	208
2	1	473	471
2	2	524	466
2	3	381	391
2	4	63	97
2	5	442	439
2	6	76	121
2	7	535	505
2	8	176	159
2	9	466	473
2	10	98	191
2	11	103	147
2	12	108	100
2	13	217	221
3	0	232	164
3	1	994	1016
3	2	193	178
3	3	575	546
3	4	176	172
3	5	640	652
3	6	78	100
3	7	711	741
3	8	88	185
3	9	242	253
3	10	194	167
3	11	499	538
3	12	229	233
3	13	115	251
4	0	252	231
4	1	676	677
4	2	795	785
4	3	649	669
4	4	436	411
4	5	219	225
4	6	81	96
4	7	400	390
4	8	567	541
4	9	409	428
4	10	479	505
4	14	318	361
4	15	332	345
4	16	244	222
5	0	670	643
5	1	243	252
5	2	254	211
5	3	73	21
5	4	400	393
5	5	249	223
5	6	704	710
5	7	89	96
5	8	191	173
5	9	218	187
5	10	103	195

TABLE 1.1A (contd.)

	H	K	FOBS	FCAL
U	5	11	108	179
	5	12	266	281
U	6	0	75	70
U	6	1	76	133
	6	2	266	256
	6	3	235	248
	6	4	266	237
U	6	5	85	75
U	6	6	89	118
	6	7	215	191
	6	8	365	361
U	6	9	101	90
	6	10	251	233
	6	14	283	244
	7	0	586	618
	7	1	489	500
	7	2	268	278
U	7	3	85	85
	7	4	202	154
	7	5	498	505
	7	6	372	350
	7	7	430	432
	7	8	308	293
U	7	9	105	176
U	7	10	109	188
	7	11	271	269
	7	12	289	289
U	8	0	89	90
	8	1	490	504
	8	2	201	121
	8	3	686	702
U	8	4	94	110
	8	5	443	449
U	8	6	99	143
	8	7	391	378
E	8	8	250	197
	8	9	586	596
	8	10	254	257
	8	13	284	259
	8	15	283	294
	9	0	429	412
	9	1	346	287
	9	2	284	276
	9	3	307	275
	9	4	199	184
	9	5	296	275
	9	6	254	285
	9	7	292	279
	9	8	273	233
U	9	9	113	142
	9	10	255	174
U	9	11	121	145
	9	12	254	256
U	10	0	102	179
	10	1	294	264
	10	2	374	381
U	10	3	103	173
	10	4	181	199
U	10	5	107	77
	10	6	260	251
U	10	7	112	137
	10	8	242	254
	11	0	426	477
	11	1	216	199
	11	2	272	262
	11	4	234	237
	11	6	449	470
	11	10	254	261
	11	12	250	262
	12	1	235	195
	12	3	528	529
	12	7	282	288
	12	9	303	355
	13	1	257	259
	13	3	261	239
	13	5	258	277
	13	7	257	240
	14	1	245	236
	15	0	315	333
	16	4	290	301
	L = 4**			
	0	1	824	817
U	0	2	43	59
	0	3	761	778
E	0	4	139	45
U	0	5	69	29
	0	6	286	275
E	0	7	402	349
	0	8	188	202
	0	9	742	746
U	0	10	101	61
U	0	11	107	78
U	0	12	112	17
	0	13	266	278
	0	14	250	215
	0	15	400	396
	1	0	655	728
	1	1	810	882
	1	2	637	635
	1	3	141	129
	1	4	453	426
	1	5	454	461
	1	6	464	442
	1	7	572	552
	1	8	360	343
	1	9	187	196
	1	10	260	259
	1	11	322	321
	1	12	228	210
	1	13	302	304
	2	0	385	375
	2	1	572	586
	2	2	406	391
	2	3	169	164
	2	4	578	549
	2	5	530	508
	2	6	330	316
	2	7	496	472
	2	8	612	605
	2	9	350	327
	2	10	298	276
	2	11	383	364
U	2	12	113	86
	2	13	248	238
	2	14	290	309
	3	0	862	871
	3	1	305	303
	3	2	613	595
	3	3	473	451
	3	4	293	299
	3	5	436	433
	3	6	596	584
	3	7	523	518
	3	8	360	357
	3	9	241	260
	3	10	246	274
U	3	11	110	147
	3	12	357	371
U	4	0	65	63
	4	1	459	422
	4	2	390	402
	4	3	479	482
	4	4	434	414
	4	5	279	302
	4	6	196	180
	4	7	249	236
	4	8	326	301
	4	9	347	331
	4	10	315	315
	4	11	285	302
	4	14	251	220
E	4	15	307	265
	5	0	225	196
	5	1	664	665
	5	2	330	325
U	5	3	78	80
	5	4	164	143
	5	5	459	459
U	5	6	89	134
	5	7	530	530
	5	11	283	279
	6	0	174	182
	6	1	664	654
U	6	2	81	133
	6	3	299	284
U	6	4	87	67
	6	5	225	223
	6	6	339	300
	6	7	357	337
	6	8	262	236
	6	9	292	275
	6	10	218	211
U	6	11	116	146
U	6	12	121	164
	6	13	318	326
	7	0	549	625
U	7	1	87	94
	7	2	236	214
	7	3	254	270
	7	4	360	321
	7	5	344	350
	7	6	414	385
	7	7	268	247
	7	8	207	212
	7	9	297	317
	7	10	242	219
U	7	11	120	172
	7	12	280	256
	8	0	281	302
	8	1	281	268
	8	2	360	353
U	8	3	95	135
	8	4	239	230
	8	8	387	382
	8	10	231	187
	9	0	182	182
	9	1	458	447
U	9	2	100	44
	9	3	377	361
	9	5	340	337
	9	6	203	262
	9	7	249	257
U	9	8	115	46
	9	9	240	173
	10	0	271	305
	10	3	339	318
	10	4	258	247
	10	6	262	243
	10	9	301	275
	11	0	272	290
	11	1	279	276
	12	5	278	252
	L = 5**			
E	0	1	245	351
U	0	2	35	49
	0	3	215	203
E	0	4	362	352
	0	5	145	130
	0	6	296	304
	0	7	486	497
U	0	8	73	75
U	0	9	77	65
U	0	10	82	29
	0	11	244	217
U	0	12	92	195
	0	13	385	374
	0	14	306	300
	0	17	266	276
E	1	0	192	177
E	1	1	237	285
	1	2	230	248
	1	3	361	354
	1	4	266	264
	1	5	257	252
	1	6	473	464
U	1	7	69	100
U	1	8	73	86
	1	9	420	439
	1	10	334	348
	1	12	200	216
	2	0	360	364
	2	1	209	230
	2	2	361	356
	2	3	387	407
U	2	4	54	122
	2	5	393	372
	2	6	422	438
	2	7	327	345
	2	8	322	287
	2	9	434	455
	2	10	164	149
U	2	11	89	74
	2	12	293	308
U	2	13	97	135
	2	14	236	251
	3	0	372	377
	3	1	403	390
	3	2	489	459
	3	3	130	141
	3	4	549	560
	3	5	344	329
U	3	6	68	51
	3	7	299	298
	3	8	520	555
	3	11	260	278
	4	0	556	565
	4	1	513	505
U	4	2	56	50
	4	3	232	202
	4	4	382	351
	4	5	526	548
	4	6	264	257
	4	7	337	373
U	4	8	79	66
	4	9	283	282
U	4	10	87	123
	4	11	258	282
	4	12	207	187
	5	0	552	571
	5	1	693	716
	5	2	317	317
	5	3	525	549
	5	4	237	245
	5	5	197	170
	5	6	397	398
	5	7	427	429
U	5	8	81	123
	5	9	279	282
	6	0	711	654
	6	1	209	212
	6	2	332	312
U	6	3	69	25
	6	4	551	551
	6	5	168	186
	6	6	219	157
	6	7	375	383
	6	8	325	340
U	6	9	88	120
	6	10	264	281
	6	11	259	222
E	6	12	278	198
	7	0	187	193
	7	1	183	154
	7	2	331	314
	7	3	150	175
	7	4	286	314
	7	5	211	163
U	7	6	81	106
U	7	7	84	80
	7	8	313	310
	7	10	258	255
	8	0	166	192
U	8	1	76	145
U	8	2	77	105
	8	3	197	154
	8	4	306	281
U	8	5	83	146
	8	6	332	342
	8	8	198	180
	8	10	175	185
	8	12	229	246
U	9	0	81	56
	9	1	272	259
	9	2	269	282
	9	3	235	240
	9	5	235	262
	9	8	244	202
	9	9	215	210
	9	11	257	243
E	10	0	189	234
	10	1	283	300
	10	2	305	330
	10	4	254	231
	10	5	259	274
	10	8	252	228
	10	10	248	233
	10	11	242	204
	10	13	241	229
E	11	0	269	235
	11	1	228	232
	11	2	200	178
	11	3	376	368
	11	4	198	191
	11	6	207	168
	11	7	253	259
	11	9	283	287
	12	0	288	309
	12	2	232	215
	12	4	267	285
	13	1	207	200
	13	2	213	211
	13	4	255	210
	13	5	221	241
	13	7	205	235
	13	8	252	276
	14	5	223	218
	15	3	212	200
	L = 6**			
U	0	1	27	38
	0	2	180	186
U	0	3	44	10
	0	4	310	289
	0	5	177	182
	0	6	372	358
	0	10	352	367
	0	12	253	242
U	1	0	27	41
	1	1	227	267
	1	2	249	255
	1	3	365	394
	1	4	125	88
	1	5	202	197
	1	6	178	181
	1	7	173	171
	1	8	224	206
	1	9	251	244
	1	14	257	265
	2	0	138	137
	2	1	226	244
	2	2	109	116
	2	3	173	149
	2	6	186	197
	2	7	209	216
	2	10	212	231
	2	11	222	234
	3	0	186	196
	3	1	324	329
	3	3	389	391
	3	5	327	333
	3	7	153	151
	3	8	182	158
	3	9	435	438
	4	0	444	471
	4	1	290	285
	4	2	178	146
	4	4	241	242
	4	5	184	178
	4	6	468	455
	4	7	316	311
	4	10	221	209
	4	12	240	246
	4	13	216	211
U	5	0	60	12
U	5	1	61	19
	5	2	474	474
	5	3	238	245
	5	4	365	366
	5	6	161	139
	5	8	326	332
	5	10	237	269
	5	14	238	244
	6	0	467	448
E	6	1	185	124
	6	2	292	276
	6	3	143	130
	6	4	154	158
	6	6	292	294
E	7	0	208	97
	7	2	278	260
	7	3	259	244
	7	4	389	391
	7	5	163	168
	7	7	261	230
	7	8	346	336
	7	9	258	260
U	8	0	78	88
	8	1	340	329
	8	2	214	172
	8	5	405	394
	8	6	190	166
	8	7	300	294
	8	11	281	307
U	9	0	83	32
	9	1	210	191
	9	2	424	422
	9	3	205	175
	9	4	285	274
	9	7	190	178
	9	8	257	237
	9	10	222	229
	10	0	441	444
	10	4	305	265
	10	6	303	314
	10	10	223	224
	11	2	463	504
	11	3	194	224
	11	4	358	365
	11	8	331	358
	11	10	249	257
	12	1	313	345
	12	5	339	344
	12	7	268	274
	13	3	321	304
	L = 7**			
	0	2	122	141
	0	3	174	148
U	0	4	53	36
	0	5	135	162
	0	6	162	164
	0	7	248	234
	0	11	190	184
	0	13	263	288
E	1	0	91	101
E	1	1	120	149
	1	2	88	88
	1	3	189	196
	1	4	245	255
	1	5	149	139
	1	6	261	223
	1	7	153	149
	1	9	267	272
	1	10	254	267
	2	0	332	381
	2	1	306	318
	2	2	154	161
	2	3	255	278
	2	4	145	150
	2	5	163	169
	2	6	266	267
	2	8	181	180
	2	9	245	244
	2	10	176	174
	2	11	187	181
	2	12	240	237
	3	0	212	229
	3	2	489	481
	3	3	146	149
	3	4	365	379
	3	7	241	231
	3	8	390	364
	3	10	204	201
	4	0	413	408
	4	1	362	360
	4	2	213	217
	4	4	204	190
	4	5	348	316
	4	6	291	282
	4	7	253	265
	4	11	206	184
	5	0	365	367
	5	1	331	317
	5	3	481	475
	5	5	182	185
	5	7	325	298
	5	9	260	273
	5	12	211	220
	6	0	258	232
	6	2	204	217
	6	4	367	360
	6	5	158	148
	6	6	195	185
	6	7	205	218
	6	8	246	263
	7	0	221	191
	7	2	182	192
	7	4	221	231
	7	8	281	269
	8	6	243	231
	8	8	202	165
	9	1	251	244
	9	2	235	229
	10	1	226	224
	10	2	294	310
	10	4	195	181
	10	5	212	224
	11	3	288	304
	11	5	227	231
	11	7	209	203
	12	0	249	270
	12	1	188	180
	12	6	244	243
	13	2	258	256

TABLE 1.1B FRIEDEL PAIRS (F_{hk1}, $F_{h\bar{k}1}$): Na $(+)_{546}$[Co mal$_2$ en].2H$_2$O: $|F_c|$ calculated for the incorrect Λ configuration.

	k	F_o $hk1$	F_o $h\bar{k}1$	F_c $hk1$	F_c $h\bar{k}1$
$h = 1$,	3	588	622	732	535
	4	475	444	207	351
	5	538	513	436	552
	7	486	503	521	404
	8	478	486	472	378
	9	466	440	378	471
	10	383	427	319	232
	11	320	U	62	120
	13	320	371	190	158
$h = 2$,	4	456	493	417	274
	10	450	427	367	405
	13[a]	U	263	90	99
$h = 3$,	4	220	436	259	81
	5	416	355	143	271
	10	427	459	471	328
	11	355	302	90	210
$h = 4$,	5	402	U	24	169
	12	364	263	149	255
$h = 5$,	1	436	366	116	235
$h = 5$,	12	263	346	199	150
$h = 6$,	4	436	416	214	337
	10	236	364	227	127
$h = 7$,	2	521	504	461	567
	3	450	440	279	348
	4	416	450	378	214
	5	440	428	254	333
	8	450	402	328	443
	10	427	402	261	339
$h = 8$,	1	288	383	191	114
	2	459	440	295	359
	4	416	288	142	269
$h = 9$,	6	364	194	150	240
	10	334	U	156	191
$h = 10$,	5	416	383	215	318
$h = 11$,	2	355	288	95	194
	3	371	416	306	206
	4	383	302	152	251
	6	346	263	62	176

a. (2, ± 13, 1) is the only pair in agreement with a Λ configuration.

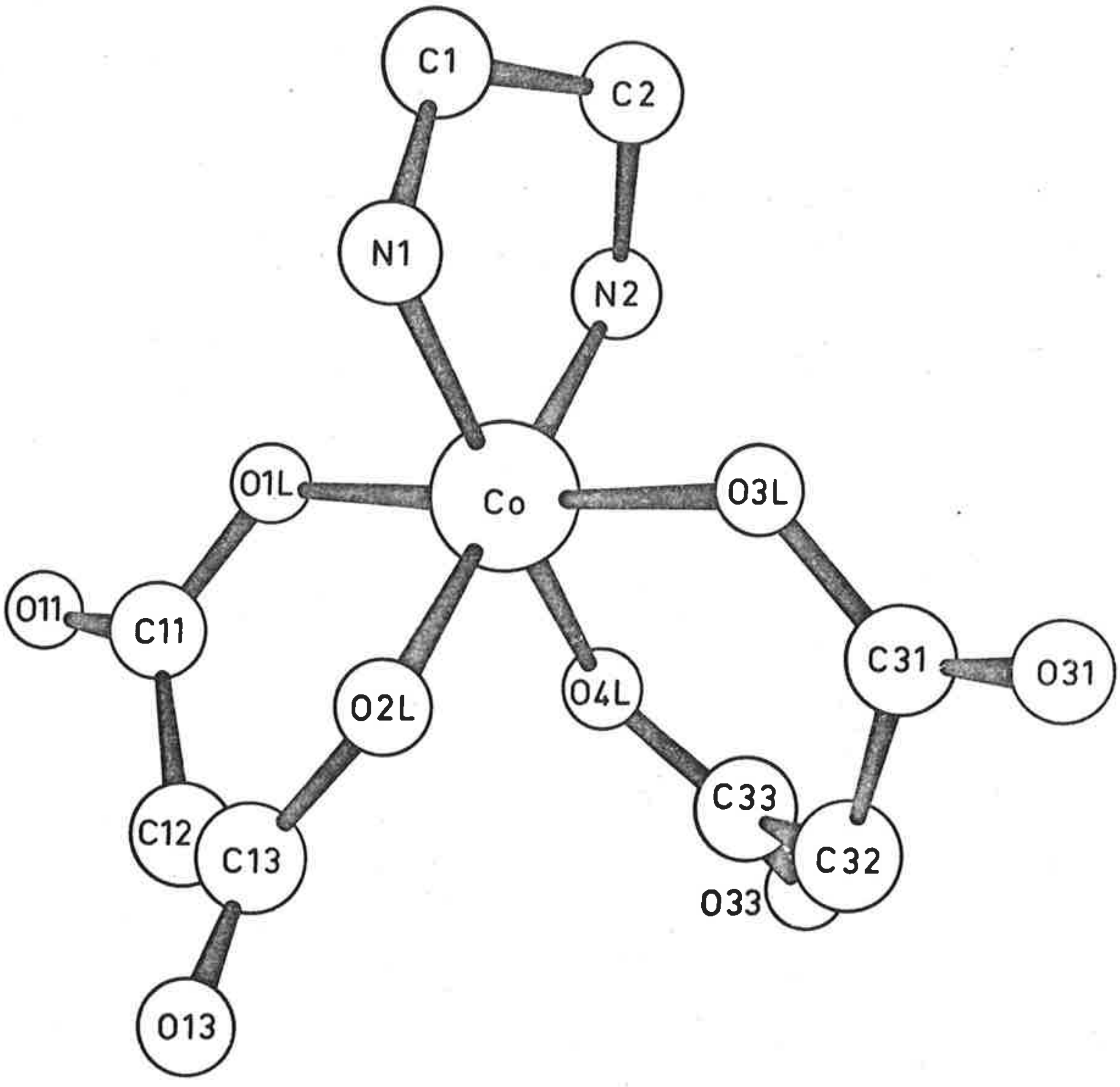
C1
C2
N1
N2
O1L
Co
O3L
O11
C11
C31
O31
O2L
O4L
C33
C12
C13
C32
O33
O13

FIGURE 1.1: PSEUDO C_3 PROJECTION OF $(+)_{546}[\mathrm{Co\ mal_2\ en}]^-$.

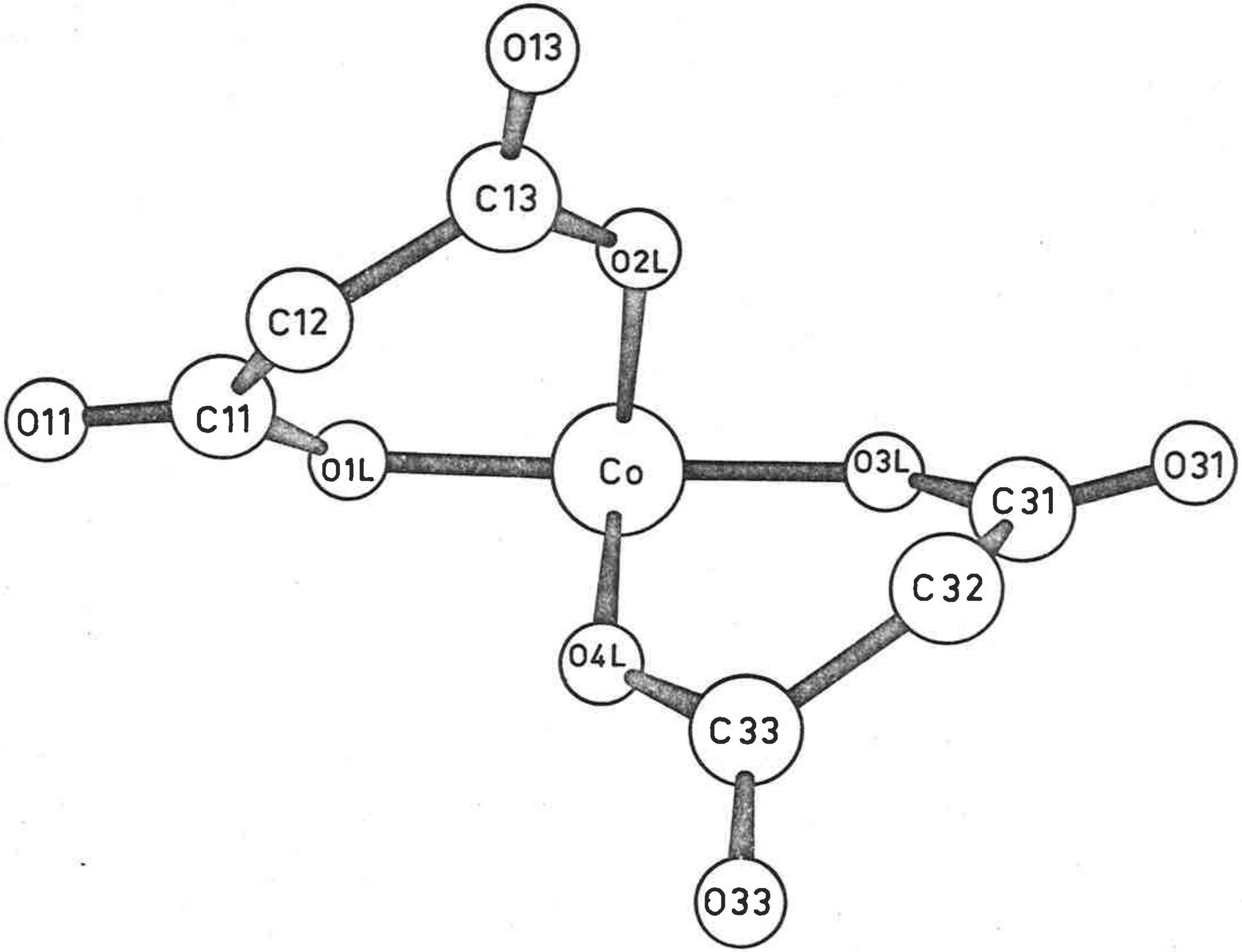
O13
C13
O2L
C12
O11
C11
O1L
Co
O3L
C31
O31
C32
O4L
C33
O33

FIGURE 1.2: PSEUDO C_2 PROJECTION OF $(+)_{546}[\mathrm{Co\ mal_2\ en}]^-$; en ligand omitted.

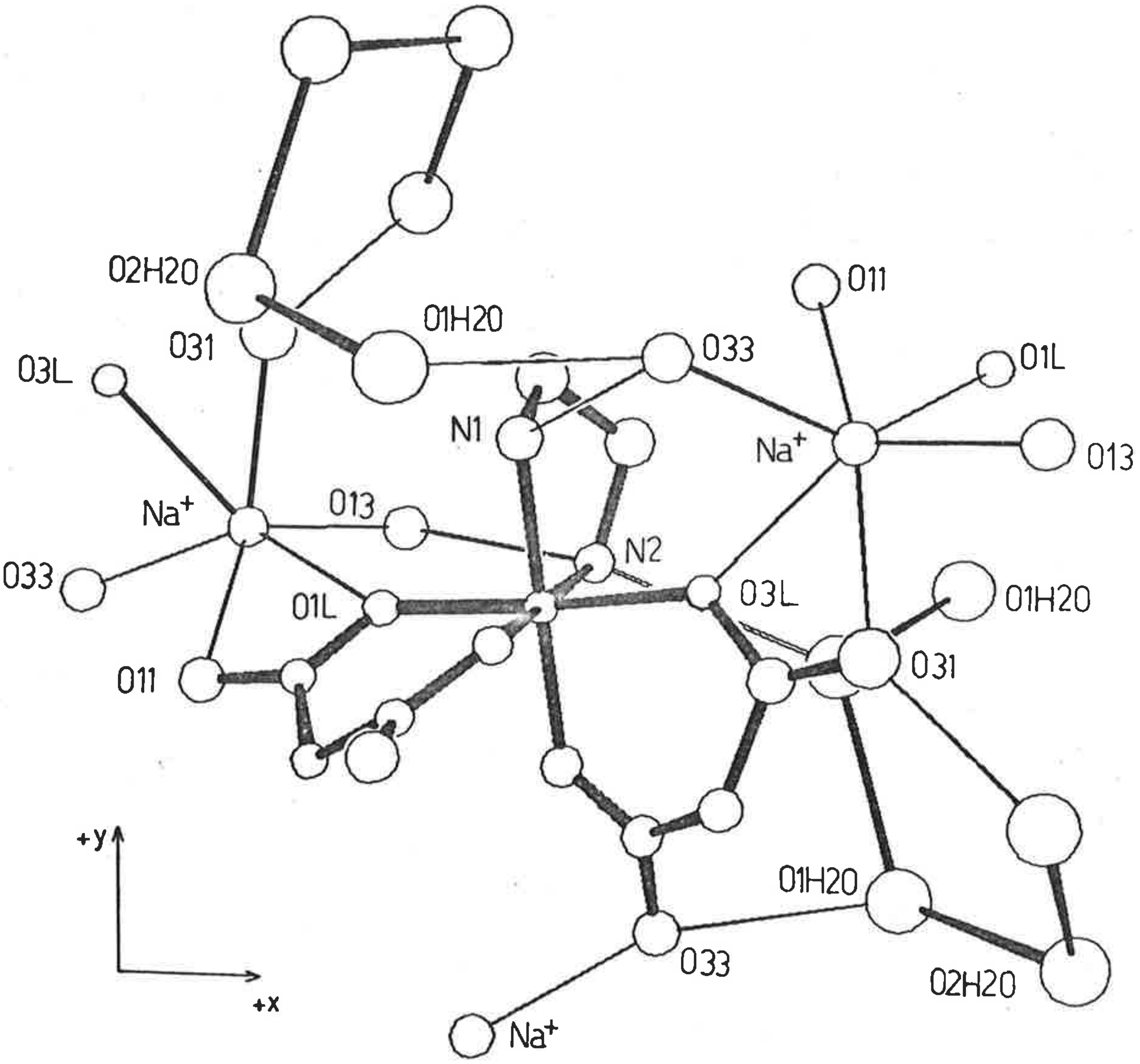
02H20
031
03L
01H20
033
011
01L
013
N1
N2
Na+
033
01L
011
03L
01H20
031
+y
+x
01H20
033
02H20
Na+

FIGURE 1.3: REPRESENTATION OF HYDROGEN BONDING AND IONIC CLOSE CONTACT SCHEME FOR Na $(+)_{546}[\text{Co mal}_2\ \text{en}].2H_2O$.

TABLE 1.2 POSITIONAL AND THERMAL PARAMETERS FOR Na $(+)_{546}$[Co mal$_2$ en].2H$_2$O^a: Δ CONFIGURATION.

Atom	*x*	*y*	*z*	*B* (Å^2)
Co	-0970 (03)	1642 (03)	0815 (05)	*anisotropic*
Na	-3538 (08)	1681 (09)	-2504 (14)	*anisotropic*
Malonate Ligand 1				
O_{1L}	-2299 (14)	1449 (13)	1017 (25)	1.41 (32)
C_{11}	-2955 (20)	1039 (18)	0968 (37)	1.32 (44)
O_{11}	-3789 (15)	0854 (15)	0270 (26)	2.18 (43)
C_{12}	-2782 (21)	0742 (20)	2922 (36)	1.25 (46)
C_{13}	-2083 (19)	1337 (18)	4003 (38)	1.34 (45)
O_{13}	-2206 (15)	1374 (14)	5667 (31)	2.35 (39)
O_{2L}	-1341 (14)	1790 (14)	3282 (24)	1.48 (34)
Malonate Ligand 2				
O_{3L}	0345 (14)	1931 (13)	1546 (23)	1.16 (33)
C_{31}	0872 (25)	1427 (20)	2674 (39)	2.14 (55)
O_{31}	1609 (19)	1760 (19)	3354 (32)	3.52 (51)
C_{32}	0496 (24)	0468 (23)	3218 (41)	1.94 (55)
C_{33}	-0093 (25)	-0073 (22)	1876 (37)	1.84 (55)
O_{33}	0049 (17)	-0941 (16)	1737 (27)	2.24 (40)
O_{4L}	-0769 (14)	0326 (13)	1001 (27)	1.85 (37)
Ethylenediamine Ligand				
N_1	-1176 (19)	2960 (18)	0386 (32)	2.14 (53)
C_1	-1005 (29)	3167 (24)	-1549 (43)	2.90 (63)
C_2	-0237 (27)	2519 (25)	-2319 (46)	2.86 (67)
N_2	-0520 (18)	1573 (19)	-1673 (29)	1.82 (41)
Water				
O_1H_2O	-2128 (21)	4104 (20)	4403 (39)	4.64 (60)
O_2H_2O	-3391 (30)	4258 (29)	1420 (54)	7.88 (105)

(contd.)

TABLE 1.2 (contd.)

Atom	x	y	z	B (Å^2)
Final calculated hydrogen atom positions - fixed[b]				
N_1H_1	-1839	3123	0701	
N_1H_2	-0726	3314	1109	
N_2H_1	-1040	1334	-2415	
N_2H_2	0039	1167	-1743	
C_1H_1	-1654	3085	-2249	
C_1H_2	-0765	3843	-1679	
C_2H_1	-0243	2541	-3706	
C_2H_2	0452	2693	-1853	
$C_{12}H_1$	-2508	0075	2907	
$C_{12}H_2$	-3453	0747	3571	
$C_{32}H_1$	1103	0069	3541	
$C_{32}H_2$	0065	0553	4346	

Anisotropic thermal parameters

	β_{11}	β_{22}	β_{33}	β_{12}	β_{13}	β_{23}
Co	140 (16)	107 (14)	410 (81)	-23 (20)	-55 (31)	0 (30)
Na	215 (65)	305 (63)	792 (21)	22 (71)	88 (84)	149 (103)

a. positional parameters (x 10^4)

anisotropic thermal parameters (x 10^5).

b. hydrogen atoms attached to N had B fixed at 3 Å^2;

those bonded to C had B fixed at 4 Å^2.

TABLE 1.3 BOND DISTANCES AND ANGLES

Atoms	*Distance* (Å)	*Atoms*	*Angle (deg.)*	*Atoms*	*Angle (deg.)*
Malonate Ligand 1					
$Co-O_{1L}$	1.902 (19)	$O_{1L}-Co-O_{2L}$	93.6 (8)	$C_{11}-C_{12}-C_{13}$	116.2 (25)
$Co-O_{2L}$	1.891 (18)	$Co-O_{1L}-C_{11}$	123.5 (17)	$Co-O_{2L}-C_{13}$	122.5 (17)
$C_{11}-O_{1L}$	1.268 (30)	$O_{1L}-C_{11}-O_{11}$	119.5 (25)	$O_{2L}-C_{13}-O_{13}$	118.9 (25)
$C_{11}-O_{11}$	1.262 (32)	$O_{1L}-C_{11}-C_{12}$	123.0 (24)	$O_{2L}-C_{13}-C_{12}$	123.3 (25)
$C_{11}-C_{12}$	1.514 (37)	$O_{11}-C_{11}-C_{12}$	117.6 (23)	$O_{13}-C_{13}-C_{12}$	117.8 (25)
$C_{13}-O_{2L}$	1.301 (32)				
$C_{13}-O_{13}$	1.235 (38)				
$C_{13}-C_{12}$	1.495 (39)				
Malonate Ligand 2					
$Co-O_{3L}$	1.895 (19)	$O_{3L}-Co-O_{4L}$	93.5 (8)	$C_{31}-C_{32}-C_{33}$	118.2 (26)
$Co-O_{4L}$	1.899 (20)	$Co-O_{3L}-C_{31}$	124.6 (19)	$Co-O_{4L}-C_{33}$	126.1 (20)
$C_{31}-O_{3L}$	1.306 (34)	$O_{3L}-C_{31}-O_{31}$	119.5 (28)	$O_{4L}-C_{33}-O_{33}$	121.1 (29)
$C_{31}-O_{31}$	1.207 (36)	$O_{3L}-C_{31}-C_{32}$	119.0 (28)	$O_{4L}-C_{33}-C_{32}$	119.7 (29)
$C_{31}-C_{32}$	1.510 (44)	$O_{31}-C_{31}-C_{32}$	121.4 (29)	$O_{33}-C_{33}-C_{32}$	119.0 (29)
$C_{33}-O_{4L}$	1.251 (36)				
$C_{33}-O_{33}$	1.256 (36)				
$C_{33}-C_{32}$	1.481 (43)				
Ethylenediamine Ligand					
$Co-N_1$	1.922 (26)	N_1-Co-N_2	86.6 (11)		
$Co-N_2$	1.928 (22)	$Co-N_1-C_1$	109.4 (20)	$Co-N_2-C_2$	109.8 (20)
N_1-C_1	1.470 (39)	$N_1-C_1-C_2$	110.5 (29)	$N_2-C_2-C_1$	105.3 (27)
N_2-C_2	1.478 (43)				
C_1-C_2	1.496 (48)				

Interligand angles at Co

Atoms	*Angle (deg.)*	*Atoms*	*Angle (deg.)*	*Atoms*	*Angle (deg.)*
$O_{1L}-Co-O_{3L}$	175.6 (9)	$O_{2L}-Co-O_{3L}$	87.2 (8)	$O_{3L}-Co-N_1$	88.2 (10)
$O_{1L}-Co-O_{4L}$	90.8 (8)	$O_{2L}-Co-O_{4L}$	94.5 (9)	$O_{3L}-Co-N_2$	89.2 (9)
$O_{1L}-Co-N_1$	87.4 (10)	$O_{2L}-Co-N_1$	90.6 (9)	$O_{4L}-Co-N_1$	174.7 (10)
$O_{1L}-Co-N_2$	89.8 (9)	$O_{2L}-Co-N_2$	175.5 (10)	$O_{4L}-Co-N_2$	88.5 (10)

TABLE 1.4 UNWEIGHTED BEST PLANES THROUGH THE LIGANDS

Planes equations $AX + BY + CZ + D = 0$

where $X = ax$, $Y = by$, $Z = cz$ (i.e. orthogonalized coordinates).

Plane	*A*	*B*	*C*	*D*	*Distance from plane* (Å)
Malonate Ligand 1					
$O_{1L}, O_{2L}, C_{11}, C_{13}$[a]	0.499	-0.861	-0.097	3.326	O_{1L}, 0.003 : O_{2L}, -0.003 : C_{11}, -0.003 : C_{13}, 0.003 : Co, 0.603 : C_{12}, 0.339
O_{1L}, O_{11}, C_{12}	0.345	-0.885	-0.313	2.899	C_{11}, -0.006
O_{2L}, O_{13}, C_{12}	-0.594	0.795	-0.126	-2.792	C_{13}, 0.014
Malonate Ligand 2					
$O_{3L}, O_{4L}, C_{31}, C_{33}$	0.576	-0.189	-0.795	1.211	O_{3L}, 0.055 : O_{4L}, -0.058 : C_{31}, -0.059 : C_{33}, 0.062 : Co, -0.459 : C_{32}, -0.409
O_{3L}, O_{31}, C_{32}	0.531	-0.390	-0.752	1.681	C_{31}, 0.035
O_{4L}, O_{33}, C_{32}	0.666	0.191	-0.721	1.131	C_{33}, 0.034
Ethylenediamine Ligand					
Co, N_1, N_2	-0.935	-0.189	-0.300	-0.600	C_1, 0.155 : C_2, -0.468

a. The C...C vector is slightly skewed with respect to O...O in both six-membered chelate rings, as shown by the signed distances from the mean four atom plane.

TABLE 1.5 INTERPLANAR DIHEDRAL ANGLES[a]

Plane 1	*Plane 2*	*Angle (deg.)*	*Plane 1*	*Plane 2*	*Angle (deg.)*
Interligand angles					
Co,O_{2L},O_{1L}	Co,O_{3L},O_{4L}	94.5 (9)			
Co,O_{2L},O_{1L}	Co,N_1,N_2	87.4 (10)			
Co,O_{3L},O_{4L}	Co,N_1,N_2	89.2 (9)			
Intraligand angles					
Malonate Ligand 1			*Malonate Ligand 2*		
Co,O_{2L},O_{1L}	O_{1L},O_{2L},C_{11},C_{13}	27.6[b,c]	Co,O_{3L},O_{4L}	O_{3L},O_{4L},C_{31},C_{33}	20.8
C_{13},C_{12},C_{11}	O_{1L},O_{2L},C_{11},C_{13}	25.2	C_{31},C_{32},C_{33}	O_{3L},O_{4L},C_{31},C_{33}	32.5
Co,O_{2L},O_{1L}	C_{13},C_{12},C_{11}	52.8 (25)	Co, O_{3L},O_{4L}	C_{31},C_{32},C_{33}	53.4 (30)
Ethylenediamine					
Co,N_1,N_2	Co,C_1,C_2	24.8 (22)			

a. atoms of triatomic planes listed in sequential order required to maintain a right-handed set.

b. values of dihedral angles involving four atom planes are given as $< 90^{o}$.

c. see Appendix IV, note 2.

TABLE 1.6 TORSION ANGLES IN THE CHELATE RINGS

Bond	*Angle (deg.)*	*Bond*	*Angle (deg.)*	*Bond*	*Angle (deg.)*
Malonate Ligand 1		*Malonate Ligand 2*		*Ethylenediamine Ligand*	
Co-O_{1L}	33.4 (21)	Co-O_{3L}	31.5 (21)	Co-N_1	6.4 (23)
O_{1L}-C_{11}	6.3 (35)	O_{3L}-C_{31}	10.5 (36)	N_1-C_1	31.2 (35)
C_{11}-C_{12}	30.7 (38)	C_{31}-C_{32}	31.7 (41)	C_1-C_2	46.2 (36)
C_{12}-C_{13}	30.2 (38)	C_{32}-C_{33}	45.3 (42)	C_2-N_2	40.0 (30)
C_{13}-O_{2L}	7.0 (36)	C_{33}-O_{4L}	14.0 (39)	Co-N_2	19.6 (21)
Co-O_{2L}	33.5 (21)	Co-O_{4L}	19.0 (23)		

TABLE 1.7 CLOSE CONTACTS WITH Na LESS THAN 2.6 Å

Atom	*Symmetry Transform*[a]	*Distance* (Å)
O_{13}	2	2.282 (24)
O_{33}	3	2.358 (25)
O_{3L}	8	2.581 (22)
O_{31}	8	2.314 (30)
O_{1L}	10	2.513 (21)
O_{11}	10	2.377 (22)

[a] see Table 1.10.

TABLE 1.8 POSSIBLE A-H...B BONDS WITH A...B LESS THAN 3.25 Å

A	*B*	*Symmetry Transform on B*	*H*	*A...B* (Å)	*B...H* (Å)	*Angle at H (deg.)*
N_2	O_{13}	2	N_2H_1	3.007 (32)	2.110	157
N_2	O_2H_2O	6	N_2H_2	3.105 (47)	2.210	149
N_1	O_{33}	9	N_1H_2	3.035 (34)	2.111	163
O_1H_2O	O_2H_2O	10		2.781 (49)		
O_1H_2O	O_2H_2O	4		2.851 (51)		
O_1H_2O	O_{33}	9		2.920 (36)		
O_2H_2O	O_{3L}	8		3.241 (44)		

TABLE 1.9 INTERMOLECULAR DISTANCES LESS THAN 3.5 Å [a]

A	*B*	*Symmetry Transform on B*	*A...B* (Å)	*A*	*B*	*Symmetry Transform on B*	*A...B* (Å)
O_{13}	O_{1L}	1	3.199 (29)	C_{12}	O_{13}	3	3.440 (35)
O_{13}	C_2	1	3.444 (42)	O_{4L}	C_{12}	3	3.351 (33)
Na	C_{13}	2	3.265 (28)	C_{12}	O_{1L}	5	3.481 (33)
Na	C_{33}	3	2.975 (34)	C_{31}	Na	6	2.812 (32)
Na	O_{4L}	3	3.202 (23)	C_{31}	O_2H_2O	6	3.312 (48)
O_{1L}	C_{12}	3	3.481 (33)	O_{31}	C_1	6	3.476 (45)
C_{11}	O_{13}	3	3.451 (33)	C_1	O_{11}	6	3.423 (43)
O_{11}	C_{13}	3	3.461 (33)	C_2	O_{11}	6	3.381 (42)
O_{11}	O_{13}	3	3.456 (29)	O_{31}	O_{13}	7	3.181 (33)
O_{11}	C_{32}	3	3.331 (38)	O_{3L}	O_{33}	9	3.324 (28)
O_{11}	C_{33}	3	3.117 (35)	O_1H_2O	C_{33}	9	3.345 (43)
O_{11}	O_{33}	3	3.102 (28)	C_{11}	Na	10	2.820 (29)

[a] not involving hydrogen atoms and in addition to the distances listed in Tables 1.7 and 1.8.

TABLE 1.10 SYMMETRY TRANSFORMS REFERENCED IN TABLES 1.7, 1.8 AND 1.9

1.	x,	y,	$1 + z$
2.	x,	y,	$-1 + z$
3.	$-\frac{1}{2} - x$,	$-y$,	$-\frac{1}{2} + z$
4.	$-\frac{1}{2} - x$,	$1 - y$,	$\frac{1}{2} + z$
5.	$-\frac{1}{2} - x$,	$-y$,	$\frac{1}{2} + z$
6.	$\frac{1}{2} + x$,	$\frac{1}{2} - y$,	$-z$
7.	$\frac{1}{2} + x$,	$\frac{1}{2} - y$,	$1 - z$
8.	$-\frac{1}{2} + x$,	$\frac{1}{2} - y$,	$-z$
9.	$-x$,	$\frac{1}{2} + y$,	$\frac{1}{2} - z$
10.	x,	y,	z

1.5 DESCRIPTION OF STRUCTURE AND DISCUSSION

The $(+)_{546}[\mathrm{Co\ mal_2\ en}]^-$ anion has the Δ absolute configuration (see discussion in Chapter 5). In the NADCOMALEN structure the complex ion exhibits approximate non-crystallographic two-fold symmetry with the six-membered malonate ligands adopting flattened boat conformations and folding toward each other. The ethylenediamine C-C bond is oblique to the pseudo-C_3 axis of the complex ion. There is extensive hydrogen bonding involving the two water molecules per asymmetric unit and the diamine nitrogens; Na^+ makes six close contacts with the malonate carboxyl and carbonyl oxygens but none with the water molecules. The conformational features of the Δ complex ion and the atom labelling are shown in Figures 1.1 and 1.2; Figure 1.3 is an *ab* projection of the immediate environment of the anion with a small angular tilt around the horizontal (*a*) axis to better show the oxygen environment of Na^+. The water molecules form a right-handed hydrogen bonded spiral of density around the 2_1 screw axes parallel to *c*; the hydrogen atoms of the water molecules were not located in the final difference map.

The various types of intermolecular and interion close contacts are listed in Tables 1.7, 1.8 and 1.9; not all are significant; the Na^+ ionic radius is 0.97 Å,[80] van der Waals radius of oxygen, 1.40 Å,[81] and acceptable hydrogen bond ranges are given[74] as N...O, 2.73-3.22 Å, and O...O, 2.49-3.15 Å. When comparing close contacts in the solid state with appropriate van der Waals radii sums it should be remembered that weak attractive forces between "non-nearest" neighbour atoms tend to contract the lattice; [82,83] limiting contacts 0.3-0.4 Å less than the van der Waals radii sum are not uncommon.[84] All close contacts in Table 1.9 are satisfactory.

Tables 1.3-1.6 detail the geometry of the anion. Failure to refine the non-metal atoms anisotropically has resulted in large estimated standard deviations (esd's) in their positional coordinates and the derived bond lengths and angles. The chemically equivalent Co-O, Co-N, N-C and C-C (malonate) bond lengths agree to better than one esd of an individual bond length. The mean Co-O bond length of 1.897 (8) Å is within 3σ (see Appendix IV, note 3) of that reported for $Co(acac)_3$, namely 1.898 (6) Å [85] and 1.872 (8) Å.[86] The less accurately determined[87] $Co(ox)_3^{3-}$ has two independent Co-O bonds of length 1.90 (3) Å and 1.95 (3) Å. The mean Co-N length (1.925 (17) Å) is close to that found[88] in $[Co(NH_3)_6]I_3$ but more than 2σ shorter than the average Co^{III}-N bond length in any of the tris (five-membered diamine ring) complexes listed in Table 8.1. The analogous bond lengths reported[89] for this anion in the $(-)_{589}[Co\ en_2(NO_2)_2](+)_{589}[Co\ mal_2\ en]$ structure[90] were Co-O 1.90 (2) Å, Co-N 1.94 (2) Å; that structure refinement was based on visually estimated data and was limited to isotropic refinement of all thermal parameters. The esd's from the present refinement (NADCOMALEN) and Matsumoto and Kuroya's structure[89] are similar and the limiting factor would seem to be failure to perform full-anisotropic least-squares cycles rather than the quality of the visually estimated data as opposed to the microdensitometer intensities.[91]

The C-C bonds in all three ligands show the expected[74] shortening from the 1.54 Å paraffinic value; the mean C-N bond length, 1.474 (29) Å, is that listed[74,92] for a paraffin four-covalent nitrogen bond length. The mean carboxyl, 1.282 (17) Å, and carbonyl, 1.240 (18) Å, bond lengths agree to within 3σ of the two mean values; all four exocyclic oxygen atoms are involved in close contacts with Na^+ and/or possible hydrogen bonds (Tables 1.7 and 1.8, Figure 1.3). As only three structures of complexes containing chelated malonate ions have been reported[89,93] protracted discussion of the bond and torsion angles is not informative especially in view of their large esd's; in general the chemically equivalent bond angles agree within one standard deviation. The average C-C-C angle (117°) is closer to an ideal sp^2 value (120°) than sp^3 (109.5°) but is not as strained as that quoted in ref. 89, namely 125°.

Apart from the determination of the absolute configuration of the anion, the conformations of the two six-membered malonate rings are of special interest. There are several ways of describing the observed conformations, of which the torsion angle description (Table 1.6) is the most rigorous but at the same time the least conceptually satisfying. A more descriptive analysis is possible in terms of the two carboxyl oxygens and carbons of each malonate ligand, i.e. O_{1L}, O_{2L}, C_{11}, C_{13} and O_{3L}, O_{4L}, C_{31}, C_{33}; these four atom groups are closely planar whereas the Co and methylene carbon atom are significantly displaced to the same side of each plane (Table 1.4), giving two boat conformations. An equally satisfying description of these boat conformers is that given in Table 1.5 where the displacement of the Co and methylene carbon from the respective ligand plane is expressed as an interplanar dihedral angle, it being understood that the Co and carbon atoms (C_{12}, C_{32}) lie on the same side of the relevant four atom plane.

Dreiding models give no clear indication of a preferred conformation for a chelated malonate ring, especially when the steric role of the carboxyl oxygen lone pairs is uncertain. This doubt concerning the lone-pairs precluded an energy minimization analysis analogous to those performed[94,95] for the five- and six-membered diamine ring systems. NMR studies[31,32] of $[\mathrm{Co\ mal_2\ en}]^-$ and $[\mathrm{Co\ mal\ en_2}]^+$ were equally ambiguous. In view of the interionic contacts and hydrogen bonding in the NADCOMALEN structure it seemed probable that the conformation observed reflected crystal packing forces as much as any minimum energy conformation of the isolated ion. This hypothesis was supported by our subsequent determination of the CRMALTCOPN structure (Chapter 2) in which the malonate rings are significantly distorted from the boat conformation and also by the recent publication[89,90] of the structure of triclinic $(-)_{589}[\mathrm{Co\ en_2(NO_2)_2}](+)_{589}[\mathrm{Co\ mal_2\ en}]$.

The anion in this latter structure also exhibits approximate non-crystallographic two-fold symmetry with the en ligand again adopting an oblique conformation relative to the pseudo-C_3 axis; the malonate rings, however, are more flattened than those found in the present study. In neither structure analysis were weighted least-squares planes calculated and the esd's in the deviations of the atoms from the mean planes are not available. Matsumoto and Kuroya have described[89] the malonate rings in their structure as "approximately planar"; given that the deviations from planarity are small (and probably lack significance) both malonate rings in the [Co $en_2(NO_2)_2$][Co mal_2 en] structure are more accurately described as distorted skew conformations. It is not possible to decide the orientation of the ring backbones relative to the pseudo C_3-axis (i.e. whether *lel* or *ob*[96]) from the distortions as listed; calculations from the positional coordinates are required. Intermolecular hydrogen bonding is again seen[89] to be important in determining the precise conformation of the Co-malonate chelate rings. Further discussion of malonate ring conformation is made in Chapter 2.

A final point of interest is the oblique conformation[1] observed for the ethylenediamine ligand in the [Co mal_2 en]$^-$ ion in both structures; this particular ring conformation has now been observed in structures of several transition metal complexes and the precise geometry seems to depend on the hydrogen bonding[92,97] and van der Waals interactions. In NADCOMALEN the carbon atoms of the en ligand are dissymmetrically placed either side of the CoN_1N_2 plane; similar ring asymmetry has been found in the structure of [Cu en_2]$(SCN)_2$.[98]

CHAPTER 2 THE STRUCTURE OF $(-)_{589}$-TRIS($(-)_{589}$1,2-DIAMINOPROPANE)-COBALT(III)$(+)_{589}$-TRIS(MALONATO)CHROMATE(III) TRIHYDRATE.

$(-)_{589}[Co(-)pn_3](+)_{589}[Cr\ mal_3].3H_2O$, CRMALTCOPN.

2.1 STRUCTURE ABSTRACT

The absolute configuration of the $(+)_{589}$-tris(malonato)chromate anion, $(+)_{589}[Cr(CH_2(CO_2)_2)_3]^{3-}$, has been determined as Λ by a single crystal structure analysis of the salt formed with Δ$(-)_{589}$-tris-((−)propylenediamine)cobalt, $(-)_{589}[Co(-)(C_3H_{10}N_2)_3]^{3+}$ as cation. The structure $(-)[Co(-)pn_3](+)[Cr\ mal_3].3H_2O$ has been refined by full-matrix least-squares to a conventional *R* factor of 0.073 using 435 integrated photographic data. The lattice is rhombohedral, space group R_{32} (No. 155), hexagonal parameters *a* = 16.12 (2), *c* = 10.07 (2) Å, *U* = 2265 (7) Å^3, *Z* = 3, D_c = 1.53, D_m = 1.52 (2) g. cm^{-3}. Both complex ions are disordered on 32-symmetry sites in the hexagonal unit cell and are linked to each other and to the water molecules by hydrogen bonds. The cation adopts the expected Δ(λλλ) conformation with the exocyclic methyl groups equatorial; the metal-malonate ring skeleton in the anion is planar except for the methylene carbon. The absolute configuration of the anion is opposite an earlier assignment based on circular dichroism data.

2.2 EXPERIMENTAL

Partial resolution of $K_3[Cr\ mal_3]$ as the strychnine salt has been reported previously.[99] Attempted resolution of the complex by this method was unsuccessful: crystallization of the racemic potassium salt proved difficult because of its extreme solubility and apparent sensitivity to slight changes in pH. The dichroic blue-green microcrystalline powder obtained by reduction of potassium dichromate[99,100] was similar (IR-visible spectrum, analysis, X-ray powder photos) to the product derived from a preparation after the method of Lapraik[101,102] starting with freshly prepared $Cr(OH)_3$.

Analysis	$K_3[Cr(C_3H_2O_4)_3].3H_2O$			
calc.	Cr, 9.82:	K, 22.16:	C, 20.41:	H, 2.28.
found	9.40:	22.49:	20.81:	2.06.

(C,H, by microanalysis: permanganate determination[103-105] of malonate was not reproducible. Cr, spectrophotometrically as chromate at 370 nm on oxidation with hydrogen peroxide over three days.[102] K, gravimetric analysis as $K_2Na[Co(NO_2)_6].H_2O$ dried at 110°C to constant weight.[104])

Elution of independently prepared K_3- and $Na_3[Cr\ mal_3]$ samples from AG1-X4 anion exchange resin in the chloride form showed three to five bands for all preparations. No attempt was made to determine the nature of the species in the minor bands (probably bis- and mono-malonates[106]) since the major component always eluted last with aqueous chloride solution suggesting a predominance of the trivalent tris-chelate. An infra-red spectrum of a potassium bromide disc of one preparation was almost identical with the published spectrum[107] and as all preparations were subsequently shown to give identical crystalline precipitates with $(-)[Co(-)pn_3]^{3+}$ further characterization was not considered necessary.

Attempted resolution of $[Cr\ mal_3]^{3-}$ with $(+)[Co\ en_3]^{3+}$, $(+)[Ni\ phen_3]^{2+}$ and strychnine gave no precipitation from moderately concentrated solutions. $(-)[Co(-)pn_3]^{3+}$, however, initiated instantaneous growth of fine needles from dilute solutions;[†1] these crystals had appreciable solubility only at pH levels well removed from neutrality and since such conditions could be expected to induce racemization, if not complete rupture of one or both complex ions, larger crystals clearly could not be prepared by recrystallization. Crystals suitable for intensity data collection were prepared by layering a solution of *trans*-$(-)[Co(-)pn_3]Br_3$ on a more dense solution of $K_3[Cr\ mal_3].3H_2O$, well-formed crystals growing over several hours. *trans*-$Co(pn)_3^{3+}$ precipitated crystals of larger cross-section than did the *cis*-cation but subsequent determination of the space group and lattice constants of both types of crystal showed them to be identical. The bronze prisms were equilateral-triangular in section and showed extinction parallel to the needle axis; the triangular section was isotropic, the crystal morphology suggesting a trigonal system. Precipitation studies (see Chapter 5) showed that $(-)[Co(-)pn_3]^{3+}$ co-crystallizes with the $(+)_{589}[Cr\ mal_3]^{3-}$ enantiomer.

[†1] P.F. Crossing[95] had been attempting to verify a claimed[108] separation of the *cis*- and *trans*- geometric isomers of $(-)[Co(-)pn_3]^{3+}$: samples supplied by Dr. T.E. MacDermott. All anions tested had given precipitates of the two samples which were indistinguishable[109,110] by X-ray powder diffraction. It was decided to try $[Cr\ mal_3]^{3-}$ and the ensuing crystallization was so rapid that it was difficult to prepare sufficiently large crystals for space group determinations.

Preliminary Weissenberg and precession photographs of several crystals confirmed the trigonal system: indexing on hexagonal axes established the condition limiting observed reflections as $-h + k + l = 3n$. Coupled with the requirement for optical activity this condition restricts the possible space groups to R_3 and R_{32}. *CuKα/Nif* photographs confirmed 32-point symmetry and hence space group R_{32}; with $Z = 3$ the Co and Cr atoms lie on 32-symmetry sites and the cation must be disordered since its maximum symmetry is C_1 for *trans* and C_3 for *cis*. Subsequent structure refinement showed that the anion is similarly disordered although 32-symmetric skew conformations of $[\mathrm{Cr\ mal_3}]^{3-}$ are possible.

Crystal data - as in structure abstract.

$[\mathrm{Co(C_3H_{10}N_2)_3}][\mathrm{Cr(C_3H_2O_4)_3}].3\mathrm{H_2O}$; $M = 693.6$;
$\mu_{MoK\alpha} = 10.3\ \mathrm{cm^{-1}}$.

Lattice constants from *MoKα/Zrf* ($\lambda = 0.7107$ Å) precession films.

D_m by flotation in carbon tetrachloride/chloroform at 24°C.

Microanalysis on crystals

	C	N	H
calc.	C, 31.17:	N, 12.12:	H, 6.11.
found	30.26:	11.52:	5.71.

(Qualitative microanalysis on crushed crystals of the diastereoisomer was negative for K^+ and Br^-.)

The *trans* $(-)[\mathrm{Co}(-)\mathrm{pn_3}](+)[\mathrm{Cr\ mal_3}].3\mathrm{H_2O}$ crystal used to generate the intensity data set was a needle 0.40 mm. long and triangular in section; triangle edges 0.15 mm.. It was mounted along the needle axis. Preliminary oscillation photographs showed the intensity of the $l = 2n + 1$ layers to be much less than that of the even layers, a destructive interference effect consequent on the Co and Cr atoms being separated by $c/2$ in the real unit cell. Using $MoK\alpha/Zrf$ radiation integrated triple film packs of Weissenberg equi-inclination layers *hk0*-*hk8*, *hk10* were recorded, exposure times ranging 1-5 days for $l = 2n$ and 4-8 days for the $l = 2n + 1$ layers. The structure of the film pack was identical to that described in Chapter 1. Reciprocal layers *h0l*-*h3l* were recorded as integrated precession photographs for the same crystal without remounting. Triple exposures ranging 12-72 hours were recorded for the four levels. The integrated data were measured photometrically with a Nonius II microdensitometer.

2.3 STRUCTURE SOLUTION AND REFINEMENT

The scaling of the photographic intensity data is described in Appendix II. Lack of meshing precession data necessitated introduction of the *hk7* Weissenberg reflections at a subsequent stage and initial structure solution was made excluding this set of 25 unique reflections (initial data set: 426 unique reflections of which 35 were unobserved). Anomalies in the distribution of $Av.\ w\Delta^2$ vs. $|F_o|$ in the final stages of refinement again indicated a relative overweighting of the most intense data in the original AUFAC inter-film scaling procedure, resulting in chemically unreasonable bond lengths and angles. The initial weighting scheme was modified in the final stages of refinement when the *hkl* Weissenberg data were introduced to the reflection list.

For (-)[Co(-)pn_3](+)[Cr mal_3].$3H_2O$ in space group R_{32} (Z = 3) the metal atoms occupy the 32-symmetry positions at *(0,0,0)* and *(0,0,½)*. An initial Fourier map phased on Co and Cr atoms at these two sites showed the expected $\bar{3}$m Laue symmetry. This map, using only the $l = 2n$ data, had an additional inversion centre at *(0,0,1/4)* due to an effective halving of the *c* lattice repeat. The $l = 2n + 1$ data were excluded from the initial Fouriers because of the relatively small contribution of the metal atoms to these odd order reflections. This was, however, an unfortunate approach since the Co and Cr sites then become identical and only one unique donor atom position (2 Å from the metal and lying on a mirror plane of $\bar{3}$m) was found; the implication of this in terms of the relative orientation of the CoN_6 and CrO_6-cores was initially unclear. Smaller peaks at distances further removed from the metal atoms were also observed.

This large donor atom peak (at 0.062, 0.124, 0.100) corresponded to an orientation of the ML_6-cores which maintained the C_3 and pseudo-C_2 axes of the complex ions parallel to the crystallographic axes but although a Fourier map based on this model (CrO_6, CoN_6 only) gave several possible new atom sites, the malonate and propylenediamine ligands remained convoluted about both metal positions, making interpretation difficult (R_1 = 0.292). Introduction of the (-)[Co(-)pn_3]$^{3+}$ complex with the correct $\Delta(\lambda\lambda\lambda)$ configuration at one site gave $R_1 = 0.234$ ($R_{l = 2n} = 0.147$, $R_{l = 2n + 1} = 0.508$) but inclusion of possible water and malonate ligand atoms at this stage gave no significant improvement. Two cycles of least-squares refinement of the light atom positions and isotropic temperature factors of all atoms in this preliminary model lowered R_1 to 0.209.

Inclusion of the even and odd data in a Fourier calculation based on this most recent model gave a 32-symmetric map lacking a false 32-position at *0,0,1/4*. This map revealed the position of the one unique water molecule and suggested a Λ configuration for (+)[Cr mal$_3$]$^{3-}$ with the malonate ligand spanning the $+x$ axis: for the Δ(−)[Co(−)pn$_3$]$^{3+}$ ion the pn ligand spanned the $-x$ axis. The choice of the Λ or Δ absolute configuration for the anion corresponds not merely to a choice of absolute configuration but to a choice between two different structures, namely ΔCoΔCr and ΔCoΛCr. Even knowing the relative absolute configurations of the two complex ions, however, there remained the problem of fixing the malonate ligand conformation since the anion appeared to be disordered on the 32-symmetry site rather than adopting a 32-symmetric tris-skew conformation. The carboxyl carbon and oxygen atoms were approximately coplanar with Cr and corresponded to 32-symmetry but the methylene carbon atom lay just off the two-fold axis and the carbonyl oxygen peak was broad and of indeterminate weight. Introduction of all atoms to the model (including the carbonyl oxygen O_2C_1 with unit multiplier) resulted in the following R factors after two cycles of least-squares refinement of the positional parameters of the light atoms and the isotropic temperature factors of the metals –

$R_1 = 0.145$ ($R_{l = 2n} = 0.125$, $R_{l = 2n + 1} = 0.209$) for 426 data of which 377 were included in the least-squares cycles, unit weights. Changing to the weighting scheme refined in the data scaling routine gave, after two further cycles of full-least-squares positional and isotropic refinement ($n = 33$ variable parameters), $R_1 = 0.092$ ($l = 2n$, 0.087; $2n + 1$, 0.152). At this stage gross outliers in the data set were checked for incorrect measurement.

Fourier and difference maps computed for this model revealed appreciable anisotropy in the metal vibrations and also showed the carbonyl oxygen as included to be an average of two positions of approximately equal weight; this latter is as expected for a puckered non two-fold symmetric malonate ring. The Co^{2+} and Cr^{2+} scattering curves were modified to allow for anomalous dispersion (see Appendix IV, note 1) and all atoms refined anisotropically, except OH_2OCo which was restricted to a position on the two-fold axis through the Co atom and refined isotropically with its multiplier fixed at ½. The agreement factors at convergence were $R_1 = 0.072$, $R_2 = 0.063$, $R_{l = 2n} = 0.069$, $R_{l = 2n + 1} = 0.106$, $G = 1.98$ for 426 data of which 377 were included in the least-squares refinement cycles. $R_{l = 2n + 1}$ is most sensitive to the refinement of the light atoms since the metal contribution to the odd data corresponds to a maximum of only three electrons. The methylene carbon atom (C_2) and the split carbonyl oxygen (O_2C_1, O_2C_1A) were non-positive definite. The correlation matrix showed several large correlation factors (ca. 0.5-0.8) between positional parameters which could be related by $\bar{3}$m operations (see also ref. 45). Derived bond lengths and angles showed some disturbing deviations from the expected values, e.g. the C-C bond of the pn ligand was 1.62 Å (see discussion and Table 2.9).

Inclusion of the 25 *hk7* data at this point increased R_2 to 0.112 and worsened the distribution of *Av.* $w\Delta^2$ vs. $|F_o|$. As with the NADCOMALEN structure (Chapter 1) the fault seemed to lie in the initial weighting schemes chosen in the data scaling routine, but rather than apply a modified weighting scheme in the least-squares cycles it was decided to adopt a more realistic curve in the inter-film scaling sequence, at the same time introducing the *hk7* data. The unscaled Weissenberg and precession data were weighted independently applying average schemes derived from the earlier data reduction sequence. The parameters for the new schemes were (with those used initially in parentheses) - Weissenberg; a = 0.0484 (0.0113), b = -0.0037 (0.0066), c = 0.3024 (0.0928), d = 0.0109 (0.0078) - Precession; a = 0.0420 (0.0749), b = -0.0017 (-0.0040), c = 0 (0.0073), d = 0 (0.0086). These weighting scheme changes resulted in a relative "down-weighting" of the more intense Weissenberg data: the final data set comprised 451 unique reflections of which 38 were unobserved (*U*) and 16 unreliable (*E*).

The hydrogen atoms bonded to the N and C atoms of the pn ligand were included at calculated positions (program PLANEH) with fixed positional and isotropic thermal parameters; no attempt was made to introduce the methyl group hydrogens or the disordered hydrogen atoms attached to the methylene carbon of the malonate ligand. The 38 unobserved reflections were included in the least-squares data set and after three cycles of anisotropic refinement (OH$_2$OCo isotropic) employing the modified weighting scheme all variable parameter shifts were less than 1/3 of the relevant esd (except for the anisotropic thermal parameters of O$_2$C$_1$A which remained non-positive definite). The agreement factors at convergence were - R_1 = 0.073, R_2 = 0.083, $R_{l = 2n}$ = 0.064, $R_{l = 2n + 1}$ = 0.121, G = 2.01 for 451 data of which 435 were included in the least-squares cycles, 80 variable parameters; the distribution of $Av.\ w\Delta^2$ vs. $|F_o|$ was flat. The bond lengths and angles were more chemically reasonable and apart from atom O$_2$C$_1$A the thermal parameters seemed realistic (the problem with O$_2$C$_1$A is thought to arise because of its high correlation with O$_2$C$_1$ to which it is related by an approximate non-crystallographic mirror plane coincident with the Cr, O$_1$, C$_1$O$_1$, atoms[45]). High coefficients in the correlation matrix are considered to reflect non-orthogonality of the crystal a and b axes.[45,111]

A final difference Fourier revealed peaks of ca. $\frac{1}{2}$-electron in height on the z axis adjacent to the metal atom sites and also showed some anisotropy of OH$_2$OCo parallel to z. The light atoms all occupied saddle points between peaks 0.05 e$^-$ in height.

Observed and calculated structure factor amplitudes from the final least-squares cycle are listed in Table 2.1 with F_o, F_c both × 10.

TABLE 2.1 FINAL $|F_o|$ AND $|F_c|$ FOR (-)[Co(-)pn_3](+)[Cr mal_3].$3H_2O$: ΔΛ CONFIGURATION.

```
   H   K  FOBS  FCAL     H   K  FOBS  FCAL     H   K  FOBS  FCAL     H   K  FOBS  FCAL     H   K  FOBS  FCAL     H   K  FOBS  FCAL     H   K  FOBS  FCAL     H   K  FOBS  FCAL
   **L =    0****       12   5    97    81     4   8   250   233     4  10    68    68     0  11   196   210    14   2   110   124    10   3    64    50     8   9    88    61
   3   0   273   231     1   6   155   143     7   8   162   163     2  11   119   118     3  11   183   179     0   3   209   199    13   3    73    50     0  10   145   123
   6   0   173   186     4   6   107   114    10   8    84    81     5  11    53    29     6  11   143   142     3   3   280   277     2   4    45    29     3  10   153   148
   9   0   109    86  U  7   6    31    43     2   9   157   157     0  12   151   134     9  11   107    90     6   3   201   220     5   4    61    57     1  11   117    93
  12   0   199   192     2   7   126   129     5   9   174   173     **L =    4****        1  12   191   184     9   3    81    73     0   5    70    61     2  12    96    77
  15   0   143   122     5   7    99   101     8   9   182   151     1   0   219   202     4  12   205   203    12   3   144   137  U  3   5    23    30     0  13    89    67
  18   0   164   160  U  8   7    34    34     0  10   174   194     4   0   477   472     7  12   132   117     1   4   143   136     6   5    84    72     1  14   108    97
E  1   1   624   984    11   7    62    54     3  10   116   105     7   0   381   384     2  13   155   157     4   4   242   261     1   6   120   102  U  2  15    54    69
   4   1   465   436     0   8    84    88     6  10   203   184    10   0   245   272     5  13   143   124     7   4   113   112     4   6    61    54     0  16   116    93
   7   1   237   246     3   8   100    89  U  9  10    57    99    13   0   242   246     0  14   152   130    10   4   159   157     2   7    96    88     3  16   107    82
  10   1   141   149  U  1   9    29    18  U  1  11    45    35     2   1   388   391     3  14    92    91    13   4   139   136     0   8   108   111     1  17   105    69
U 13   1    70    80     4   9    57    52     4  11   188   181     5   1   315   329     **L =    5****        2   5    98    98     1   9    79    75     **L =   10****   
  16   1   194   164     2  10    89    37     7  11   145   151     8   1   272   289     2   0    35    32     5   5   149   148     2  10    52    45     1   0   267   264
   2   2   157   131     0  11    81    97  U 10  11    61    75    11   1   261   256     3   1    57    56     8   5   132   125  E  0  11    68    48     4   0    56    55
   5   2   137   149     3  11    68    45     2  12    80    80    14   1   108   108  E  6   1    69    59    11   5   148   145     **L =    8****     U  7   0    22    32
   8   2   247   241     1  12   121   124     5  12   213   199     0   2   101    71     1   2   200   200    14   5    94    83     2   0   319   326    10   0    81    72
  11   2   156   154     **L =    2****        8  12   137   116     3   2   356   358  U  4   2    17    25  U  0   6    26    43     5   0   209   214    13   0   101   103
  14   2   128   127     2   0   136   134  U  0  13    48    50     6   2   276   281     7   2    68    59     3   6   196   184     8   0   206   193     2   1   105   130
   3   3   272   209     5   0   128   138     3  13   186   171     9   2   214   222    10   2    46    42     6   6    59    52  U 11   0    42    18     5   1    34    38
   6   3   357   355     8   0   176   181     6  13   134   138    12   2   183   181     2   3   131   121     9   6   174   170     0   1   347   343     8   1    72    62
   9   3   301   305    11   0   319   332     1  14   137   133     1   3   492   495     5   3    99    93    12   6   118   114     3   1   283   273    11   1   104   107
U 12   3    71    81    14   0   162   142     4  14   144   142     4   3   312   325  E  8   3    65    67     1   7   183   169     6   1   165   147    14   1    74    72
  15   3   145   114  E 17   0   147   127     2  15   100   126     7   3   149   157    11   3    50    66     4   7   131   125     9   1   119   107     0   2   181   173
E  4   4   372   351     0   1   745   742     0  16   121   119    10   3   159   154  E  0   4    76    67     7   7   120   114  U 12   1    46    11     3   2    81    76
   7   4   449   471     3   1    68    75     3  16   106   107    13   3   132   127     3   4   143   138    10   7   128   129    15   1    96   107     6   2    78    92
  10   4   159   163     6   1   130   123     **L =    3****        2   4   511   511     6   4    58    54    13   7    87    83     1   2   225   221     9   2    99   107
  13   4   135   111     9   1   233   257     0   0   510   488     5   4   215   225     9   4    96    88     2   8   220   219     4   2   158   137    12   2    68    66
E  5   5   481   462    12   1   276   338     3   0    98    59     8   4   130   118     1   5   138   137     5   8   109   101     7   2   151   132     1   3   129   149
   8   5   363   358    15   1    99    84     6   0    93    58    11   4   157   156     4   5    49    45     8   8   139   147    10   2    95    76     4   3    99   117
  11   5   131    96     1   2   635   585     9   0   107    97    14   4    98    72  U  2   6    19    10    11   8   112   101    13   2    88    80     7   3   105   110
E  6   6   464   487     4   2   183   189  U 12   0    26    27     0   5   682   704     5   6   142   129     0   9   174   184    16   2    90    75    10   3    92    91
   9   6   155   131     7   2   115   138     1   1   243   239     3   5   316   327     8   6    62    50     3   9   190   192     2   3   107    82     2   4   136   135
E  7   7   263   246    10   2   269   297     4   1   194   192  U  6   5    37    23     0   7    52    46     6   9   111   121     5   3   193   178     5   4   109   119
E  8   8   177   136    13   2   119   102     7   1    51    67     9   5   109   109     3   7    81    67     9   9    94    93     8   3   176   160     8   4   134   153
U  9   9    78    70    16   2    99    85    10   1    55    41    12   5   158   142     6   7    60    54    12   9    91    77    11   3    84    89     0   5   173   198
   **L =    1****        2   3   274   307     2   2   108   115    15   5    95    69     9   7    53    35     1  10   221   228    14   3   104    89     3   5   129   130
   4   0   366   336     5   3   263   240     5   2   137   136     1   6   332   350     1   8    61    68     4  10   132   137     0   4    91    84     6   5   114   122
   7   0   227   204     8   3   307   313     8   2    51    29     4   6   128   129     4   8   111   110     7  10    85    70     3   4   210   209     9   5    80    83
U 10   0    29     8    11   3   149   175  E  0   3    34    43  U  7   6    41    29     2   9    70    69    10  10    82    72     6   4   178   161     1   6   135   136
   2   1   315   300  U 14   3    55    55     3   3    87    58    10   6   128   132  U  5   9    26    35     2  11   205   196     9   4   171   149     4   6   126   126
   5   1   284   259     0   4   935   947  U  6   3    21    13  U 13   6    53    87     3  10    56    43     5  11    77    79    12   4   102    84     7   6   108   111
   8   1    89    68     3   4   422   412     9   3    47    28     2   7   255   253     6  10    60    48     0  12   271   258  U  1   5    29    31     2   7   124   117
  11   1    91    99     6   4   254   272     1   4    57    39  U  5   7    39    24  E  1  11    64    54     3  12   109   111     4   5   236   228     5   7   107   116
   0   2   276   222     9   4   243   252     4   4   163   165     8   7   167   164     **L =    6****        1  13   149   148     7   5   204   182     0   8   111   113
   3   2   176   166    12   4    98    84     7   4    49    37    11   7   116   116     3   0   400   421     2  14    86    86    10   5   119   102     3   8   101   104
   6   2    86    62     1   5   772   817     2   5   100    76     0   8   369   379     6   0   336   328     0  15    97   103     2   6   148   123     6   8    89    88
   9   2    61    24     4   5   342   367     5   5    54    42     3   8   119   111     9   0   296   313     **L =    7****        5   6   221   206     1   9    74    76
   1   3   490   452     7   5   300   316     8   5    62    88     6   8   143   139  U 12   0    38    31     2   1    89    95     8   6   141   128     4   9    99   103
   4   3   127    96  U 10   5    49    72     3   6   118   101     9   8   157   152    15   0    82    88     5   1    90    87  U  0   7    33    21     7   9    57    62
   7   3   155   126     2   6   393   405     6   6    53    48    12   8   115    92     1   1   167   158  U 11   1    30    21     3   7   186   161  U  2  10    29    46
  10   3    70    81     5   6   290   288     1   7   152   140     1   9   310   312     4   1   472   494    14   1    61    64     6   7   174   154     5  10    84    80
   2   4   149   122  E  8   6   137   145     4   7    69    85     4   9   111    94     7   1   324   341     0   2    66    68     9   7   111    96     8  10    79    70
E  5   4    62    33  U 11   6    53    46  U  7   7    26    31     7   9   160   172    10   1    89    96  U  3   2    18    20     1   8   117   104  U  0  11    29    20
   8   4    70    56     0   7   682   690     2   8    71    49    10   9   110    98    13   1    89    77     6   2   100   102     4   8   217   195     3  11    70    74
   0   5   303   287     3   7   191   209     5   8    87    85     2  10   105    93     2   2   363   367     1   3   124   129     7   8   105    94     3  14    71    68
   3   5   121    99     6   7   192   191     0   9    82    82     5  10   183   179     5   2   295   300     4   3   111   109     2   9   180   166     1  15    75    83
   6   5    73    56     9   7   117   102  E  3   9    61    72     8  10   137   126     8   2   177   160     7   3    72    65     5   9   125   114     0  16    32    87
   9   5    97    97     1   8   319   309     1  10    57    33  U 11  10    56    58    11   2    65    76
```

2.4 STRUCTURE FIGURES AND TABLES

The figures and tables of structural parameters for the CRMALTCOPN structure are collected together here preliminary to the discussion of section 2.5. The structural parameters as given in the following tables correspond to the atom labelling and orientation of figures 2.1 and 2.2, where a ' superscript denotes a two-fold related atom.

2.5 DESCRIPTION OF STRUCTURE AND DISCUSSION

$(+)[\mathrm{Cr\ mal}_3]^{3-}$ has a Λ absolute configuration by comparison with the known Δ(λλλ) configuration of $(-)[\mathrm{Co}(-)\mathrm{pn}_3]^{3+}$; this assignment is contrary to an earlier assignment[27,28] based on the aqueous solution CD spectrum. Both complex ions are C_3 symmetric but are disordered[†2] on 32-symmetry sites of the R_{32} space group with the water molecules occupying two-fold sites between the pn ligands of the cation, directly under (and above) each malonate ring.

The Co and Cr atoms are 5 Å apart along *c* with the pn and mal ligands spanning the −*a* and +*a* crystallographic directions respectively. The carboxyl oxygen (O_1) of the malonate ligand is strongly hydrogen bonded to N_1 through N_1H_2 while the water oxygen makes close contacts with N_1 through N_1H_1 and with the carbonyl oxygens of anions on adjacent three-fold axes (Table 2.7, Figures 2.2 and 2.3). If a freely rotating methyl group is taken[80] as having an effective non-bonded radius of

---

[†2] This disorder renders the *cis*- and *trans*-cations indistinguishable and single crystal *CuKα/Nif* equi-inclination and precession photographs of several $(-)[\mathrm{Co}(-)\mathrm{pn}_3](+)[\mathrm{Cr\ mal}_3].3\mathrm{H}_2\mathrm{O}$ crystals grown from the supposedly *cis*- and *trans*-$(-)[\mathrm{Co}(-)\mathrm{pn}_3]\mathrm{Br}_3$ samples confirmed the R_{32} space group in all cases (this preliminary study in conjunction with P.F. Crossing).

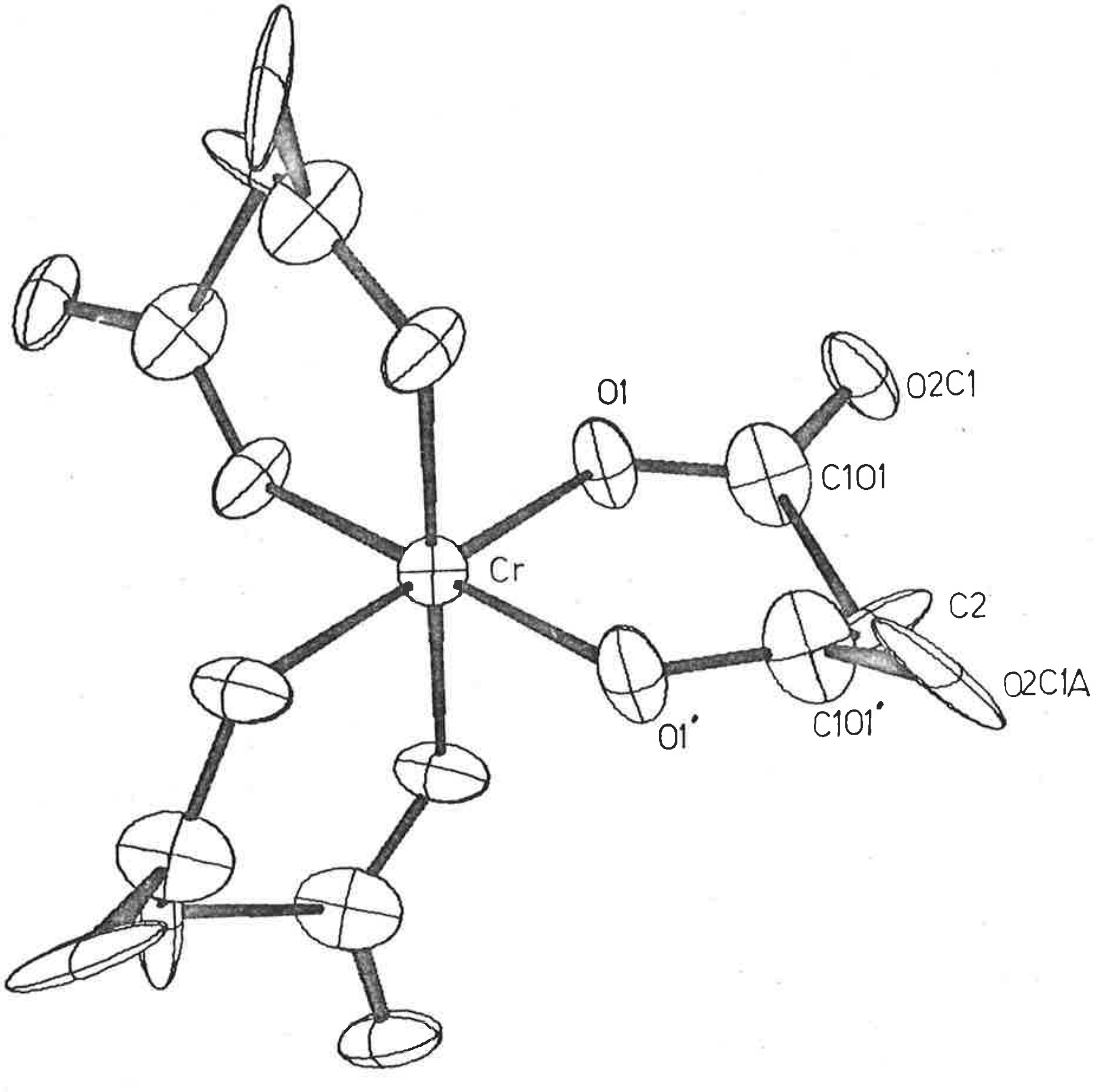
O2C1
O1
C1O1
Cr
C2
O2C1A
O1'
C1O1'

FIGURE 2.1: (+)[Cr mal_3]$^{3-}$ VIEWED DOWN THE *c* AXIS (not 32-disordered).

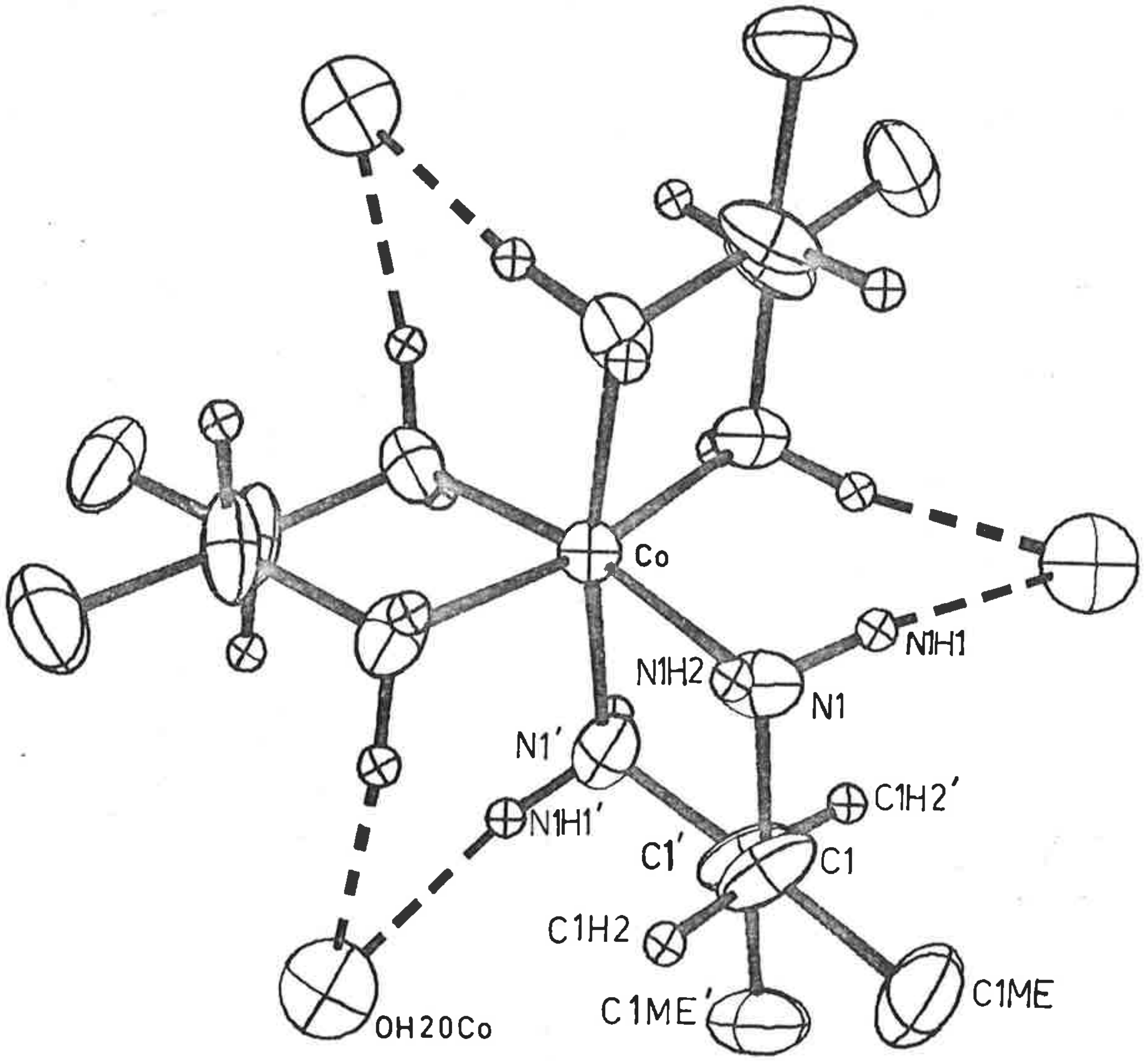
Co
N1H1
N1H2
N1
N1'
C1H2'
N1H1'
C1'
C1
C1H2
C1ME
C1ME'
OH2OCo

FIGURE 2.2: (-)$[Co(-)pn_3]^{3+}$ VIEWED DOWN THE *c* AXIS (32-disorder shown).

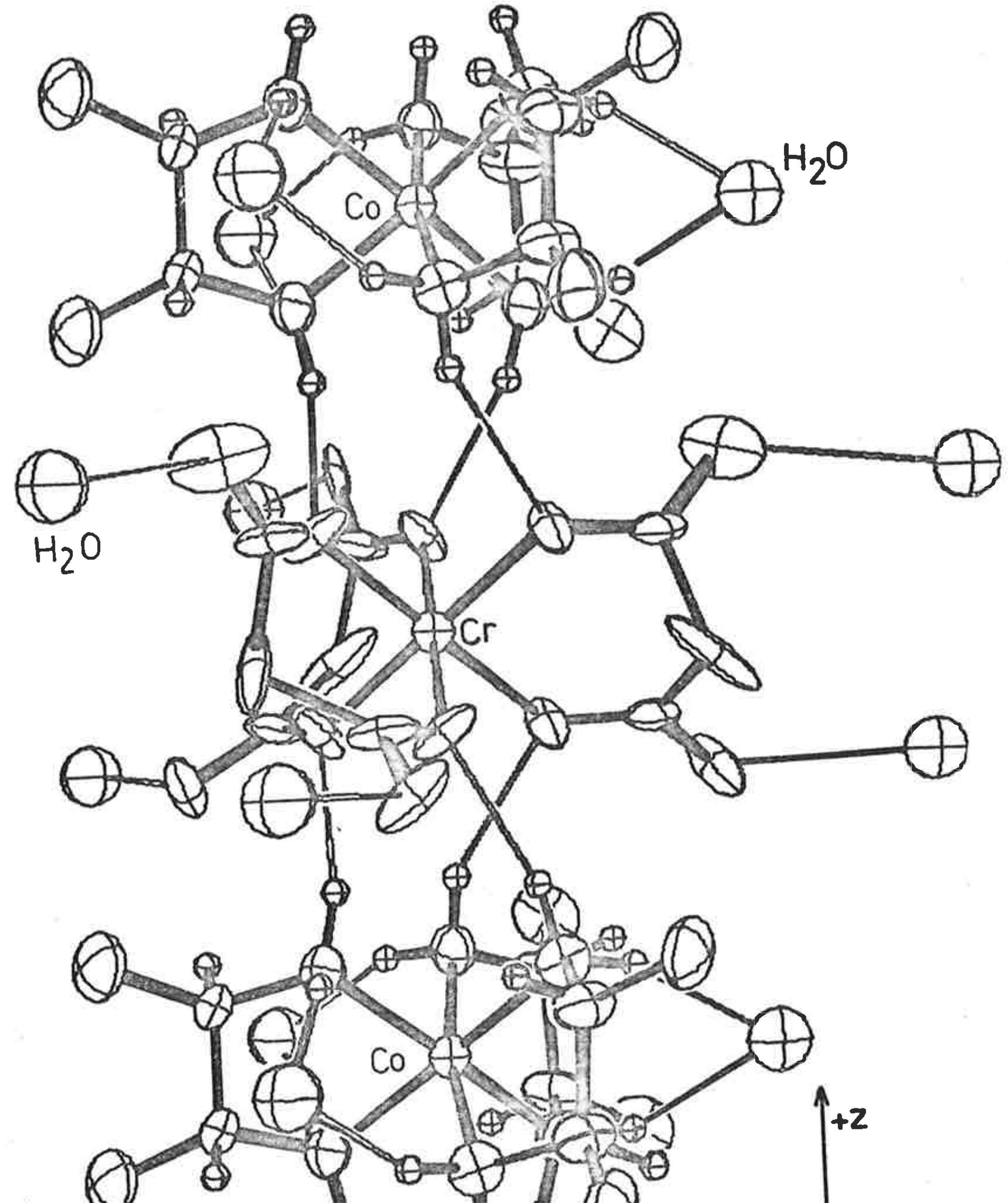
H$_2$O
Co
H$_2$O
Cr
Co
+Z
+X

FIGURE 2.3: (−)[Co(−)pn$_3$](+)[Cr mal$_3$].3H$_2$O. THE ARRANGEMENT OF THE COMPLEX IONS ALONG THE *c* AXIS.

(*a* and *c* in the plane of the paper, as shown.)

TABLE 2.2 POSITIONAL AND THERMAL PARAMETERS FOR (−)[Co(−)pn$_3$](+)[Cr mal$_3$].3H$_2$O:^{a,b} ΔΛ CONFIGURATION.

Atom	*x*	*y*	*z*	β_{11}	β_{22}	β_{33}	β_{12}	β_{13}	β_{23}
Cation									
Co^f	0	0	0	248(26)	248	552(30)	124	0	0
N_1	0677(10)	1145(07)	1122(08)	254(77)	390(74)	784(87)	123(68)	—008(57)	009(47)
C_1	1677(10)	1706(09)	0735(11)	391(89)	309(79)	573(124)	—030(69)	—097(66)	—031(69)
C_1ME	2264(24)	2689(22)	1325(23)	630(228)	283(174)	1290(270)	137(175)	—123(170)	021(137)
Anion									
Cr	0	0	½	277(29)	277	526(36)	139	0	0
O_1	1124(05)	0564(10)	3845(06)	226(54)	531(72)	777(73)	169(66)	115(38)	433(60)
C_1O_1	1851(10)	0463(11)	3899(09)	425(94)	708(116)	279(102)	270(89)	092(65)	139(68)
^{c} C_2	0432(29)	2205(21)	4620(32)	1622(462)	414(198)	1726(528)	706(257)	—1443(350)	—560(208)
O_2C_1	2647(24)	1022(22)	3226(35)	212(168)	504(251)	1189(289)	015(166)	—089(125)	488(197)
^{c} O_2C_1A	2391(33)	0601(28)	3001(34)	−598(244)	676(297)	1130(316)	−259(219)	011(171)	255(234)
Water									
OH_2OCo	2427(10)	0	0	4.74(27)					
Calculated hydrogen atom positions - fixed									
N_1H_1	0378	1534	1020	4.0					
N_1H_2	0631	0966	2026	4.0					
^{,e} C_1H_1	1949	2393	1040	4.0					
C_1H_2	2040	1411	1142	4.0					

a. positional parameters (x 10^4): anisotropic thermal paramaters (x 10^5).

b. isotropic thermal parameters for OH_2OCo and hydrogen atoms.

c. a symmetry related atom is represented in the figures.

d. this atom not represented in the figures.

e. atoms C_1ME, C_2, O_2C_1, O_2C_1A, OH_2OCo and C_1H_1 were input with multipliers of 1/2.

f. anisotropic thermal parameters for Co and Cr symmetry restricted (ref. 54).

TABLE 2.3 BOND LENGTHS AND ANGLES

Atoms	*Distance* (Å)	*Atoms*	*Angle (deg.)*	*Atoms*	*Angle (deg.)*
Cation					
$\mathrm{Co{-}N_1}$	1.964 (10)	$\mathrm{N_1{-}Co{-}N_1'}$	83.2 (8)	$\mathrm{N_1{-}C_1{-}C_1ME}$	117.9 (1.6)
$\mathrm{N_1{-}C_1}$	1.453 (22)	$\mathrm{Co{-}N_1{-}C_1}$	110.7 (10)	$\mathrm{C_1ME{-}C_1{-}C_1'}$	114.5 (1.3)
$\mathrm{C_1{-}C_1ME}$	1.503 (36)	$\mathrm{N_1{-}C_1{-}C_1'}$	106.9 (9)		
$\mathrm{C_1{-}C_1'}$	1.481 (26)				
Anion					
$\mathrm{Cr{-}O_1}$	1.953 (7)	$\mathrm{O_1{-}Cr{-}O_1'}$	91.9 (7)	$\mathrm{O_1{-}C_1O_1{-}C_2}$	119.2 (17)^a
$\mathrm{O_1{-}C_1O_1}$	1.262 (18)	$\mathrm{Cr{-}O_1{-}C_1O_1}$	128.3 (9)	$\mathrm{O_1'{-}C_1O_1'{-}C_2}$	114.3 (13)^b
$\mathrm{C_1O_1{-}C_2}$	1.563 (38)^a	$\mathrm{O_1{-}C_1O_1{-}O_2C_1}$	122.4 (21)^a	$\mathrm{O_2C_1{-}C_1O_1{-}C_2}$	117.9 (24)^a
$\mathrm{C_1O_1'{-}C_2}$	1.606 (35)^b	$\mathrm{O_1'{-}C_1O_1'{-}O_2C_1A}$	125.4 (28)^b	$\mathrm{O_2C_1A{-}C_1O_1'{-}C_2}$	118.1 (29)^b
$\mathrm{C_1O_1{-}O_2C_1}$	1.328 (46)^a	$\mathrm{C_1O_1{-}C_2{-}C_1O_1'}$	108.1 (24)		
$\mathrm{C_1O_1'{-}O_2C_1A}$	1.196 (54)^b				

a,b. The malonate ring is not mirror symmetric about the $\mathrm{Cr{-}C_2}$ line; the bond lengths and angles involving the carboxyl carbon fall into two groups designated a and b.

Interligand angles at the metals

Co	*Symmetry operation relating the donor atoms*	*Angle (deg.)*	*Cr*	*Symmetry operation relating the donor atoms*	*Angle (deg.)*
	3	90.3 (4)		3	88.2 (3)
	2	97.1 (10)		2	91.7 (9)
	32	170.2 (11)		32	179.9 (10)

TABLE 2.4 UNWEIGHTED BEST PLANES THROUGH THE LIGANDS

Plane	*A*	*B*	*C*	*D*	*Distance from plane* (Å)
Malonate (orientation as in figures 2.1 and 2.2)					
O_1,O_1',C_1O_1,C_1O_1'	0	-0.845	-0.535	2.693	O_1,-0.043 : O_1',+0.043 C_1O_1,+0.047 : C_1O_1',-0.047 Cr,O^a : C_2,+0.714
Cr,O_1,O_1'	0	-0.828	-0.561	2.821	C_1O_1,+0.086 : C_1O_1',-0.086
Cr,C_1O_1,C_1O_1'	0	-0.864	-0.504	2.536	O_1,-0.094 : O_1',+0.094
C_1O_1,C_2,C_1O_1'	-0.767	-0.554	-0.323	3.629	O_2C_1,-0.853 : O_2C_1A,-0.767
O_1,C_2,O_2C_1	-0.074	-0.562	-0.824	3.733	C_1O_1,-0.059
O_1',C_2,O_2C_1A	0.016	-0.995	-0.099	-0.189	C_1O_1',-0.115
1,2-diaminopropane					
Co,N_1,N_1'	-0.749	0.433	-0.501	0	C_1,-0.336 : C_1',+0.336

a. Since the two carboxyl oxygens and carboxyl carbons are two-fold symmetric the Cr atom lies in their mean plane.

TABLE 2.5 INTERPLANAR DIHEDRAL ANGLES

	Plane 1	*Plane 2*	*Angle (deg.)*
Cation	Co,N_1,N_1' (ligand 1)	Co,N_1,N_1' (ligand 2)	97.1 (10)
	Co,C_1,C_1' (ligand 1)	Co,C_1,C_1' (ligand 2)	119.7 (13)
	Co,N_1,N_1'	Co,C_1,C_1'	26.9 (15)
Anion	Cr,O_1,O_1' (ligand 1)	Cr,O_1,O_1' (ligand 2)	91.7 (10)
	Cr,C_1O_1,C_1O_1' (ligand 1)	Cr,C_1O_1,C_1O_1' (ligand 2)	96.9 (10)
	Cr,O_1,O_1'	C_1O_1,C_2,C_1O_1'	50.2 (27)
	Cr,O_1,O_1'	Cr,C_1O_1,C_1O_1'	3.9 (10)
	Cr,C_1O_1,C_1O_1'	C_1O_1,C_2,C_1O_1'	50.1 (30)
	O_1,O_1',C_1O_1,C_1O_1'	C_1O_1,C_2,C_1O_1'	50.1

TABLE 2.6 TORSION ANGLES IN THE CHELATE RINGS

Bond	*Angle (deg.)*	*Bond*	*Angle (deg.)*
Malonate ligand		*Propylenediamine ligand*	
$Cr-O_1$	5.0 (12)	$Co-N_1$	14.3 (7)
$O_1-C_1O_1$	21.9 (28)	N_1-C_1	39.1 (19)
$C_1O_1-C_2$	54.9 (31)	C_1-C_1'	50.3 (24)
$C_2-C_1O_1'$	62.7 (30)		
$C_1O_1'-O_1'$	38.4 (29)		

TABLE 2.7 POSSIBLE A-H...B BONDS WITH A...B LESS THAN 3.25 Å

A	*B*	*Symmetry Transform on B*[a]	*H*	*A...B* (Å)	*B...H* (Å)	*Angle at H (deg.)*
N_1	O_1	1	N_1H_2	3.097 (15)	2.219	154
N_1	O_1	2	N_1H_2	3.243 (20)	2.496	136
N_1	OH_2OCo	2	N_1H_1	2.998 (24)	2.090	155
OH_2OCo	O_2C_1A	1		3.182 (40)		
OH_2OCo	O_2C_1	3		2.668 (41)		
OH_2OCo	O_2C_1A	3		2.788 (61)		

a. see table 2.8.

TABLE 2.8 INTERMOLECULAR DISTANCES < 3.5 Å[a]

A	*B*	*Symmetry Transform on B*	*A...B* (Å)	*A*	*B*	*Symmetry Transform on B*	*A...B* (Å)
C_1	O_2C_1	1	3.417 (33)	C_1ME	C_1ME	3	3.064 (76)
C_1	O_2C_1A	1	3.428 (57)	N_1	C_1O_1	2	3.474 (19)
N_1	O_2C_1A	2	3.323 (42)	O_2C_1	C_1ME	4	3.066 (47)

Symmetry transforms referenced in Tables 2.7 and 2.8.

1.	$x,$	$y,$	z
2.	$\bar{y},$	$x - y,$	z
3.	$2/3 - x,$	$1/3 + y - x,$	$1/3 - z$
4.	$2/3 - y,$	$1/3 + x - y,$	$1/3 + z$

a. not involving hydrogen atoms and in addition to the values listed in table 2.7.

TABLE 2.9 SOME BOND LENGTHS AND ANGLES FROM THE REFINEMENT WITH THE INITIAL WEIGHTING SCHEME (c.f. Table 2.3)

Bond	*length* (Å)	*Angle*	*Degrees*
Cation			
Co-N_1	1.983	N_1-Co-N_1'	82.9
N_1-C_1	1.426	N_1-C_1-C_1'	104.2
C_1-C_1ME	1.445	ω^a	48.6
C_1-C_1'	1.627		
Anion			
Cr-O_1	1.930	O_1-Cr-O_1'	94.0
O_1-C_1O_1	1.268	ω	62.5
C_1O_1-C_2	1.579		
C_1O_1-O_2C_1	1.291		

a. the angle ω is defined by figure 7.1. The values at completion of refinement with the new weighting scheme were 48.0° and 60.2° for the cation and anion respectively (Chapter 8).

2.0 Å the two close contacts less than 3.1 Å (Table 2.8) are noteworthy; however, they are avoidable by a more specific ordering of the ions on adjacent symmetry sites.

Some relevant literature bond lengths are quoted in Chapter 1 and are comparable with those observed here, particularly for the cation which has the predicted tris(lel) conformation with the C-C bond of the pn ring being held parallel to the C_3 axis by the requirement that the methyl substituent occupy the energetically most favourable equatorial position.[1] The extent of this parallelism is emphasized by the inter-ligand Co,C_1,C_1' interplanar dihedral angle, 119.7 (1.3)°. The interplanar dihedral angle between the Co, N_1,N_1' planes, 97.1 (1.0)°, indicates significant distortion of the CoN_6 first coordination sphere from an idealized geometry having interplanar angles of 90° (this distortion is discussed further in Chapter 8). C_1H_1 in the atoms list (Table 2.2) corresponds to the position of the two-fold disordered methyl group, C_1ME; both were input with multipliers of $\frac{1}{2}$.

A tris-malonate anion has D_3 symmetry only if the methylene carbon (C_2) lies on a two-fold axis through the metal ion, i.e. a completely flattened ring conformation or a symmetrical skew form; in CRMALTCOPN C_2 is displaced 0.71 Å from the mean five atom plane through Cr,O_1,O_1',C_1O_1,C_1O_1'. The methylene carbon atom is also displaced from the hypothetical mirror plane of an ideal chair, boat or flattened conformer (viz. C_1O_1-C_2 is 1.56 (4) Å whereas C_1O_1'-C_2 is 1.61 (4) Å) with consequent changes in bond and torsion angles (Tables 2.3 and 2.6).

Therefore in the 32-disordered arrangement the methylene carbon and the carbonyl oxygen atoms are split. The non-symmetry equivalent O_2C_1 and O_2C_1A sites are 0.63 (5) Å apart.

The Cr-O_1 bond length, 1.953 (7) Å, compares well with that found in Cr(acac)$_3$,[112] 1.956 (7) Å, Cr(gly)$_3$,[113] 1.964 (1) Å, and (+)Cr((+)atc)$_3$,[114,115] 1.968 (10) Å. The carboxyl carbon-oxygen bond length (O_1-C_1O_1, 1.262 (18) Å) is the same as the average carbonyl bond length (C_1O_1-O_2C_1, C_1O_1-O_2C_1A). The mean anion C-C bond length, 1.585 (25) Å, is significantly longer than that found in the NADCOMALEN structure (1.50 (2) Å); associated with this bond lengthening is a contraction of the angle at the methylene carbon from a value approximating the ideal sp^2 value to within one esd of the ideal tetrahedral angle, e.g. in CRMALTCOPN the C-C-C angle is 108.1 (2.4)°, in NADCOMALEN 117.2 (1.8)° and in (-)[Co en$_2$(NO$_2$)$_2$](+)[Co mal$_2$ en][89] where the average C-C bond length in the malonate rings is 1.48 Å this angle is 125°. The high standard deviations in the individual bond angles in all three structures preclude detailed discussion of the individual bond and torsion angles.

The relative skew of the $O_1 \ldots O_1'$ and $C_1O_1 \ldots C_1O_1'$ lines about the two-fold axis is barely significant at a 3σ level (3.85 (98)°) although larger than that found in NADCOMALEN; the displacement of the carboxyl oxygens ± 0.09 Å either side of the Cr,C_1O_1,C_1O_1' plane is about half that observed in Matsumoto and Kuroya's structure[89] (see Chapter 1). In CRMALTCOPN the skew is such that the Cr,C,C plane is more nearly parallel to the three-fold axis of the anion than is the Cr,O,O plane, as shown by the interligand interplanar dihedral angles (96.86 (98)° and 91.65 (96)° respectively). This twisting of the ligand backbone relative to the ML_6-core in $[Cr\ mal_3]^{3-}$ is discussed in section 8.2.

Mean-square amplitudes of thermal vibration were not computed but the anisotropic thermal ellipsoids of the non-metal atoms are shown in the figures; the temperature factor of atom O_2C_1A was non-positive definite and the minimum thermal ellipsoid as drawn serves only to indicate the direction of maximum vibration. Unfortunately, because figures 2.1 and 2.2 are views parallel to *c*, the thermal ellipsoids as drawn are of limited value in deciding the directions of maximal vibration. The methylene carbons of the pn ligand vibrate appreciably perpendicular to the Co,C,C plane while the ellipsoid of C_1ME is elongated radially. In the anion the methylene carbon shows maximum vibration perpendicular to the C,C,C plane while the other malonate ring atoms exhibit appreciable vibration perpendicular to the mean $Cr,O_1,O_1',C_1O_1,C_1O_1'$ plane.

The most alarming feature of the CRMALTCOPN structure refinement was the significant change in some of the bond lengths and angles of the converged model on modification of the weighting of the intensity data: see Table 2.9 for some bond length and angle parameters for the converged structure based on the initial weighting scheme. For the tris-malonate ion the relevant angular parameters (see Chapters 7 and 8) from the final converged model are not significantly different from those of a

D_{3d} symmetric ML_6-core; it would be more satisfactory if we could feel certain that this represents reality and not just a fortuitous dependence on the particular weighting of the intensity data. The structure refinement should be repeated, preferably using an excess of "correctly" weighted diffractometer data; it is important that more $l = 2n + 1$ data be used in the refinement since these are relatively most sensitive to the refinement of the light atoms. The time required to record such data photographically became increasingly prohibitive at high μ angles.

Malonate Ring Conformation -

Two important conclusions emerge from the three known structures of chelated malonate ligands. Firstly, the exocyclic carbonyl oxygens are always likely to participate in strong intermolecular hydrogen bonds and ionic close contacts resulting in a greater variety of conformations than is to be expected for the analogous six-membered diamine ring complexes. Second, because of this strong inter-molecular interaction the carbonyl oxygen bond is unlikely to be found significantly shorter than the intra-ring carboxylic C-O bond, at least not when using photographic intensities.

Notwithstanding the probable importance of intermolecular forces in determining the malonate ring conformations some observations of an intramolecular nature are worthwhile.

The mean intra-ring inter-carboxyl oxygen distance in the malonate rings of NADCOMALEN (i.e. $O_1L \ldots O_2L$, $O_3L \ldots O_4L$) is 2.77 Å; the mean inter-carboxyl carbon atom distance ($C_{11}...C_{13}$, $C_{31}...C_{33}$) is 2.56 Å. The corresponding distances in CRMALTCOPN are $O_1...O_1' = 2.72$ Å, $C_1O_1...C_1O_1' = 2.57$ Å. In the present structure the C,C,C plane makes an angle of 50.1° with the O_1,O_1',C_1O_1,C_1O_1' plane whereas in NADCOMALEN this angle averages 28.9°. The agreement of the intra-ring non-bonded vectors in these two structures suggests that the smaller average value of this intra-ring dihedral angle in the $[Co\ mal_2\ en]^-$ ion may in part be due to potential unfavourable intra-molecular close contacts between the two malonate ligands; the relevant interactions in the refined NADCOMALEN structure are $C_{12}H_1...C_{33}$, 3.34 Å, $C_{12}H_1...O_4L$, 2.75 Å, $C_{32}H_2...O_2L$, 2.70 Å, $C_{32}H_2...C_{13}$, 3.11 Å. Increasing the intra-ring dihedral angle beyond ca. 30° in the $[Co\ mal_2\ en]^-$ ion would result in strong repulsion between the above atom pairs. Although the malonate methylene hydrogen atoms were not included in the CRMALTCOPN refinement it is not difficult to see that the planarity of the five atoms ($Cr,O_1,O_1',C_1O_1,C_1O_1'$) permits a larger dihedral angle with the C_1O_1,C_2,C_1O_1' plane before there is appreciable interaction of a donor oxygen of one malonate ligand with a methylene hydrogen of the other ligand. The dihedral angle between the tri-atomic M,O,O and C,C,C planes is ca. 52° for the three independent malonate rings (CRMALTCOPN, 50.1 (2.7)°; NADCOMALEN, 52.8 (2.5)°, 53.4 (3.0)°), a geometry quite different from that found[89] in the $[Co\ en_2(NO_2)_2][Co\ mal_2\ en]$ structure.

If the malonate ligands in $[Co\ mal_2\ en]^-$ folded toward the en ligand to the same degree that they fold toward each other in the NADCOMALEN structure the interaction between the amine hydrogen atoms and the malonate methylene protons would be impossibly short; that a more flattened conformation of the malonate ring is acceptable has already been shown.[89] As mentioned previously, lack of suitable potential functions incorporating the steric effects of electron lone-pairs has precluded vapour-phase energy minimization calculations of the chelated malonate systems. Lone-pair/lone-pair repulsions have elsewhere been considered[116-118] stronger than atom/atom interactions with lone-pair/bonded-pair repulsions being intermediate in strength.[81,119] Only in the completely flattened ring conformation are all lone-pairs (on the donor oxygens) and bonding-pairs (M-L, C=O, C-H) maximally staggered; for a chair conformation they are maximally eclipsed and for boat and skew conformers some interactions are eclipsed and others are gauche. Correct representation of these interactions will be important in assessing the relative energies of the various malonate ring conformations but it is perhaps noteworthy that the low energy chair conformation commonly found[94,120-126] for chelated tn ligands (all ring atoms except the coordinated metal tetrahedral) is not approximated by any of the five crystallographically independent malonate rings in the three structures discussed here.

Similar consideration[31] was taken of the steric role of the carboxyl oxygen lone-pairs in discussing the nmr spectra of $[\mathrm{Co\ mal_2\ en}]^-$ and $[\mathrm{Co\ mal\ en_2}]^+$; there, however, the interaction of the oxygen axial lone-pairs with the orthogonally placed donor atoms of adjacent ligand rings was also considered. For an "isolated" M-mal ring the boat and skew conformers were thought more favourable than the chair; introduction of donor nitrogens or oxygens (with their attendant amine hydrogens or oxygen lone-pairs) was considered to increase the relative favourability of the skew form. The single resonance observed[31] for the malonate methylene protons in the [Co mal $en_2]^+$ ion was interpreted as indicating rapid flipping of the malonate ring between the two symmetrical skew forms (λ and δ);[127,128] the [Co mal_2 en$]^-$ resonance[31,32] was compatible with either a two-fold symmetric bis(chair) or bis(boat) conformation but rapid conformational interchange was again thought likely. In the two independent crystal structures containing [Co mal_2 en$]^-$ the complex ion maintains an approximate non-crystallographic two-fold symmetry, although the malonate ring conformations are distinctly different, as indicated above.

CHAPTER 3 THE STRUCTURE OF POTASSIUM CALCIUM $(+)_{589}$-TRIS(DITHIO-OXALATO) COBALTATE(III) TETRAHYDRATE

$K.Ca(+)_{589}[Co\ thiox_3].4H_2O$, CADCOTHIOX.

3.1 STRUCTURE ABSTRACT

The crystal structure of $K.Ca(+)_{589}[Co(S_2C_2O_2)_3].4H_2O$ has been solved and refined by full-matrix least-squares to convergence with $R_1 = 0.062$; the Λ configuration previously assigned to the $(+)_{589}[Co\ thiox_3]^{3-}$ anion on the basis of circular dichroism correlations is confirmed by the present refinement. Structure solution was based on 2374 equi-inclination counter data recorded with *CuKα/Nif* radiation. The structure is orthorhombic, $P2_12_12_1$ (No. 19), $a = 12.381$ (5), $b = 12.791$ (5), $c = 11.801$ (5) Å, $U = 1869$ (2) $Å^3$, $Z = 4$, $D_c = 2.03$, $D_m = 2.01$ g. cm^{-3}. Although the angles, S-Co-S, subtended at the Co atom by the three thio-oxalate ligands are close to 90° (Av. $89.7 \pm 0.15^\circ$) the CoS_6 first coordination sphere lacks O_h symmetry showing significant elongation along the pseudo-C_3 axis of the complex ion. The cations and water molecules make numerous close contacts with each other and with the complex anion.

3.2 EXPERIMENTAL

The complex ion was prepared and resolved following the literature procedure[129] except that Ca^{++}, rather than Ba^{++}, was chosen as the co-crystallizing cation with K^+ in order to reduce the scattering from atoms external to the complex ion (atomic number of calcium = 20, barium = 56). In view of the subsequent difficulty in distinguishing the three metal atoms in the preliminary Patterson and Fourier maps ($Z_K = 19$, $Z_{Co} = 27$) the presence of a dominant barium ion would have been an advantage in choosing a correct starting model.

Dithio-oxalic acid from Eastman-Kodak Co., Rochester, N.Y., U.S.A.. The resolving agent, (+)[Co $en_2(NO_2)_2$]Br from F.R. Keene.

Recrystallization of K.Ca(+)[Co $thiox_3$] from aqueous solution gave burgundy coloured rectangular prisms of the tetrahydrate, elongated along c^* and bearing (1,1,1) and ($\bar{1},\bar{1}$,1) bevels at one end in most cases; the faces parallel to the needle axis were of the form {1,1,0}. Absorption and ORD spectra suggested the first coordination sphere contained some sulphur atoms and stability of the complex ion in light and its failure to racemize at a perceptible rate in aqueous solution pointed to all three ligands being bidentate through sulphur donor atoms.

Preliminary photographic investigation of several crystals revealed that twinning parallel to the c^* axis was a serious problem and although crystals suitable for integrated photographs could be readily found, there were few which met the more rigorous requirements of a diffractometer study. The films showed the space group to be $P2_12_12_1$ with a = 12.33, b = 12.74, c = 11.77 Å ($\lambda_{CuK\alpha}$ = 1.5424 Å); non-integrated Weissenberg equi-inclination films were recorded for reciprocal lattice levels up all three axes to facilitate setting of the diffractometer for recording the individual layers. Two crystals (coated with a thin film of Canada Balsam to reduce possible dehydration), one mounted about c^*

and the other about a^*, were used to determine more accurate lattice constants on a semi-automated Buerger-Supper Equi-inclination X-ray diffractometer using a pinhole collimator. The lattice repeats were calculated from the α_1 component of high order zero layer reflections using non-monochromated *CuKα/Nif* radiation ($\lambda_{K\alpha_1} = 1.54051$ Å).

Crystal data - as in structure abstract.

$K.Ca(+)[Co(S_2C_2O_2)_3].4H_2O$; $M = 570.6$; $\mu_{CuK\alpha} = 175\ cm^{-1}$.

D_m by flotation in 1,2-dibromopropane/1,2-dibromoethane at 23°C.

Microanalysis - *calc.*	C 12.63,	S 33.71,	H 1.42,	H_2O 12.63.
found	12.40,	33.4,	1.32,	11.3 (by weight loss).

$[\alpha]^{28}_{589} = +1042^\circ$, $[M]_{589} = +6680^\circ$ (ref. 129, $[M] = +5000^\circ$ for K.Ba salt).

Details of the diffractometer data collection routine and subsequent data reduction process are given in Appendix III. Using the c^* mounted crystal, reflections for layers $l = 0 \rightarrow 9$ were measured along lines of constant k, varying h through + and - values within a machine limited upsilon range of $\Upsilon = 10\text{-}140^\circ$; the equi-inclination angle for layer $hk9$ was 36.03°. With *CuKα* radiation, the pronounced anomalous dispersion effect for this crystal reduces the symmetry of the reciprocal lattice from the Laue symmetry mmm to the point symmetry 222 resulting in non-equivalent $\overset{+}{h}kl$ and $\bar{h}kl$ octants; structure refinement based on this non-averaged data set was expected to yield the absolute configuration of the complex ion directly.

The a^* mounted crystal was used to generate reciprocal layers $0kl \rightarrow 8kl$, measuring the +++ octant only (along lines of constant l index). The μ angle for $8kl$ was 29.89°. This crystal was smaller than that used to generate the c^* data and consequently measurement of individual layers was somewhat slower; since two octants of c^* data had been recorded one octant of a^* data was adequate to achieve correct interlayer scaling of the anomalous dispersion data.

3.3 STRUCTURE SOLUTION AND REFINEMENT

Lorentz and polarization (but not absorption) corrections were applied to the raw reflection intensities (see Appendix III) and the three octants merged to give a unique data set of 1548 reflections having all indices positive. Although the first Patterson map based on this incorrectly averaged data showed two peaks at approximately 2.3 Å from the origin, consistent with an approximately octahedral CoS_6 coordination sphere, the number of heavy atoms per asymmetric unit (Co, Z = 27; Ca, Z = 20; K, Z = 19; six S, Z = 16) rendered location of the metal atoms uncertain; the problem is ideally suited to solution by direct methods. There were numerous peaks on the Harker ($\frac{1}{2}$) sections and inclusion of a Co atom at several of the possible solutions for these vector sets gave R_1 ca. 0.67 compared with a random value of 0.83: however, further structural features could not be determined from the resultant Fourier maps even though the face-centred subcell pattern of the Patterson map suggested a precise positioning of the calcium and potassium ions relative to the oriented CoS_6 core.

The structure was solved by making use of the intensity differences (Bijvoet differences) between Friedel pair reflections due to the anomalous scattering by the heavy atoms. All three metal atoms have $\Delta f''_{CuK\alpha} > 1.0$ and $\Delta f''$ for sulphur is 0.6 but the Co coefficient is dominant (3.9) and a Patterson map based on the Bijvoet differences between the $\overset{+}{h}kl$ and $\bar{h}kl$ c^* axis data could be expected to show a dominant peak on each Harker section corresponding to the Co-Co vectors in $P2_12_12_1$. When comparing Friedel pairs rigorous absorption corrections should be applied[44b] but since the "c^* crystal" was approximately uniform, other than for the bevels at one end, these corrections were not applied; comparison of some $\overset{+}{h}k0$ and $\bar{h}k0$ pairs indicates this approximation is not entirely satisfactory. Data for which only one reflection of a Friedel pair was observed were prematurely excluded from the data set; this was invalid since such data, especially at high sinθ,[44b,130b,131] can be expected to be most sensitive to anomalous dispersion, but fortunately this omission did not prevent the finding of a unique solution for the Co atom.

The +++ and −++ c^* axis data sets comprised ca. 1200 reflections each. Two anomalous Patterson syntheses were computed,

(a) one based on $|\Delta F|^2 = |\bar{F} - \overset{+}{F}|^2$ for all data showing any difference in intensity of the Friedel pairs, 851 $|\Delta F|^2$ output,

(b) and the other based on $\Delta I = (\bar{I} - \overset{+}{I})$ where $|\Delta I| > (\sigma_{\overset{+}{I}} + \sigma_{\overset{-}{I}})$, 417 data output:

an analogous significance test should have been applied in case (a). Reflections having at least one index zero were automatically excluded from the data set. Synthesis (a) is the "anomalous squared synthesis"[130a,b] and (b) a modification of the "anomalous difference Patterson" proposed by Okaya and Pepinsky.[44b,130b] In the ideal case synthesis (a) is more direct showing only the Harker peaks for the anomalous scatterer whereas (b) also gives peaks due to interaction of the anomalous scatterer with the normal scatterers. Interactions involving normal scatterers only should be absent from both maps.

Although the disposition of peaks was similar in the two maps there were some differences in relative peak heights. Interpretation of the dominant peaks on the Harker (1/2) sections gave a starting position for Co at (± 0.078, 0, ± 0.213). A structure factor calculation with Co at (0.078, 0, 0.213) had R_1 = 0.675 and suggested further improvement was possible with lowering of the scale and isotropic temperature factors. A Fourier map phased by this model showed the expected mirror symmetry about the xz plane, but no further atomic positions could be decided. A β-anomalous synthesis[130a] computed using the 417 signed ΔI values with Co at (0.078, 0, 0.213) yielded six possible sulphur atom sites, five of which were consistent with the strong 2.3 Å peaks in the original Patterson map. Inclusion of these six atoms in a subsequent calculation lowered R_1 to 0.512 but it was not possible to locate the Ca and K atoms with certainty in the resulting Fourier.

Comparing the original Patterson map with the anomalous squared synthesis, the Ca-Ca and K-K vectors in the latter should be considerably reduced in peak height compared with those in the former, taking the Co-Co Harker peaks as reference. Two such sets of vectors were found and deconvolution gave two possible starting positions for Ca and K at (0.078, 0.440, -0.207) and (0.070, -0.280, -0.075). Inclusion of the Ca in the above model gave R_1 = 0.478; the alternate structure with the mirror image set of sulphur atoms gave R_1 = 0.503. Positional refinement of this limited eight-atom model lowered R_1 to 0.305 for the 1548 unique data. A difference map computed at this stage confirmed the K position and introduction of this atom together with four carbonyl oxygens further reduced R_1 to 0.250. The two remaining carbonyl oxygens, the six ligand carbon atoms and the four water oxygens were located in the subsequent difference and Fourier maps. R_1 dropped to 0.190 on inclusion of these additional atoms. Positional and isotropic refinement of all twenty-five atoms gave R_1 = 0.133 (R_2 = 0.123 using individual weights based on counting statistics - see Appendix III). The isotropic temperature factor for K^+ was approximately three times those of Co and Ca^{++} consistent with the large spread of electron density at this site in both the difference and Fourier maps. These maps indicated that the thermal vibration of all atoms was significantly anisotropic.

There is no point in making a full anisotropic refinement of a model for a structure having a large linear absorption coefficient unless absorption corrections are first applied to the intensity data;

otherwise the temperature factors correct for this systematic error by adjusting to smaller values, generally with the complication of non-positive definite anisotropic thermal ellipsoids.[45] The raw data were checked for counting and punching errors before application of absorption corrections. Both crystals were described as regular parallelepipeds of square cross section neglecting the (1,1,1) and ($\bar{1}$,$\bar{1}$,1) bevels and the slight inequality of the edge lengths perpendicular to the needle axis. The crystals were measured on a travelling microscope calibrated in 0.001 mm. — the c^* crystal was 0.128 x 0.146 in section and 0.321 in overall length; the effective length was considered to be less due to the angular truncations and it was described as being 0.137 x 0.137 x 0.283 mm. having a volume of 5.296 x 10^{-6} cm^{-3}. The a^* needle was 0.134 x 0.125 in section and 0.214 in maximum length; for the purpose of applying absorption corrections it was described as 0.129 x 0.129 x 0.182 mm., having an effective volume of 3.044 x 10^{-6} cm^{-3}. A more rigorous description of the crystal shapes may have facilitated improved fitting of the refined model to the intensity data.

Comparison of observed/unobserved reflections in the a^* set with those in the +++ and -++ c^* octants indicated that the a^* data corresponded to the +++ c^* octant. Interlayer scaling of the absorption corrected a^* data with the two c^* octants separately, confirmed this assignment. The -++ c^* data were introduced with scale factors derived in the interlayer scaling of the +++ data; the unique data set comprised 2374 $\overset{+}{h}kl$ and $\bar{h}kl$ reflections. Introduction of the absorption corrected data to the structure refinement reduced the esd's of the positional coordinates and increased the isotropic temperature factors.[45] The large temperature factor for K^+ was disturbing but attempts to represent the broad Fourier and difference peak at this site by several atoms having fractional multipliers gave no significant improvement in the least-squares agreement factors[55] or in the esd's of the coordinates. The isotropic stage of refinement was concluded with $R_1 = 0.109$, $R_2 = 0.100$, $G = 2.862$ for the Λ configuration of the complex ion (Co^{+1}, Ca^{+2}, K^{+1} scattering anomalously — details of scattering factors used in this structure are summarized in Appendix IV, note 1), $n = 101$. The Δ configuration gave $R_1 = 0.148$ confirming that the correct absolute configuration can be derived from Patterson functions based on the Friedel pair intensity differences.

Anisotropic thermal parameters were introduced in stages; anisotropic refinement of Co, Ca, K ($n = 116$) gave $R_1 = 0.090$, $R_2 = 0.079$. Introduction of anisotropic thermal parameters for the six sulphur atoms lowered R_1 to 0.073 and R_2 to 0.063, $G = 1.849$ ($n = 146$). An attempted anisotropic refinement of all light atoms was unsuccessful at this stage due to non-positive definite temperature factors for several atoms of one thio-oxalate ligand. The distribution of $Av.\ w\Delta^2$ versus $|F_o|$ indicated relative over-weighting of the more intense reflections; the low angle, $(\sin\theta)/\lambda < 0.2$, reflections showed little evidence of an extinction effect and the few reflections affected were excluded from subsequent least-squares cycles. Initially reflections having $I \leq 2\sigma_I$ were excluded from the data set — of 3652 c^* data 848 were unobserved, of 1532 a^* data 416 were unobserved on this $2\sigma_I$ criterion. Examination of $|F_o|$ and $|F_c|$ indicated that many of the weakest intensity reflections had $|F_o| > |F_c|$, a phenomenon usually seen with "unobserved" reflections in film data. A $3\sigma_I$ cut-off was imposed[97,132] and all reflections having $2\sigma_I < I \leq 3\sigma_I$ were retained in the data set as "unobserved" but were excluded from subsequent least-squares refinement cycles — 3920 data condensed to a unique $\overset{+}{h}kl/\overset{-}{h}kl$ set of 2374, of which 2086 were included in the least-squares cycles.

The anomalous scattering contribution was included for the six sulphur atoms (as well as Co, Ca, K) and the whole structure refined anisotropically (alternate cycles refining the positions, $n = 76$, and temperature factors, $n = 151$) to convergence with $R_1 = 0.062$, $R_2 = 0.060$, $G = 1.753$ ($n = 76$), $G = 1.785$ ($n = 151$) in two complete cycles. The anisotropic temperature factors for atoms C_5 and C_6 remained non-positive definite, probably reflecting inadequate absorption correction of the intensity data.[45] The distribution of $Av.\ w\Delta^2$ vs $|F_o|$ was satisfactory except in the high intensity ranges and neither a Hughes[133] nor a Cruickshank[44a] weighting scheme promised any improvement; time did not permit the application of an arbitrary weighting scheme to the raw data. As indicated in Appendix III, the standard deviation assigned to the raw peak intensity is the minimum value determined by the counting statistics; in program AULAC some account is taken of the agreement of the symmetry equivalent reflections such that σ for a multiply observed reflection is most commonly less than that of a "once only" observation of comparable intensity. Many of the weaker reflections were not observed in the a^* data set and as "once only" observations carry a relatively high standard deviation. Coupled with the already over-optimistic σ values assigned to the most intense-data from counting statistics this results in a relative over-weighting of the most intense data. An additional error should be included[45] in σ to correctly represent the random errors not represented by the counting statistics.

A final difference map showed no further peaks of any significance, the minor peaks which did occur being close to supplied atom sites. The hydrogen atoms of the four water molecules could not be located. Their non-inclusion in the model and the unsatisfactory representation of the K^+ disorder can also be expected[44a] to influence the trend in $Av.\ w\Delta^2$. Derivation of the estimated standard deviations of the variable parameters is formally invalid for weighting schemes showing this increasing trend in $Av.\ w\Delta^2$ to high $|F_o|$; the effect is most noticeable in the esd's of the thermal parameters.[44a]

$|F_o|$ and $|F_c|$, both × *10*, are listed in Table 3.1.

3.4 STRUCTURE FIGURES AND TABLES

The figures and tables of structural parameters presented in this section are discussed in section 3.5.

In Figures 3.1 and 3.2 the non-positive definite C_5 and C_6 atoms

TABLE 3.1 FINAL $|F_o|$ AND $|F_c|$ FOR K.Ca(+)[Co thiox$_3$].4H_2O: Λ CONFIGURATION.

	H	K	FOBS	FCAL
	**L =		0****	
E	2	0	2346	2622
	4	0	224	188
	6	0	1834	1851
	8	0	1401	1369
	10	0	306	261
	14	0	203	189
	2	1	380	360
	3	1	341	388
	4	1	438	387
	5	1	435	415
U	7	1	130	149
	8	1	401	449
	9	1	803	815
	10	1	304	319
	14	1	176	172
	0	2	2989	2981
	1	2	841	823
	2	2	1042	970
	3	2	204	169
	4	2	316	273
	5	2	929	904
	6	2	718	768
	8	2	779	846
	9	2	597	536
	12	2	204	214
U	13	2	163	146
	14	2	244	242
	1	3	293	219
	2	3	562	604
	3	3	536	443
	4	3	604	609
	5	3	160	144
	6	3	171	154
	8	3	240	252
	10	3	564	482
	11	3	275	171
	14	3	167	170
	0	4	1021	983
	2	4	254	274
	3	4	450	411
	4	4	927	918
	5	4	637	624
	6	4	509	504
	7	4	581	539
	8	4	269	204
	9	4	182	249
	12	4	460	475
	13	4	307	287
	14	4	358	297
	1	5	604	628
	2	5	288	256
	3	5	473	470
	4	5	301	302
	5	5	248	285
	6	5	637	615
	8	5	456	431
	9	5	207	174
	10	5	388	425
	11	5	325	358
U	12	5	163	94
	13	5	213	173
	14	5	238	180
	0	6	1750	1709
	1	6	865	850
	2	6	271	282
	3	6	304	293
	4	6	512	540
	7	6	386	432
	8	6	448	410
	9	6	302	350
U	11	6	177	154
	12	6	368	318
	13	6	225	216
	1	7	430	411
	2	7	333	354
	3	7	1525	1583
	4	7	612	656
	5	7	667	662
	6	7	404	406
	7	7	177	194
	8	7	351	386
	9	7	449	385
	10	7	186	173
	11	7	370	333
	0	8	614	592
	1	8	725	752
	2	8	227	231
	4	8	212	200
	6	8	224	221
	7	8	474	414
U	8	8	166	198
	9	8	324	256
	11	8	250	239
	12	8	166	107
	1	9	176	159
	2	9	349	339
	3	9	585	649
	4	9	368	394
	5	9	425	430
	6	9	420	405
	8	9	283	262
	9	9	405	425
	10	9	358	391
	11	9	271	293
U	12	9	122	82
	0	10	423	404
	1	10	199	204
	2	10	379	367
	3	10	355	349
U	5	10	154	166
U	9	10	146	94
	1	11	480	476
	2	11	194	182
	4	11	233	229
	5	11	485	489
	6	11	403	423
	7	11	264	202
	8	11	517	486
	9	11	244	203
	10	11	254	245
	2	12	314	338
	3	12	260	245
U	3	13	164	149
	4	13	203	152
	8	13	211	206
U	0	14	176	135
U	3	14	141	152
	6	14	174	190
U	1	15	119	127
	2	15	462	441
U	3	15	129	120
	**L =		1****	
	2	0	379	396
	3	0	381	376
	4	0	482	486
	5	0	258	268
	7	0	550	643
	8	0	348	358
	9	0	266	277
	10	0	275	208
	11	0	320	350
	12	0	476	432
	13	0	188	197
U	14	0	152	141
	1	1	135	120
	2	1	1218	1294
	-2	1	1353	1325
	3	1	584	604
	-3	1	649	613
	4	1	328	368
	-4	1	615	607
	5	1	429	490
	-5	1	467	514
	6	1	212	237
	-6	1	257	262
	7	1	611	679
	-7	1	625	638
	8	1	920	1027
	-8	1	968	989
U	9	1	152	167
	10	1	446	425
	-10	1	380	396
	11	1	328	353
	-11	1	312	363
	12	1	237	198
U	-14	1	143	174
	0	2	208	212
	1	2	834	841
	-1	2	940	868
	2	2	242	233
	-2	2	296	253
	3	2	1610	1717
	-3	2	1774	1711
	4	2	259	266
	-4	2	345	325
	5	2	401	444
	-5	2	539	553
	6	2	205	240
	-6	2	257	278
	7	2	672	675
	-7	2	749	750
	8	2	420	489
	-8	2	437	487
	9	2	332	330
	-9	2	347	369
	11	2	215	195
	-11	2	190	196
U	12	2	164	189
	0	3	206	133
	1	3	299	329
	-1	3	240	272
	2	3	871	931
	-2	3	1183	1134
	3	3	656	700
	-3	3	776	787
	4	3	634	652
	-4	3	755	732
	5	3	585	605
	-5	3	666	685
	7	3	735	754
	-7	3	671	692
	8	3	283	325
U	-8	3	138	210
	9	3	280	292
	-9	3	186	217
U	10	3	169	160
U	-10	3	153	204
	11	3	525	471
	-11	3	427	454
	12	3	289	328
	-12	3	232	266
	13	3	198	181
	-13	3	192	195
	14	3	194	149
	-14	3	200	154
	0	4	836	862
	1	4	486	491
	-1	4	633	626
	2	4	918	940
	-2	4	965	945
	3	4	218	209
	-3	4	210	183
	4	4	808	844
	-4	4	876	874
	5	4	522	545
	-5	4	521	547
	6	4	387	414
	-6	4	418	418
U	-7	4	137	189
	8	4	529	497
	-8	4	428	462
	9	4	226	199
	-9	4	238	254
	11	4	185	173
	-11	4	215	213
	12	4	296	261
	-12	4	228	260
	13	4	257	263
	-13	4	253	317
	0	5	951	949
	1	5	1099	1134
	-1	5	1038	1057
	2	5	250	260
U	-2	5	108	112
	3	5	1182	1202
	-3	5	1212	1196
	4	5	997	1054
	-4	5	1046	1090
	5	5	793	829
	-5	5	844	908
	6	5	418	415
	-6	5	467	453
	7	5	289	286
	-7	5	281	296
	8	5	232	204
	-8	5	202	141
	9	5	292	281
	-9	5	243	253
U	10	5	167	129
	11	5	512	509
	-11	5	436	476
U	12	5	154	74
	13	5	202	189
	-13	5	198	204
	14	5	142	126
U	-14	5	124	128
	1	6	898	923
	-1	6	941	960
	2	6	366	357
	-2	6	365	375
	3	6	463	484
	-3	6	534	515
	5	6	1072	1134
	-5	6	1035	1097
	6	6	262	218
U	-6	6	150	191
	7	6	428	482
	-7	6	362	392
	11	6	412	394
	-11	6	393	433
	12	6	178	176
U	-12	6	135	155
	13	6	302	308
	-13	6	312	332
	1	7	608	642
	-1	7	511	533
	2	7	238	250
	-2	7	198	179
	3	7	810	829
	-3	7	854	838
	4	7	475	511
	-4	7	500	515
	5	7	515	523
	-5	7	520	501
	6	7	337	330
	-6	7	364	360
	7	7	385	395
	-7	7	448	436
U	8	7	166	167
	9	7	556	532
	-9	7	582	578
	10	7	246	269
	-10	7	188	223
	11	7	184	193
	-11	7	180	187
	0	8	366	372
	1	8	816	854
	-1	8	769	808
	2	8	191	182
	3	8	641	677
	-3	8	668	687
	4	8	491	519
	-4	8	500	524
	5	8	425	422
	-5	8	397	389
	6	8	231	250
	-6	8	228	214
	7	8	473	469
	-7	8	379	409
	8	8	254	294
	-8	8	199	302
	10	8	194	191
	-10	8	170	195
	11	8	369	334
	-11	8	296	304
	12	8	230	205
	-12	8	222	227
	0	9	274	298
	1	9	487	558
	-1	9	485	545
	2	9	450	472
	-2	9	464	462
	3	9	428	441
	-3	9	433	462
	6	9	341	327
	-6	9	265	294
	7	9	305	344
	-7	9	334	370
	9	9	412	437
	-9	9	417	450
	10	9	171	166
	11	9	192	159
	-11	9	206	210
U	12	9	118	82
	0	10	794	799
	1	10	476	489
	-1	10	468	456
	2	10	549	582
	-2	10	577	541
	3	10	277	296
	-3	10	325	305
	4	10	365	357
	-4	10	368	382
U	5	10	161	119
	-5	10	242	201
	6	10	247	239
	-6	10	296	289
	7	10	424	408
	-7	10	405	409
	8	10	401	374
	-8	10	360	353
	9	10	163	127
	11	10	218	219
	-11	10	177	179
	1	11	379	340
	-1	11	344	392
	2	11	210	231
	-2	11	220	225
	3	11	387	394
	-3	11	373	378
	4	11	227	210
U	-4	11	160	243
	5	11	486	494
	-5	11	427	449
	6	11	408	452
	-6	11	349	408
	7	11	313	276
	-7	11	298	292
	10	11	152	103
	0	12	352	351
	2	12	314	320
	-2	12	248	278
U	3	12	161	180
	-3	12	220	207
	6	12	167	183
	-6	12	256	251
	7	12	200	187
	-7	12	202	188
	8	12	286	277
	-8	12	251	245
	-9	12	140	95
	1	13	355	349
	-1	13	305	314
	2	13	354	378
	-2	13	420	435
	3	13	307	301
	-3	13	237	239
	4	13	192	174
	-4	13	210	201
U	-5	13	150	141
	8	13	189	158
	-8	13	201	202
	0	14	421	409
	1	14	193	129
	2	14	181	129
	5	14	215	228
	-5	14	209	235
	6	14	321	335
	-6	14	297	333
	0	15	156	129
	**L =		2****	
E	0	0	1779	1432
	1	0	203	201
	2	0	499	518
	4	0	791	789
	5	0	471	535
	6	0	862	939
	7	0	254	283
	8	0	911	1018
	10	0	328	304
	11	0	200	251
	12	0	423	423
	13	0	438	445
	0	1	1091	976
	1	1	808	898
	-1	1	938	908
	2	1	243	207
	-2	1	350	303
	3	1	623	625
	-3	1	608	581
	4	1	320	321
	-4	1	349	346
	5	1	1100	1159
	-5	1	1073	1077
	6	1	653	693
	-6	1	679	659
	7	1	222	250
	-7	1	263	256
	8	1	342	355
	-8	1	368	355
	9	1	297	347
	-9	1	363	360
	10	1	221	201
	-10	1	192	191
	11	1	224	252
U	-11	1	187	187
U	13	1	169	131
U	-13	1	146	139
	14	1	205	186
	-14	1	216	208
	0	2	1538	1489
	1	2	697	727
	-1	2	680	659
	2	2	841	866
	-2	2	710	668
	3	2	1056	1104
	-3	2	1164	1077
	4	2	1611	1705
	-4	2	1808	1809
	5	2	1173	1246
	-5	2	1264	1215
	6	2	514	572
	-6	2	661	677
	7	2	293	257
	-7	2	330	302
	8	2	776	791
	-8	2	870	853
	9	2	187	134
	11	2	238	224
	-11	2	194	219
	12	2	305	299
	-12	2	265	270
	13	2	303	266
	-13	2	294	276
	14	2	178	161
	0	3	112	79
	1	3	688	728
	-1	3	712	711
	2	3	914	938
	-2	3	971	902
	3	3	645	689
	-3	3	592	560
	4	3	1075	1153
	-4	3	1158	1133
	5	3	840	864
	-5	3	780	760
	6	3	388	413
	-6	3	485	465
	7	3	362	323
	-7	3	297	256
U	9	3	154	118
	10	3	487	471
	-10	3	444	476
	11	3	272	267
	-11	3	192	188
	12	3	361	351
	-12	3	335	374
U	14	3	147	140
	-14	3	163	183
	0	4	166	122
	1	4	641	617
	-1	4	593	535
	2	4	1089	1110
	-2	4	1156	1077
	3	4	379	362
	-3	4	492	441
	4	4	1137	1169
	-4	4	1276	1240
	5	4	557	568
	-5	4	560	583
	6	4	329	353
	-6	4	430	418
	8	4	442	470
	-8	4	529	560
	9	4	197	188
	-9	4	185	126
	10	4	344	358
	-10	4	340	363
	11	4	278	257
	-11	4	202	224
	12	4	219	209
	-12	4	234	220
	13	4	381	360
	-13	4	335	322
	14	4	197	178
	-14	4	182	172
	0	5	182	172
	1	5	683	645
	-1	5	691	648
	2	5	585	621
	-2	5	667	652
	3	5	802	884
	-3	5	898	906
	4	5	810	862
	-4	5	808	821
	5	5	764	796
	-5	5	769	770
	6	5	264	266
	-6	5	328	334
	7	5	466	494
	-7	5	396	446
	8	5	317	330
	-8	5	356	373
	-9	5	252	224
	10	5	310	382
	-10	5	331	360
	11	5	299	296
	-11	5	300	288
	12	5	274	288
	-12	5	252	288
	13	5	188	186
U	-13	5	140	155
	0	6	438	426
	1	6	486	481
	-1	6	556	554
	2	6	350	367
	-2	6	405	389
	3	6	279	296
	-3	6	246	241
	4	6	668	723
	-4	6	668	662
	5	6	281	288
	-5	6	232	223
	6	6	237	272
	-6	6	246	297
	7	6	198	134
	-7	6	236	236
	8	6	252	271
	9	6	317	296
	-9	6	191	213
	10	6	203	197
U	-10	6	154	205
	11	6	345	312
	-11	6	306	295
U	12	6	147	136
U	-12	6	136	189
	13	6	240	228
	-13	6	158	176
	1	7	379	395
	-1	7	318	358
	2	7	177	186
	-2	7	292	264
	3	7	893	924
	-3	7	899	899
	4	7	404	409
	-4	7	453	460
	5	7	713	730
	-5	7	738	804
	6	7	481	451
	-6	7	506	480
	7	7	249	220
	-7	7	297	276
	9	7	325	310
	-9	7	328	316
	10	7	252	269
	-10	7	286	313
	11	7	225	236
	-11	7	225	239
U	13	7	140	119
	0	8	189	169
	1	8	219	245
	-1	8	310	346
	2	8	403	413
	-2	8	417	394
	3	8	281	291
	-3	8	211	211
	4	8	432	444
	-4	8	383	414
	5	8	248	248
	8	8	388	415
	-8	8	368	379
	9	8	350	315
	-9	8	250	258
U	10	8	145	142
	-10	8	212	192
	11	8	336	328
	-11	8	314	332
	0	9	526	516
	1	9	477	486
	-1	9	522	552
	2	9	424	455
	-2	9	562	564
	3	9	788	796
	-3	9	694	749
	4	9	246	277
	-4	9	342	378
	5	9	321	314
	-5	9	328	344
	-6	9	232	159
	7	9	236	251
	-7	9	265	288
	8	9	304	269
	-8	9	301	298
	9	9	408	397
	-9	9	324	362
	10	9	383	368
	-10	9	453	451
U	-11	9	136	73
	0	10	239	227
	1	10	444	423
	-1	10	424	428
	2	10	283	329
	-2	10	328	389
U	-3	10	150	145
	4	10	351	340
	-4	10	239	279
	5	10	228	171
U	-5	10	154	177
	6	10	354	352
	-6	10	326	376
	7	10	406	372
	-7	10	338	312
	9	10	186	172
	10	10	317	284
	-10	10	327	313
	1	11	265	271
	-1	11	358	339
	2	11	360	405
	-2	11	314	324
U	3	11	175	199
	-3	11	216	221
	4	11	494	500
	-4	11	484	508
	6	11	251	277
	-6	11	216	243
	8	11	285	249
	-8	11	241	236
	-9	11	154	184
	10	11	175	215
U	-10	11	135	196
	0	12	244	235
	1	12	258	236
U	-1	12	182	175
	2	12	231	252
	-2	12	221	281
	3	12	258	278
	-3	12	291	319
	5	12	257	280
	-5	12	304	293
	8	12	372	327
	2	13	322	314
	3	13	236	228
	4	13	342	360
	2	14	457	460
	3	14	245	249
	4	14	242	239
	5	14	214	176
U	1	15	158	99
	**L =		3****	
	2	0	113	90
	3	0	130	106
	4	0	773	749
	5	0	218	232
	6	0	475	503
	7	0	408	434
	8	0	302	315
U	9	0	159	197
	10	0	207	191
	11	0	341	359
	12	0	446	474
	0	1	525	455
	1	1	364	340
	-1	1	325	288
	2	1	273	282
	-2	1	238	246
	3	1	1156	1193
	-3	1	1236	1204
	4	1	747	799
	-4	1	671	680
	5	1	827	822
	-5	1	908	891
	6	1	471	506
	-6	1	477	491
	7	1	429	406
	-7	1	558	477
	8	1	322	356
	-8	1	272	265
	9	1	458	469
	-9	1	467	466
	10	1	560	553
	-10	1	574	560
	11	1	291	288
	-11	1	351	330
	12	1	250	245
	-12	1	217	216
U	14	1	130	71
	0	2	1199	1216
	1	2	794	782
	-1	2	969	870
	2	2	512	530
	-2	2	496	474
	3	2	554	536
	-3	2	598	537
	4	2	937	990
	-4	2	978	948
	5	2	535	527
	-5	2	510	505
	6	2	346	345
	-6	2	341	339
	7	2	161	109
U	-7	2	163	171
	8	2	374	370
	-8	2	340	322
	9	2	275	329
	-9	2	305	360
	10	2	319	333
	-10	2	388	420
U	11	2	185	209
U	-11	2	184	209
	12	2	249	248
	-12	2	266	253
	0	3	1232	1208
	1	3	1221	1174
	-1	3	1455	1305
	2	3	895	928
	-2	3	984	918
	3	3	1068	1105
	-3	3	1112	1040
	4	3	941	982
	-4	3	985	952
	5	3	920	866
	-5	3	869	873
	6	3	299	296
	-6	3	254	264
	7	3	336	373
	-7	3	458	470
	8	3	737	701
	-8	3	656	644
	9	3	376	352
	-9	3	373	336
	10	3	431	380
	-10	3	441	398
	11	3	422	439
	-11	3	458	484
	12	3	351	358
	-12	3	336	332
	0	4	582	550
	1	4	1409	1466
	-1	4	1586	1556
	2	4	577	553
	-2	4	445	448
	3	4	351	366
	-3	4	416	389
	4	4	644	666
	-4	4	664	603
	5	4	262	281
	-5	4	261	234
	6	4	259	258
	-6	4	280	254
	7	4	698	688
	-7	4	718	710
	8	4	226	241
	9	4	499	534
	-9	4	536	588
	10	4	283	277
	-10	4	320	329
	11	4	247	200
	-11	4	188	157
	-13	4	167	150

TABLE 3.1 (contd.)

	H	K	FOBS	FCAL
U	14	4	134	84
	0	5	646	633
	1	5	636	604
	-1	5	578	562
	2	5	362	373
	-2	5	506	451
	3	5	865	894
	-3	5	851	840
	4	5	666	694
	-4	5	707	692
	5	5	602	646
	-5	5	609	640
	6	5	275	266
	-6	5	306	306
	7	5	538	534
	-7	5	471	475
	8	5	301	299
	-8	5	295	261
	9	5	395	374
	-9	5	407	401
	11	5	370	341
	-11	5	328	342
	12	5	203	230
	-12	5	183	237
	0	6	767	779
	1	6	750	762
	-1	6	782	755
	2	6	335	342
	-2	6	306	284
	3	6	791	873
	-3	6	877	896
U	4	6	139	168
	-4	6	196	173
U	5	6	179	197
	-5	6	213	238
	6	6	293	276
	-6	6	285	286
	7	6	687	664
	-7	6	656	667
	8	6	279	247
	-8	6	290	229
	9	6	236	236
	-9	6	271	276
	10	6	205	197
U	11	6	154	78
U	12	6	155	147
	13	6	267	262
	-13	6	295	298
	1	7	855	883
	-1	7	873	861
	2	7	520	532
	-2	7	526	521
	3	7	303	315
	-3	7	378	397
	4	7	263	263
	-4	7	257	265
	5	7	296	258
U	-5	7	159	163
	6	7	506	516
	-6	7	465	459
	7	7	496	487
	-7	7	425	444
	9	7	501	518
	-9	7	539	563
	10	7	253	233
U	11	7	159	105
	12	7	251	204
	-12	7	243	219
	0	8	668	687
	1	8	390	400
	-1	8	282	290
	2	8	467	469
	-2	8	517	505
	3	8	476	469
	-3	8	535	554
	4	8	431	462
	-4	8	422	441
	5	8	197	164
	-5	8	257	236
	6	8	271	294
	-6	8	228	207
	7	8	241	249
	-7	8	187	230
	9	8	207	190
	-9	8	204	205
	10	8	224	230
	11	8	331	327
	-11	8	321	333
U	0	9	204	216
	1	9	998	1034
	-1	9	1023	1017
	2	9	578	598
	-2	9	532	531
	3	9	318	311
	-3	9	366	370
	4	9	346	328
	-4	9	336	355
	5	9	471	466
	-5	9	471	445
U	6	9	177	225
	7	9	463	424
	-7	9	468	467
	8	9	278	237
U	-8	9	175	176
	9	9	253	213
	-9	9	254	243
	10	9	210	209
	-10	9	195	174
	11	9	174	110
	3	10	234	220
	-3	10	339	296
	5	10	272	298
	-5	10	322	357
	6	10	332	336
	-6	10	279	257
	8	10	307	339
	-8	10	261	302
U	-10	10	132	51
	0	11	411	411
	1	11	500	500
	-1	11	483	535
	2	11	272	272
	-2	11	256	234
U	3	11	188	146
	5	11	475	442
	-5	11	432	417
	6	11	204	180
	-6	11	218	177
	7	11	339	326
	-7	11	366	377
	8	11	225	239
	-8	11	202	213
U	9	11	136	149
	-9	11	174	113
	10	11	183	149
	-10	11	144	152
	0	12	582	559
	1	12	308	270
	-1	12	318	307
	2	12	340	296
	-2	12	314	267
U	3	12	173	230
	4	12	225	235
	-4	12	216	212
U	-5	12	146	137
	6	12	429	406
	-6	12	404	421
U	7	12	151	118
U	-7	12	155	119
	8	12	323	272
	-8	12	281	277
	0	13	477	508
	1	13	190	170
	-1	13	198	184
U	-2	13	157	120
U	3	13	149	174
	-3	13	173	147
	4	13	269	294
	-4	13	262	278
U	-5	13	133	41
	6	13	172	219
	-6	13	237	258
	0	14	217	226
	1	14	377	382
	-1	14	346	364
	2	14	290	301
	-2	14	322	321
	3	14	243	269
U	-3	14	154	213
U	4	14	140	136
	1	15	175	195
	-1	15	149	166
L = 4**				
	0	0	208	240
	1	0	975	895
	2	0	181	198
	3	0	414	422
	4	0	767	796
U	7	0	166	100
	8	0	343	382
	9	0	323	340
	10	0	304	239
	11	0	293	228
	12	0	426	412
U	0	1	123	121
	1	1	766	832
	-1	1	798	754
	2	1	205	217
	-2	1	354	311
	3	1	200	236
U	-3	1	106	119
	4	1	242	239
	-4	1	251	246
	5	1	203	272
	-5	1	248	281
	6	1	440	490
	-6	1	436	490
	7	1	500	465
	-7	1	466	417
	8	1	390	392
	-8	1	501	495
	9	1	524	506
	-9	1	480	430
	12	1	548	499
	-12	1	514	467
	13	1	207	187
	-13	1	245	202
	14	1	289	256
	-14	1	279	274
	0	2	619	619
	1	2	188	186
	-1	2	241	219
	2	2	698	728
	-2	2	623	611
	3	2	482	475
	-3	2	699	619
	4	2	876	894
	-4	2	1007	952
	5	2	468	475
	-5	2	456	407
	6	2	672	685
	-6	2	574	556
U	7	2	180	95
	8	2	404	406
	-8	2	318	323
	9	2	338	307
	-9	2	432	403
	11	2	236	294
U	-11	2	189	227
	12	2	241	189
	13	2	253	225
	-13	2	251	219
	14	2	220	184
U	-14	2	155	128
	0	3	1607	1573
	1	3	827	842
	-1	3	807	744
	2	3	1064	1109
	-2	3	1121	1037
	3	3	237	221
U	-3	3	140	95
	4	3	499	522
	-4	3	586	566
U	5	3	140	131
U	-5	3	168	122
	6	3	542	530
	-6	3	554	517
	7	3	624	686
	-7	3	614	657
	8	3	599	587
	-8	3	670	624
	9	3	573	563
	-9	3	504	512
U	10	3	215	117
U	11	3	211	169
	12	3	403	342
	-12	3	310	277
U	14	3	146	98
	-14	3	175	135
	0	4	1517	1468
	1	4	1282	1305
	-1	4	1359	1307
	2	4	690	704
	-2	4	686	629
	3	4	1119	1181
	-3	4	1276	1224
	4	4	355	342
	-4	4	431	378
	5	4	703	745
	-5	4	668	661
	6	4	631	636
	-6	4	666	642
	7	4	258	274
U	-7	4	184	261
	9	4	597	591
	-9	4	675	663
	11	4	333	320
	-11	4	222	249
	12	4	214	209
	-12	4	253	263
U	-13	4	179	122
	0	5	921	911
	1	5	1260	1303
	-1	5	1248	1241
U	-2	5	149	130
	3	5	345	383
	-3	5	241	237
	4	5	386	381
	-4	5	355	342
	5	5	709	715
	-5	5	754	760
	6	5	569	557
	-6	5	464	455
	7	5	549	555
	-7	5	552	550
	8	5	662	675
	-8	5	638	668
	9	5	560	468
	-9	5	483	460
	11	5	217	210
	12	5	245	187
	13	5	298	253
	-13	5	207	189
	0	6	408	454
	1	6	1112	1133
	-1	6	1151	1122
	2	6	495	515
	-2	6	470	480
	3	6	288	299
	-3	6	248	239
	4	6	531	509
	-4	6	565	515
	5	6	287	249
U	-5	6	185	139
	6	6	548	550
	-6	6	659	636
	7	6	503	489
	-7	6	488	497
	8	6	290	269
	-8	6	369	347
	9	6	555	542
	-9	6	545	571
	10	6	253	205
U	-10	6	204	204
	12	6	254	228
	-12	6	274	252
	0	7	298	274
	1	7	219	208
	-1	7	323	321
U	2	7	173	166
	4	7	311	340
	-4	7	304	318
	5	7	666	705
	-5	7	671	691
	7	7	271	262
U	-7	7	192	228
	8	7	542	462
	-8	7	486	443
U	-9	7	200	172
	10	7	263	190
	-10	7	285	224
U	11	7	167	183
	0	8	225	156
U	-1	8	164	109
	2	8	274	174
	-2	8	272	240
	3	8	339	389
	-3	8	224	243
	4	8	245	282
	-4	8	379	317
	5	8	253	211
	-5	8	311	272
	6	8	355	396
	-6	8	433	442
	7	8	329	367
	-7	8	331	388
	9	8	251	237
	-9	8	260	223
	-10	8	204	212
U	12	8	140	53
	0	9	263	212
	1	9	314	315
	-1	9	406	405
	3	9	508	502
	-3	9	511	518
U	4	9	191	207
	-4	9	263	275
	5	9	467	461
	-5	9	439	429
	6	9	368	355
	-6	9	445	420
	8	9	244	121
U	0	10	198	168
	1	10	267	274
	-1	10	257	253
U	-2	10	214	193
	3	10	384	358
	-3	10	282	267
	4	10	388	417
	-4	10	442	478
	6	10	330	367
	-6	10	305	333
	7	10	399	389
	-7	10	361	369
U	-10	10	161	175
U	0	11	208	129
	1	11	267	247
U	-1	11	212	199
	2	11	542	551
	-2	11	509	567
	3	11	434	477
	-3	11	433	459
	4	11	528	575
	-4	11	565	585
	6	11	312	290
	-6	11	288	327
U	7	11	184	129
	-7	11	251	171
U	9	11	177	167
U	-9	11	177	196
	0	12	272	310
U	-1	12	205	130
	2	12	719	691
	-2	12	708	675
	4	12	594	593
	-4	12	604	609
	5	12	238	189
	6	12	435	413
	-6	12	423	394
	7	12	236	222
	-7	12	209	170
	8	12	204	193
U	-8	12	167	153
U	1	13	175	151
	2	13	283	247
U	-2	13	196	228
U	3	13	166	105
	4	13	367	340
	-4	13	363	336
	6	13	241	228
	2	14	231	267
	-2	14	253	275
	3	14	235	235
	-3	14	287	255
U	4	14	150	176
	-4	14	212	172
L = 5**				
	1	0	1038	1007
	2	0	1057	1034
	3	0	483	441
	4	0	1534	1538
	6	0	248	186
	7	0	289	296
	8	0	262	215
	9	0	446	455
U	10	0	225	230
	1	1	1202	1218
	-1	1	1441	1297
	2	1	780	813
	-2	1	926	844
	3	1	301	286
	-3	1	296	245
	4	1	829	820
	-4	1	896	797
	5	1	685	694
	-5	1	716	642
	6	1	393	401
	-6	1	411	391
	7	1	311	338
	-7	1	372	391
	8	1	255	273
U	-8	1	204	246
U	-9	1	195	192
	10	1	282	253
	-10	1	321	251
	11	1	280	269
	-11	1	308	265
	12	1	232	134
U	-12	1	188	120
	13	1	332	253
	-13	1	345	241
	0	2	1165	1108
	1	2	772	779
	-1	2	860	772
	2	2	1326	1350
	-2	2	1310	1205
	3	2	976	952
	-3	2	1058	931
	4	2	1389	1383
	-4	2	1571	1448
	5	2	306	313
	-5	2	352	344
	6	2	255	238
	-6	2	320	307
	7	2	332	306
	-7	2	309	294
	8	2	347	376
	-8	2	286	301
	9	2	277	236
	-9	2	246	214
	10	2	449	372
	-10	2	491	438
U	-11	2	210	130
U	12	2	184	103
	-13	2	219	176
	0	3	554	531
	1	3	723	725
	-1	3	958	876
	2	3	582	591
	-2	3	639	570
	3	3	237	230
	-3	3	283	278
	4	3	384	380
	-4	3	414	385
	5	3	289	284
	6	3	283	343
	-6	3	390	334
	7	3	361	359
	-7	3	410	384
	8	3	657	577
	-8	3	607	535
	-9	3	253	251
	10	3	245	259
U	-10	3	212	229
U	13	3	186	144
	0	4	502	515
	1	4	387	389
	-1	4	454	388
	2	4	489	520
	-2	4	648	585
	3	4	396	406
	-3	4	528	461
	-4	4	185	187
U	5	4	171	145
	-5	4	262	232
	6	4	258	306
	-6	4	327	340
U	7	4	207	280
	-7	4	234	295
	8	4	627	570
	-8	4	595	518
	9	4	460	418
	-9	4	438	437
	10	4	401	352
	-10	4	338	364
	11	4	231	153
U	-11	4	183	144
	13	4	201	168
	-13	4	198	212
	0	5	306	247
	1	5	1345	1360
	-1	5	1494	1394
	2	5	344	347
	-2	5	356	325
	3	5	343	331
	-3	5	328	342
	4	5	346	322
	-4	5	318	302
U	5	5	169	199
	6	5	314	322
	-6	5	363	345
	7	5	951	895
	-7	5	937	823
	8	5	451	459
	-8	5	468	462
	9	5	320	253
	-9	5	335	276
	10	5	279	243
U	-12	5	207	143
	13	5	210	148
	0	6	900	838
	1	6	297	310
	-1	6	254	209
	2	6	532	573
	-2	6	739	702
	3	6	326	286
	-3	6	477	438
	4	6	260	292
	-4	6	257	247
U	5	6	204	196
	-5	6	227	227
	6	6	322	331
	-6	6	347	331
	7	6	678	654
	-7	6	685	638
	8	6	299	267
	-8	6	288	253
	9	6	360	339
	-9	6	324	310
	11	6	251	258
	-12	6	219	210
	1	7	559	533
	-1	7	527	488
	2	7	496	493
	-2	7	433	431
	3	7	269	296
	-3	7	247	248
	4	7	446	481
	-4	7	513	493
U	6	7	183	176
	7	7	688	705
	-7	7	682	648
U	8	7	219	152
U	9	7	214	195
	10	7	235	230
U	-10	7	201	208
U	11	7	180	91
	3	8	367	401
	-3	8	340	363
	5	8	266	242
	7	8	290	273
	-7	8	355	270
	9	8	352	339
	-9	8	239	257
	10	8	253	217
	-10	8	244	248
	1	9	263	260
	-1	9	267	275
	2	9	262	193
	-2	9	303	275
U	3	9	189	220
U	-3	9	206	255
	5	9	648	602
	-5	9	600	590
	6	9	429	417
	-6	9	390	370
	7	9	302	261
	-7	9	345	319
U	-8	9	196	56
	1	10	586	566
	-1	10	561	530
U	2	10	187	177
	3	10	505	493
	-3	10	454	406
	5	10	514	484
	-5	10	492	456
	6	10	438	415
	-6	10	380	364
	7	10	279	289
	-7	10	281	221
	9	10	213	244
U	10	10	182	125
	0	11	469	430
	3	11	284	234
	-3	11	268	271
U	-4	11	220	256
	5	11	388	395
	-5	11	354	368
	6	11	415	385
	-6	11	503	458
	-7	11	239	167
	8	11	228	200
	-8	11	207	197
	-9	11	195	202
	1	12	269	258
	-1	12	310	276
	3	12	307	300
	-3	12	241	258
	4	12	245	190
U	-4	12	208	187
	5	12	237	249
	-5	12	231	256
	6	12	264	255
	7	12	258	233
U	-7	12	172	200
	0	13	526	504
	1	13	229	186
U	-1	13	202	174
	2	13	252	250
	3	13	271	271
	-3	13	222	283
U	-4	13	181	193
	6	13	247	223
	-6	13	358	336
U	0	14	172	187
	1	14	211	215
	-1	14	269	256
	2	14	190	144
U	-2	14	180	157
U	3	14	153	123
L = 6**				
	0	0	493	526
	1	0	614	609
	2	0	173	171
	3	0	665	682
	4	0	182	151
	5	0	609	661
	7	0	242	266
	8	0	312	243
	9	0	419	478
	11	0	321	317
	1	1	121	81
	-1	1	119	66
	2	1	667	704
	-2	1	794	757
	3	1	214	201
	-3	1	236	231
	4	1	1050	1074
	-4	1	1038	992
	5	1	546	505
	-5	1	471	487
	6	1	597	579
	-6	1	697	650
	7	1	240	220
	-7	1	249	201
	9	1	236	154
U	-10	1	221	114
	11	1	317	293
	-11	1	318	300
	12	1	548	513
	-12	1	506	504
	-13	1	220	190
	0	2	723	729
	1	2	243	255
	-1	2	208	191
	2	2	241	258
	-2	2	306	273
	3	2	557	613
	-3	2	592	586
U	-4	2	148	79
	5	2	382	372
	-5	2	479	432
	6	2	202	152
U	-6	2	165	112
	7	2	222	205
U	-7	2	212	169
	8	2	455	446
	-8	2	425	424
U	-10	2	211	50
	11	2	296	287
	-11	2	326	275
	12	2	358	334
	-12	2	408	364
	0	3	730	709
	1	3	348	356
	-1	3	441	441
	2	3	392	397
	-2	3	593	546
	3	3	449	500
	-3	3	531	522
	4	3	911	871
	-4	3	879	827
	5	3	583	612
	-5	3	619	647
	6	3	501	444
	-6	3	502	453
	7	3	327	311
	-7	3	384	366
	8	3	307	262
U	-8	3	217	227
	9	3	359	352
	-9	3	340	339
	11	3	424	417
	-11	3	455	464
	12	3	309	230
	0	4	171	143
	1	4	864	843
	-1	4	917	914
	2	4	332	313
	-2	4	294	286
	3	4	257	243
U	-3	4	159	145
	4	4	316	340
	-4	4	394	394
	6	4	330	297
	-6	4	388	299
U	7	4	220	205
	-7	4	303	266
	8	4	245	241
U	-8	4	198	230
	9	4	602	552
	-9	4	541	547
U	10	4	193	191
U	-10	4	213	192
	12	4	267	227
	-12	4	247	244
	0	5	1243	1220
	1	5	663	667
	-1	5	628	642
	2	5	461	450
	-2	5	371	358
	3	5	270	255
	-3	5	232	245
	5	5	664	586
	-5	5	752	658
	6	5	233	223
	-6	5	271	261
	7	5	545	515
	-7	5	575	577
	8	5	355	335
	-8	5	280	267
	9	5	372	352
	-9	5	335	337
	11	5	240	200
	-11	5	281	250
	12	5	207	195
	0	6	537	540
	1	6	931	957
	-1	6	1041	992
U	2	6	178	172
	3	6	382	364
	-3	6	385	366
	4	6	257	248
	5	6	439	401
	-5	6	392	378
	6	6	345	364
	-6	6	361	373
U	-7	6	202	268
U	-8	6	208	194
	9	6	623	565
	-9	6	570	618
U	10	6	172	167
U	-12	6	156	99
	0	7	453	447
	1	7	912	937
	-1	7	933	945
	2	7	340	349
	-2	7	318	315
	3	7	515	535

TABLE 3.1 (contd.)

H	K	FOBS	FCAL
-3	7	489	488
4	7	293	273
-4	7	323	303
U -5	7	220	201
7	7	355	359
-7	7	388	412
10	7	215	160
U-10	7	176	166
0	8	348	364
1	8	527	494
-1	8	521	527
2	8	604	602
-2	8	538	536
3	8	560	571
-3	8	601	590
4	8	394	354
-4	8	349	310
5	8	522	491
-5	8	559	536
U -7	8	217	176
8	8	521	475
-8	8	449	441
9	8	281	258
-9	8	357	334
10	8	313	310
-10	8	238	236
U 11	8	171	167
-11	8	191	213
U 0	9	199	226
1	9	353	383
-1	9	332	328
2	9	272	218
-2	9	235	275
4	9	300	290
-4	9	235	268
U 6	9	195	170
U 7	9	213	227
-7	9	296	269
U -8	9	201	196
9	9	259	212
U -9	9	198	246
0	10	569	565
1	10	340	359
-1	10	353	296
2	10	671	649
-2	10	609	592
3	10	475	450
-3	10	434	461
4	10	470	450
-4	10	443	444
5	10	239	203
U -5	10	193	192
6	10	390	360
-6	10	409	379
7	10	252	228
-7	10	214	202
8	10	299	284
-8	10	223	236
U 9	10	171	105
1	11	363	342
-1	11	417	390
2	11	304	314
-2	11	336	338
3	11	340	372
-3	11	372	406
U 5	11	205	140
1	12	219	245
2	12	338	302
-2	12	359	335
3	12	305	264
-3	12	245	216
4	12	243	220
-4	12	303	264
5	12	217	207
6	12	233	238
-6	12	205	241
0	13	386	355
U 1	13	188	204
-1	13	207	184
2	13	342	337
-2	13	369	369
0	14	198	140
L = 7**			
2	0	1549	1592
U 3	0	129	135
4	0	2071	2114
5	0	268	265
6	0	354	347
U 7	0	219	214
8	0	275	283
9	0	264	233
10	0	743	698
11	0	256	250
12	0	214	242
U 0	1	160	219
1	1	212	240
-1	1	225	233
2	1	170	158
-2	1	147	140
3	1	352	354
-3	1	465	422
4	1	354	356
-4	1	327	347
5	1	970	1018
-5	1	985	1004
6	1	263	283
-6	1	302	279
7	1	229	282
U 10	1	204	272
-10	1	249	258
11	1	250	155
12	1	257	326
-12	1	317	326
0	2	702	737
2	2	636	612
-2	2	649	631
3	2	421	437
-3	2	468	462
4	2	927	954
-4	2	1105	1093
5	2	202	220
-5	2	292	219
6	2	366	439
-6	2	405	434
8	2	309	327
-8	2	450	411
9	2	422	426
-9	2	454	444
10	2	510	488
-10	2	508	526
U-11	2	180	81
12	2	355	353
-12	2	384	393
0	3	261	223
1	3	245	261
-1	3	276	280
2	3	691	735
-2	3	767	744
3	3	670	740
-3	3	747	764
4	3	213	221
U -4	3	161	208
5	3	538	550
-5	3	452	424
6	3	413	437
-6	3	463	443
7	3	456	460
-7	3	234	300
8	3	380	330
-8	3	363	320
U 9	3	211	202
10	3	441	383
-10	3	387	365
11	3	235	202
U-11	3	200	149
0	4	558	491
1	4	193	156
-1	4	240	217
2	4	304	277
-2	4	272	231
3	4	694	684
-3	4	800	767
U 4	4	161	50
-4	4	213	197
U 5	4	182	155
-5	4	236	213
6	4	331	318
-6	4	274	276
7	4	261	198
U -7	4	206	221
8	4	330	326
-8	4	438	430
9	4	325	291
-9	4	337	348
10	4	331	304
-10	4	313	321
11	4	343	327
-11	4	410	379
12	4	198	178
-12	4	213	219
0	5	314	334
1	5	338	299
-1	5	244	223
U 2	5	181	214
U 3	5	193	207
U -3	5	191	233
4	5	320	309
-4	5	343	305
5	5	458	468
-5	5	426	450
6	5	453	466
-6	5	479	468
7	5	456	487
-7	5	314	384
8	5	271	291
U -8	5	187	250
-10	5	269	245
11	5	285	251
-11	5	213	193
1	6	378	383
-1	6	337	336
4	6	369	406
-4	6	359	348
5	6	396	434
-5	6	339	406
6	6	430	351
-6	6	351	318
U 7	6	203	196
-7	6	254	220
8	6	256	230
-8	6	283	255
U 9	6	197	215
11	6	320	280
-11	6	308	322
1	7	907	906
-1	7	972	956
2	7	477	470
-2	7	424	439
U 3	7	194	97
U -3	7	179	87
4	7	422	424
-4	7	449	454
5	7	526	492
-5	7	501	543
U 6	7	198	171
-6	7	268	241
7	7	569	465
-7	7	567	506
U 8	7	217	172
U -8	7	187	122
9	7	245	262
-9	7	261	309
10	7	272	353
-10	7	333	358
0	8	467	450
1	8	421	381
-1	8	362	334
U 2	8	212	225
-2	8	325	315
3	8	582	585
-3	8	556	567
U 4	8	218	234
U -4	8	192	206
5	8	438	395
-5	8	403	365
9	8	379	343
-9	8	283	251
U 10	8	155	143
-10	8	233	201
U 0	9	197	229
1	9	491	505
-1	9	582	565
U 3	9	213	196
-3	9	250	167
4	9	239	233
-4	9	248	283
5	9	549	528
-5	9	560	551
6	9	511	493
-6	9	480	525
7	9	268	278
-7	9	278	312
-8	9	219	221
U 9	9	173	145
0	10	353	366
2	10	236	160
U -2	10	204	196
4	10	232	227
-4	10	269	221
5	10	238	188
-5	10	218	248
7	10	295	264
-7	10	268	242
8	10	248	253
-8	10	214	232
0	11	293	314
1	11	231	221
-1	11	298	236
3	11	224	247
-3	11	222	242
4	11	235	250
5	11	378	375
-5	11	342	367
6	11	327	318
-6	11	327	312
U 7	11	175	138
2	12	305	304
-2	12	235	271
U 5	12	184	135
-5	12	218	167
1	13	289	295
-1	13	244	249
U 3	13	144	170
L = 8**			
0	0	562	507
2	0	435	472
3	0	232	234
4	0	324	379
6	0	292	251
7	0	532	550
8	0	478	491
0	1	1015	929
2	1	831	888
-2	1	929	905
3	1	270	287
-3	1	244	247
4	1	542	584
-4	1	429	463
6	1	684	673
-6	1	634	654
7	1	308	333
-7	1	352	347
8	1	553	537
-8	1	514	486
U 9	1	188	140
11	1	309	167
12	1	228	190
U-12	1	158	199
U 0	2	128	44
1	2	411	415
-1	2	586	505
2	2	409	444
-2	2	439	430
3	2	363	362
-3	2	268	293
4	2	394	423
-4	2	376	411
5	2	348	344
-5	2	499	457
6	2	249	229
U -6	2	190	192
7	2	530	493
-7	2	553	514
8	2	367	398
-8	2	368	387
9	2	268	237
-9	2	398	365
11	2	317	300
-11	2	407	398
12	2	285	241
-12	2	208	205
0	3	310	310
1	3	368	363
-1	3	353	387
2	3	525	550
-2	3	441	449
3	3	256	218
-3	3	221	192
4	3	699	688
-4	3	632	594
5	3	470	481
-5	3	392	407
6	3	264	259
-6	3	404	385
7	3	505	527
-7	3	451	477
8	3	581	586
-8	3	399	459
U 11	3	192	209
0	4	385	388
U -1	4	159	165
U 3	4	185	188
4	4	474	513
-4	4	497	486
5	4	295	339
-5	4	402	453
U -6	4	202	187
7	4	254	278
-7	4	290	300
9	4	233	259
-9	4	339	366
10	4	232	192
-10	4	265	188
U 11	4	176	173
-11	4	276	278
1	5	283	292
-1	5	358	352
3	5	251	238
-3	5	286	254
4	5	441	449
-4	5	464	411
5	5	391	384
-5	5	289	298
6	5	262	186
-6	5	254	206
7	5	601	582
-7	5	508	523
-9	5	219	209
10	5	210	169
-10	5	226	160
U-11	5	171	68
U 0	6	235	122
1	6	417	442
-1	6	446	457
3	6	649	663
-3	6	659	615
4	6	327	336
-4	6	402	396
5	6	285	248
-5	6	239	266
6	6	237	241
-6	6	342	278
8	6	281	285
-8	6	231	275
9	6	495	452
-9	6	417	448
1	7	591	581
-1	7	534	524
U 2	7	196	183
3	7	321	329
-3	7	331	273
4	7	242	250
-4	7	253	281
5	7	648	597
-5	7	606	595
6	7	356	330
-6	7	247	256
7	7	354	329
-7	7	354	344
U 8	7	202	242
-8	7	269	288
U 9	7	205	166
-9	7	217	194
-10	7	187	130
1	8	585	561
-1	8	551	547
2	8	332	309
-2	8	247	245
3	8	710	744
-3	8	790	773
4	8	368	353
-4	8	346	359
5	8	439	441
-5	8	375	388
7	8	507	461
-7	8	428	438
U 8	8	177	112
9	8	280	263
-9	8	263	267
1	9	458	453
-1	9	387	419
2	9	371	381
-2	9	364	392
3	9	171	378
-3	9	325	332
5	9	504	469
-5	9	482	493
6	9	355	381
-6	9	263	296
7	9	268	294
-7	9	301	363
8	9	222	173
U 1	10	189	146
2	10	294	270
-2	10	287	271
3	10	406	448
-3	10	468	492
4	10	307	313
-4	10	214	232
5	10	312	297
-5	10	296	272
U 7	10	192	143
U 1	11	196	207
3	11	275	273
-3	11	263	267
U 5	11	160	181
-5	11	230	202
-2	12	225	211
L = 9**			
1	0	479	516
2	0	607	647
3	0	245	233
5	0	239	253
6	0	264	163
U 7	0	193	229
8	0	849	852
9	0	448	483
10	0	306	274
0	1	614	588
1	1	900	944
-1	1	919	893
2	1	356	415
-2	1	421	401
3	1	249	264
-3	1	249	262
4	1	254	252
-4	1	339	348
U 5	1	206	106
-5	1	203	207
U -6	1	189	215
7	1	321	305
-7	1	291	270
U 9	1	216	158
10	1	464	419
-10	1	438	398
0	2	1169	1191
1	2	761	773
-1	2	813	775
2	2	519	557
-2	2	710	688
3	2	409	455
-3	2	457	441
U 5	2	198	210
-5	2	299	283
6	2	241	208
U -6	2	178	159
7	2	369	350
-7	2	361	318
8	2	367	415
-8	2	479	479
9	2	422	434
-9	2	426	416
10	2	342	282
-10	2	229	212
0	3	667	668
3	3	453	466
-3	3	559	512
5	3	213	186
U 6	3	202	198
-6	3	241	195
7	3	301	283
-7	3	220	255
8	3	306	292
-8	3	300	285
9	3	304	284
-9	3	274	247
U 10	3	201	254
U-10	3	176	215
0	4	1042	1093
1	4	384	387
-1	4	403	382
2	4	298	328
-2	4	465	458
3	4	196	174
U -3	4	189	142
4	4	321	302
-4	4	371	382
5	4	580	627
-5	4	560	603
6	4	253	304
-6	4	270	269
8	4	255	249
-8	4	315	317
9	4	378	347
-9	4	295	276
U 10	4	193	187
U-10	4	170	127
0	5	700	697
U 1	5	196	119
-1	5	273	250
2	5	545	552
-2	5	449	475
3	5	329	321
-3	5	360	373
U -4	5	181	141
5	5	362	390
-5	5	364	385
7	5	271	252
-7	5	284	245
9	5	316	340
-9	5	258	284
0	6	451	449
2	6	281	247
-2	6	280	278
3	6	296	294
-3	6	267	274
4	6	451	469
-4	6	393	480
5	6	475	484
-5	6	450	472
8	6	283	216
U -8	6	171	162
9	6	283	300
U -9	6	193	236
0	7	502	523
1	7	625	606
-1	7	713	682
2	7	246	252
-2	7	227	284
3	7	255	266
-3	7	249	241
4	7	243	213
5	7	533	515
-5	7	494	472
6	7	223	197
U -6	7	186	247
7	7	263	260
U -7	7	200	202
8	7	268	246
-8	7	211	256
9	7	257	216
-9	7	244	219
0	8	394	403
U 1	8	210	118
3	8	253	255
-3	8	253	237
4	8	256	210
5	8	267	247
U -5	8	199	198
6	8	264	252
-6	8	313	299
7	8	254	212
-7	8	249	182
U 8	8	223	181
U -8	8	172	170
0	9	307	251
1	9	384	332
-1	9	345	337
2	9	552	518
-2	9	557	548
U 3	9	203	193
U -3	9	171	144
4	9	294	297
-4	9	334	331
5	9	272	269
-5	9	285	302
6	9	379	376
-6	9	451	439
7	9	255	175
U -7	9	160	88
0	10	247	205
3	10	274	221
5	10	242	256
0	11	501	505
U 1	11	194	181
2	11	351	361
-2	11	369	381
L = 10**			
0	0	420	437
U 1	0	206	205
3	0	388	454
5	0	251	266
6	0	298	236
7	0	391	433
8	0	532	441
0	1	899	984
1	1	582	588
2	1	387	418
3	1	429	509
6	1	558	608
8	1	268	291
0	2	641	668
2	2	298	265
3	2	344	395
U 4	2	199	315
6	2	460	465
8	2	388	329
0	3	413	412
1	3	368	385
2	3	444	489
3	3	342	363
6	3	439	429
U 7	3	232	232
8	3	282	254
U 0	4	207	161
1	4	347	391
2	4	294	241
3	4	591	625
5	4	519	530
6	4	370	379
7	4	371	354
U 8	4	207	176
2	5	380	377
3	5	564	601
4	5	337	377
5	5	239	219
U 6	5	140	233
1	6	382	383
3	6	538	590
5	6	401	405
7	6	268	243
8	6	248	221
1	7	267	304
2	7	470	494
3	7	376	356
5	7	231	220
U 6	7	188	237
U 2	8	194	270
4	8	272	276
6	8	265	335
1	9	364	382
2	9	250	241
3	9	347	290
4	9	223	141
5	9	199	196
0	10	249	301
U 2	10	191	139
L = 11**			
3	0	286	321
4	0	372	394
5	0	532	652
8	0	458	451
U 0	1	212	194
2	1	488	534
5	1	281	228
8	1	333	326
1	2	274	331
2	2	265	271
3	2	366	395
4	2	506	549
5	2	324	372
U 6	2	209	134
U 7	2	225	133
1	3	250	311
2	3	775	846
4	3	678	667
5	3	284	299
U 8	3	235	180
1	4	419	434
U 2	4	200	154
3	4	391	457
4	4	385	408
5	4	682	670
7	4	255	221
0	5	330	327
1	5	438	449
2	5	417	393
3	5	355	390
4	5	648	684
5	5	433	466
0	6	313	320
U 2	6	203	244
3	6	502	539
4	6	397	423
5	6	393	439
U 0	7	237	243
2	7	261	203
3	7	252	279
U 4	7	200	190
5	7	228	301
U 6	7	159	185
U 1	8	210	235
U 3	8	183	230
U 1	9	186	247
2	9	220	270
L = 12**			
0	0	595	568
U 2	0	186	171
4	0	307	292
0	1	345	360
1	1	398	414
2	1	242	227
0	2	622	642
1	2	424	477
2	2	295	279
3	2	426	458
6	2	423	440
7	2	313	319
U 0	3	224	209
1	3	349	420
U 2	3	214	227
3	3	376	411
5	3	320	368
7	3	257	320
1	4	287	293
2	4	228	234
4	4	359	420
5	4	245	271
6	4	424	459
3	5	599	626
5	5	416	456
2	6	319	328
3	6	271	309
4	6	242	219
5	6	373	360
0	7	491	434
U 2	7	203	250
4	7	212	251
L = 13**			
U 3	0	203	296
0	1	346	385
2	1	317	378
U 4	1	183	251
1	2	336	312
4	2	216	188
0	3	531	575
U 1	3	188	195
2	3	272	337
4	3	359	398
5	3	224	168
1	4	279	293
3	4	307	323
U 3	5	179	199
1	6	394	414
L = 14**			
0	0	461	495
U 2	0	178	177
1	1	380	473
U 0	2	186	146
2	2	211	270

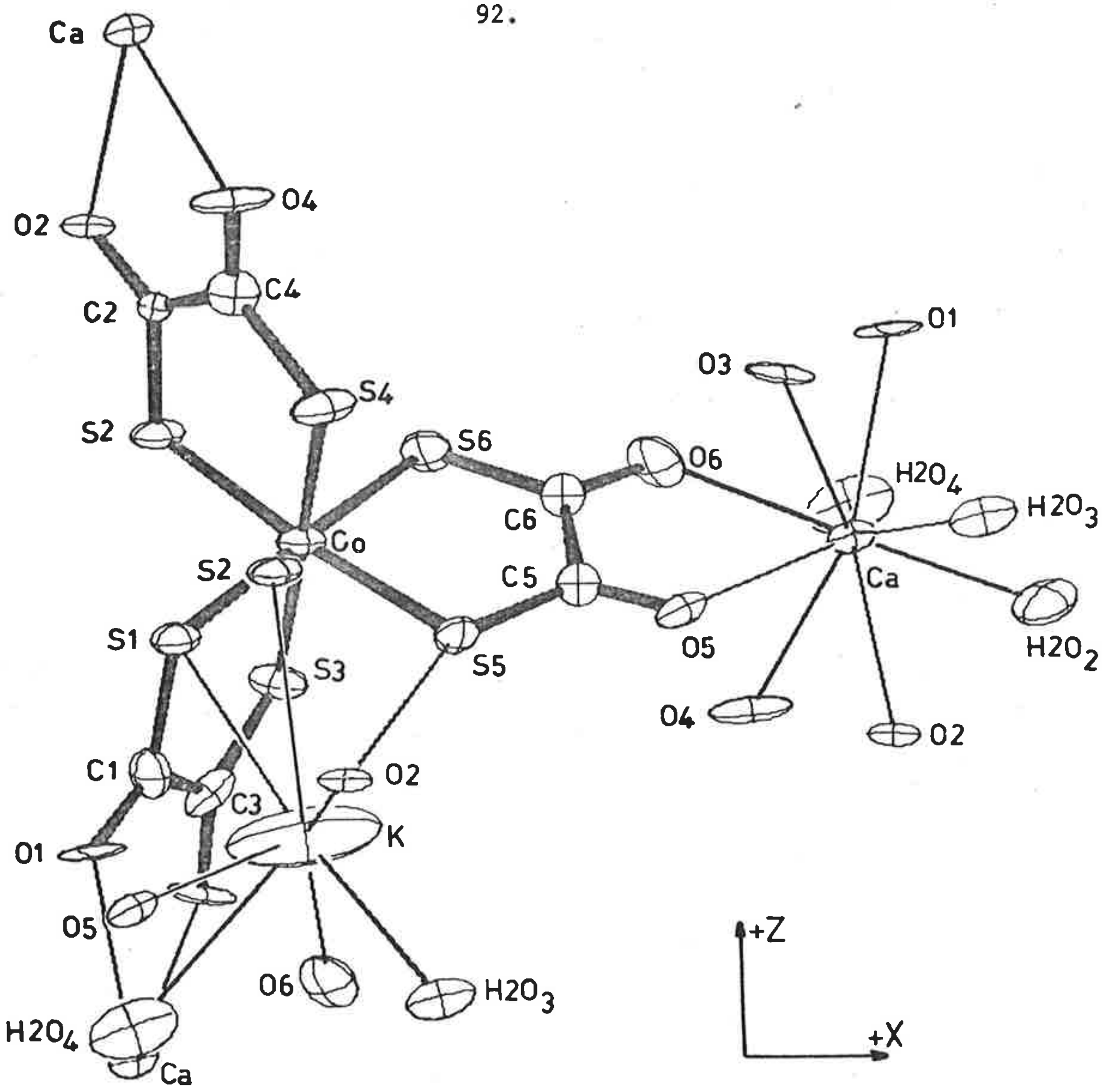
Ca
O2
O4
C2
C4
O1
O3
S4
S2
S6
O6
H2O$_4$
H2O$_3$
C6
Co
S2
C5
Ca
S1
S5
O5
H2O$_2$
S3
O4
O2
C1
O2
C3
K
O1
O5
+Z
O6
H2O$_3$
H2O$_4$
+X
Ca

FIGURE 3.1: Λ-K.Ca(+)[Co thiox$_3$].4H$_2$O, *b* AXIS PROJECTION SHOWING CLOSE CONTACTS.

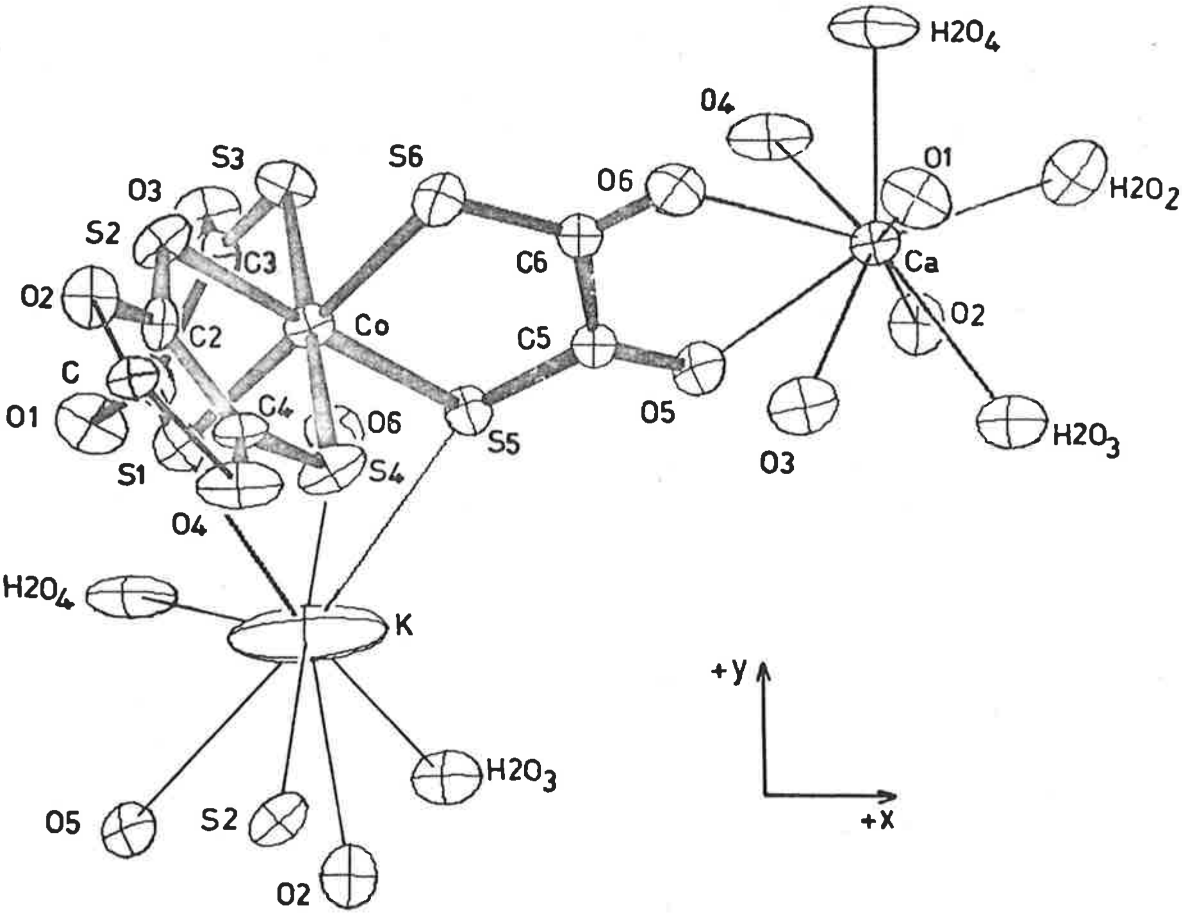
H2O4
O4
O1
H2O2
S3
S6
O6
O3
S2
C3
C6
Ca
O2
Co
C2
C5
O2
C
O1
C4
O6
O5
O3
H2O3
S1
S4
S5
O4
H2O4
K
+y
H2O3
+x
O5
S2
O2

FIGURE 3.2: Λ-K.Ca(+)[Co $thiox_3$].$4H_2O$, *c* AXIS PROJECTION (90° rotation of Figure 3.1 about *x*).

TABLE 3.2 POSITIONAL AND THERMAL PARAMETERS FOR K.Ca(+)$_{589}$[Co thiox$_3$].4H$_2$O^a: Λ CONFIGURATION.

Atom	*x*	*y*	*z*	β_{11}	β_{22}	β_{33}	β_{12}	β_{13}	β_{23}
Cations									
Ca	0780(2)	4397(2)	-2121(2)	413(21)	302(17)	214(22)	025(18)	054(21)	-007(19)
K	0778(6)	-2806(3)	-0733(4)	4089(118)	507(34)	704(46)	274(58)	538(74)	080(33)
Anion									
Co	0774(2)	-0138(2)	2130(2)	413(17)	337(15)	165(17)	021(13)	001(17)	034(14)
S$_1$	-0371(3)	-1191(3)	1187(3)	419(29)	393(24)	204(30)	-036(21)	015(25)	058(24)
S$_2$	-0529(3)	0587(3)	3171(3)	528(32)	451(25)	166(30)	191(24)	029(25)	073(23)
S$_3$	0558(3)	1085(3)	0767(3)	587(36)	359(26)	234(30)	-084(24)	-082(28)	075(22)
S$_4$	0976(3)	-1384(3)	3434(3)	722(38)	406(28)	258(32)	221(25)	125(30)	101(24)
S$_5$	2178(3)	-0869(3)	1204(3)	360(27)	396(26)	270(32)	-016(21)	053(26)	-141(24)
S$_6$	1910(3)	0961(3)	2997(3)	450(30)	463(26)	334(36)	062(22)	-021(28)	-195(27)
O$_1$	-1142(8)	-0996(8)	-0860(7)	796(100)	578(79)	055(78)	-113(72)	101(72)	-128(67)
O$_2$	-1154(8)	0100(8)	5197(7)	505(85)	611(84)	103(81)	003(68)	-012(68)	-038(67)
O$_3$	-0146(8)	0815(7)	-1279(8)	794(95)	518(78)	090(76)	077(67)	-123(73)	093(68)
O$_4$	0160(9)	-1526(7)	5454(8)	1187(120)	350(68)	144(80)	031(75)	118(80)	079(67)
O$_5$	4217(7)	-0498(7)	1423(7)	452(76)	453(67)	252(75)	024(65)	148(72)	-018(61)
O$_6$	4004(8)	1063(7)	2872(8)	562(86)	449(69)	514(93)	-034(63)	-156(83)	-243(75)
C$_1$	-0603(11)	-0620(11)	-0111(12)	302(117)	456(109)	468(133)	-131(98)	-051(109)	004(104)
C$_2$	-0553(10)	-0124(10)	4411(11)	214(113)	497(105)	172(113)	021(89)	-015(92)	019(92)
C$_3$	-0070(11)	0452(11)	-0303(12)	431(121)	451(110)	448(145)	-004(92)	236(110)	029(105)
C$_4$	0169(11)	-1051(10)	4550(12)	493(124)	207(88)	425(138)	028(88)	-003(107)	-054(99)
C$_5$	3288(10)	-0294(9)	1683(10)	453(107)	325(94)	119(110)	120(78)	267(97)	211(88)
C$_6$	3154(11)	0658(10)	2556(10)	504(114)	264(83)	105(115)	-008(86)	-135(96)	187(89)

(contd.)

TABLE 3.2 (contd.)

Atom	*x*	*y*	*z*	β_{11}	β_{22}	β_{33}	β_{12}	β_{13}	β_{23}
Water									
H_2O-1	2845(8)	2792(7)	0721(8)	691(96)	470(77)	374(93)	-022(72)	-001(84)	-041(70)
H_2O-2	2553(8)	3771(8)	-1470(8)	701(95)	693(89)	416(98)	175(73)	148(78)	291(81)
H_2O-3	2995(8)	4051(7)	2690(8)	793(92)	443(70)	320(88)	017(70)	131(79)	-024(70)
H_2O-4	0773(10)	2505(7)	-2429(8)	1336(125)	271(64)	695(110)	-009(83)	289(107)	051(71)

a. positional parameters (x 10^4): anisotropic thermal parameters (x 10^5).

TABLE 3.3 BOND DISTANCES AND ANGLES

Atoms	*Distance* (Å)	*Atoms*	*Angle (deg.)*	*Atoms*	*Angle (deg.)*
Ligand 1					
Co-S$_1$	2.250 (4)	S$_1$-Co-S$_3$	89.30 (14)		
S$_1$-C$_1$	1.721 (14)	Co-S$_1$-C$_1$	106.9 (5)	Co-S$_3$-C$_3$	104.8 (5)
C$_1$-O$_1$	1.207 (14)	S$_1$-C$_1$-O$_1$	125.1 (11)	S$_3$-C$_3$-O$_3$	123.2 (12)
C$_1$-C$_3$	1.539 (18)	S$_1$-C$_1$-C$_3$	115.9 (10)	S$_3$-C$_3$-C$_1$	121.0 (10)
C$_3$-O$_3$	1.246 (15)	O$_1$-C$_1$-C$_3$	119.0 (13)	O$_3$-C$_3$-C$_1$	115.8 (13)
S$_3$-C$_3$	1.689 (15)	Angle sum at C$_1$	360.0	Angle sum at C$_3$	360.0
Co-S$_3$	2.259 (4)	Sum of intra-chelate ring angles = 537.9°			
Ligand 2					
Co-S$_4$	2.230 (4)	S$_4$-Co-S$_2$	89.90 (15)		
S$_4$-C$_4$	1.707 (13)	Co-S$_4$-C$_4$	106.7 (5)	Co-S$_2$-C$_2$	105.1 (5)
C$_4$-O$_4$	1.228 (15)	S$_4$-C$_4$-O$_4$	123.5 (11)	S$_2$-C$_2$-O$_2$	122.0 (11)
C$_4$-C$_2$	1.493 (17)	S$_4$-C$_4$-C$_2$	117.7 (11)	S$_2$-C$_2$-C$_4$	120.1 (10)
C$_2$-O$_2$	1.224 (14)	O$_4$-C$_4$-C$_2$	118.8 (12)	O$_2$-C$_2$-C$_4$	117.9 (12)
S$_2$-C$_2$	1.724 (13)	Angle sum at C$_4$	360.0	Angle sum at C$_2$	360.0
Co-S$_2$	2.230 (4)	Sum of intra-chelate ring angles = 538.5°			

(contd.)

TABLE 3.3 (contd.)

Atoms	*Distance* (Å)	*Atoms*	*Angle (deg.)*	*Atoms*	*Angle (deg.)*
Ligand 3					
Co-S_5	2.256 (4)	S_5-Co-S_6	89.84 (15)		
S_5-C_5	1.658 (14)	Co-S_5-C_5	106.8 (5)	Co-S_6-C_6	106.9 (5)
C_5-O_5	1.220 (13)	S_5-C_5-O_5	127.0 (11)	S_6-C_6-O_6	126.5 (11)
C_5-C_6	1.603 (16)	S_5-C_5-C_6	118.1 (9)	S_6-C_6-C_5	118.1 (9)
C_6-O_6	1.231 (14)	O_5-C_5-C_6	114.9 (12)	O_6-C_6-C_5	115.3 (12)
S_6-C_6	1.672 (14)	Angle sum at C_5	360.0	Angle sum at C_6	359.9
Co-S_6	2.237 (4)	Sum of intra-chelate ring angles = 539.8°			

Interligand angles at Co

Atoms	*Angle (deg.)*	*Atoms*	*Angle (deg.)*	*Atoms*	*Angle (deg.)*
S_1-Co-S_2	93.78 (15)	S_3-Co-S_2	91.09 (15)	S_2-Co-S_5	175.31 (17)
S_1-Co-S_4	89.10 (16)	S_3-Co-S_4	178.17 (18)	S_2-Co-S_6	86.66 (15)
S_1-Co-S_5	89.87 (15)	S_3-Co-S_5	91.89 (15)	S_4-Co-S_5	87.21 (15)
S_1-Co-S_6	117.28 (17)	S_3-Co-S_6	88.01 (15)	S_4-Co-S_6	93.58 (17)

TABLE 3.4 UNWEIGHTED BEST PLANES THROUGH THE LIGANDS

Plane	*A*	*B*	*C*	*D*	*Distance from plane* (Å)
Ligand 1					
S_1, C_1, O_1)) S_3, C_3, O_3)	0.843	-0.440	-0.310	0.229	S_1, 0.077 : C_1, -0.010 : O_1, -0.087 : S_3, -0.079 : C_3, 0.013 : O_3, 0.086 : Co, 0.334
Ligand 2					
S_4, C_4, O_4)) S_2, C_2, O_2)	-0.717	-0.592	-0.368	1.331	S_4, 0.020 : C_4, 0.001 : O_4, -0.024 : S_2, -0.021 : C_2, 0.000 : O_2, 0.024 : Co, -0.177
Ligand 3					
S_5, C_5, O_5)) S_6, C_6, O_6)	-0.062	0.654	-0.754	1.984	S_5, 0.020 : C_5, -0.010 : O_5, -0.020 : S_6, -0.024 : C_6, 0.021 : O_6, 0.014 : Co, -0.085

TABLE 3.5 INTERPLANAR DIHEDRAL ANGLES

Plane 1	*Plane 2*	*Angle (deg.)*	*Plane 1*	*Plane 2*	*Angle (deg.)*
Interligand angles					
Co,S_1,S_3	Co,S_4,S_2	93.79 (15)	ligand 1[a]	ligand 2	103.31[b]
Co,S_1,S_3	Co,S_5,S_6	91.89 (16)	ligand 1	ligand 3	96.08
Co,S_4,S_2	Co,S_5,S_6	93.41 (17)	ligand 2	ligand 3	93.76
Intraligand angles					
Co,S_1,S_3	ligand 1	12.39			
Co,S_4,S_2	ligand 2	6.47			
Co,S_5,S_6	ligand 3	3.08			

a. ligand 1, 2, 3 refers to the six atom ligand planes defined in Table 3.4.

b. ORFFE does not compute angles for planes of more than three atoms.

TABLE 3.6 TORSION ANGLES IN THE CHELATE RINGS[a]

Bond	*Angle (deg.)*	*Bond*	*Angle (deg.)*	*Bond*	*Angle (deg.)*
Ligand 1		*Ligand 2*		*Ligand 3*	
Co-S_1	9.5 (5)	Co-S_4	6.2 (5)	Co-S_5	3.5 (5)
S_1-C_1	3.6 (11)	S_4-C_4	5.8 (11)	S_5-C_5	4.9 (9)
C_1-C_3	7.8 (15)	C_4-C_2	1.5 (15)	C_5-C_6	4.1 (12)
S_3-C_3	14.6 (12)	S_2-C_2	3.6 (11)	S_6-C_6	0.9 (9)
Co-S_3	12.7 (5)	Co-S_2	5.4 (5)	Co-S_6	1.5 (5)

a. The distances listed in Table 3.4 indicate that the chelate rings are closely planar; however, some of the torsion angles are still significant.

TABLE 3.7 THE SULPHUR-OXYGEN ENVIRONMENT OF THE CATIONS

Atom	*Symmetry*[a] *Transform*	*Distance* (Å)	*Atom*	*Symmetry Transform*	*Distance* (Å)
with Ca^{+2}			*with* K^+		
H_2O_2	1	2.460 (10)	S_1	1	3.380 (6)
H_2O_4	1	2.447 (9)	S_5	1	3.790 (7)
O_2	2	2.485 (9)	O_1[b]	1	3.322 (12)
O_4	2	2.573 (10)	O_6	6	2.784 (10)
O_1	3	2.476 (9)	H_2O_3	6	2.882 (11)
O_3	3	2.733 (10)	S_2	7	3.668 (6)
H_2O_3	4	2.508 (10)	O_2	7	2.791 (11)
O_5	5	2.531 (9)	H_2O_4	8	2.924 (13)
O_6	5	2.442 (10)	O_5	9	3.017 (11)

a. See Table 3.10.

b. The contact $K^+ \ldots O_1$ is not shown in Figures 3.1 and 3.2.

TABLE 3.8 POSSIBLE HYDROGEN BONDS INVOLVING WATER.

$O...O < 3.25$ Å, $O...S < 3.60$ Å.

Atom	*Symmetry Transform*	*Distance* (Å)
with H_2O_1		
O_3	10	3.130 (13)
O_4	6	2.971 (14)
H_2O_2	1	2.896 (13)
H_2O_3	1	2.833 (13)
S_3	1	3.576 (11)
S_4	6	3.558 (11)
with H_2O_2		
O_2	2	2.854 (13)
H_2O_4	1	2.959 (15)
S_2	10	3.216 (10)
S_4	6	3.557 (10)
with H_2O_3		
O_2	11	2.916 (13)
O_3	10	2.845 (13)
H_2O_2	12	3.034 (13)
S_1	2	3.522 (10)
with H_2O_4		
O_1	3	2.821 (13)
O_3	1	2.795 (13)
O_4	2	2.882 (14)
O_5	6	2.903 (12)
O_6	5	2.902 (14)

TABLE 3.9 CONTACTS LESS THAN 3.6 Å (in addition to those of Tables 3.7, 3.8).

A	*B*	*Transform for B*	*A...B* (Å)	*A*	*B*	*Transform for B*	*A...B* (Å)
S_3	O_4	2	3.494 (10)	O_6	C_3	13	3.184 (17)
Ca	C_2	2	3.268 (13)	C_2	O_5	13	3.000 (15)
Ca	C_4	2	3.304 (14)	C_2	K	2	3.362 (14)
Ca	C_1	3	3.273 (14)	C_4	O_5	13	3.064 (16)
Ca	C_3	3	3.441 (15)	C_4	C_5	13	3.599 (18)
K	C_1	1	3.358 (15)	C_4	H_2O_1	13	3.594 (17)
O_2	O_5	13	2.846 (12)	C_5	O_3	13	3.394 (16)
O_3	O_4	2	3.538 (13)	C_5	H_2O_4	13	3.232 (15)
O_4	O_5	13	2.933 (13)	C_5	Ca	10	3.332 (14)
O_4	O_6	13	3.093 (14)	C_6	O_3	13	3.394 (15)
O_4	C_5	13	3.350 (15)	C_6	Ca	10	3.291 (14)
O_4	C_6	13	3.427 (16)	C_6	H_2O_1	1	3.505 (15)
O_5	O_3	13	2.973 (13)	H_2O_1	C_3	10	3.458 (17)
O_6	O_1	13	3.041 (13)	H_2O_2	O_4	2	3.587 (14)
O_6	O_3	13	2.962 (13)	H_2O_3	O_1	10	3.463 (14)
O_6	C_1	13	3.147 (16)				

TABLE 3.10 SYMMETRY TRANSFORMS REFERENCED IN TABLES 3.7, 3.8 AND 3.9.

1.	x,	y,	z
2.	$-x$,	$\frac{1}{2} + y$,	$\frac{1}{2} - z$
3.	$-x$,	$\frac{1}{2} + y$,	$-\frac{1}{2} - z$
4.	$\frac{1}{2} - x$,	$1 - y$,	$-\frac{1}{2} + z$
5.	$-\frac{1}{2} + x$,	$\frac{1}{2} - y$,	$-z$
6.	$\frac{1}{2} - x$,	$-y$,	$-\frac{1}{2} + z$
7.	$-x$,	$-\frac{1}{2} + y$,	$\frac{1}{2} - z$
8.	$-x$,	$-\frac{1}{2} + y$,	$-\frac{1}{2} - z$
9.	$-\frac{1}{2} + x$,	$-\frac{1}{2} - y$,	$-z$
10.	$\frac{1}{2} + x$,	$\frac{1}{2} - y$,	$-z$
11.	$\frac{1}{2} + x$,	$\frac{1}{2} - y$,	$1 - z$
12.	$\frac{1}{2} - x$,	$1 - y$,	$\frac{1}{2} + z$
13.	$\frac{1}{2} - x$,	$-y$,	$\frac{1}{2} + z$

TABLE 3.11 RELEVANT THERMAL DISPLACEMENT PARAMETERS.

a) RMS Component of thermal displacement along principal axes for the three metals, (Å).

Co: 0.106 (6), 0.167 (4), 0.181 (4)

Ca: 0.119 (7), 0.157 (5), 0.183 (5)

K: 0.197 (7), 0.213 (8), 0.570 (8)

b) RMS component of thermal displacement in the unit cell axial directions for K, (Å).

a: 0.564 (8)

b: 0.205 (7)

c: 0.223 (7)

c) Angle between principal axes and the unit cell axial directions for K, (degrees).

	Axis 1	*Axis 2*	*Axis 3*
a:	90.0 (36)	80.5 (11)	9.5 (11)
b:	29.1 (20)	118.7 (20)	85.4 (09)
c:	119.1 (20)	149.5 (20)	81.7 (11)

are represented as spheres of fixed radius; their final anisotropic temperature coefficients are, however, listed in Table 3.2.

3.5 DESCRIPTION OF STRUCTURE AND DISCUSSION

The $(+)_{589}[\text{Co thiox}_3]^{3-}$ ion has the Λ configuration predicted from solution CD correlations.[27,134] In space group $P2_12_12_1$ the complex ion possesses no crystallographic symmetry, showing small distortions from an idealized D_3 (32) geometry. The atom labelling is given in Figures 3.1 and 3.2 which show the oxygen and sulphur environments of the K^+ and Ca^{+2} cations; the pseudo-C_3 axis of the complex ion is approximately parallel to the *b* crystallographic axis and one of the pseudo-C_2 axes is approximately parallel to the *a* axis. The sub-cell pattern observed in the original Patterson synthesis is immediately understandable in terms of the similarity of the Co, Ca and K coordinates (Table 3.2) and the orientation of the complex ion relative to the unit cell axes (Figures 3.1 and 3.2).

Both cations make several close contacts with the more electronegative oxygen and sulphur atoms. The Ca^{+2} is surrounded by an almost spherical arrangement of nine oxygen atoms (Table 3.7): ionic radius Ca^{++}, 0.99 Å,[80] oxygen van der Waals radius, 1.40 Å.[80] The sulphur-oxygen environment of K^+ forms a cylinder of density approximately parallel to *a* suggesting an explanation for the large thermal anisotropy of the potassium ion in this direction (Table 3.11): ionic radius K^+, 1.33 Å,[80] van der Waals radius of sulphur, 1.85 Å.[80] From the earliest Fourier and difference maps the so-called K^+ ion had always occurred as a strong peak extended parallel to *a* and of integrated density equivalent to that of the more compact Ca^{++} site. Attempts to refine fractional atoms at sites slightly displaced in *x* only resulted in further splitting of the peak density in the difference maps and produced impossibly short close contacts with the sulphur-oxygen environment. Since both the Ca^{++} and K^{+} ions have an effective "atomic" number of 18 they occur with similar integrated peak densities in the Fourier maps; the above positional assignment was based on comparison of the observed close contacts with the van der Waals radii sums. Although some of the contact distances listed in Table 3.7 are too long to realistically suggest interactions of any strength it can be seen that most of the $Ca^{++}...O$ close contacts are incompatible with the placing of a larger radius K^{+} ion at this site.

The hydrogen atoms of the four water molecules were not located in the final difference synthesis which, however, showed numerous peaks at possible suitable positions. It is probable that further significant improvement of the refined model would be achieved if these atoms were located and the thermal anisotropy (and/or splitting) of the K^{+} ion more correctly represented, even without modification of the data weighting.[44a] Several of the contacts listed in Tables 3.8 and 3.9 can not be regarded as significant in terms of the van der Waals radii sums and are included only for completeness since the large vdW radius of sulphur (1.85 Å) necessitates the specification of a larger than usual contact distance. Also, it should be remembered (section 1.5) that limiting contacts 0.3 Å less than the vdW radius sum are not uncommon.[82,84]

No structures having coordinated thio-oxalate ligands have hitherto been reported. The mean Co^{III}-S bond length found here (2.244 (5) Å) is shorter than that reported for most tris (four-membered ring) complexes, e.g. Co(dtc)$_3$, 2.258 (3) Å,[135] 2.260 (3) Å;[136] Co(exan)$_3$, 2.276 (4) Å;[137] Co(mtp)$_3$, 2.322 (3) Å;[138] Co(xan)$_3$, 2.398 (4).[139] Details of the complex ion geometry are given in Tables 3.3-3.6. The unsatisfactory thermal refinement of atoms C$_5$ and C$_6$ (represented as isotropic circles in Figures 3.1 and 3.2) results in S-C and C-C bond lengths for ligand 3 which deviate significantly from the respective means obtained for ligands 1 and 2 only; the C=O bond lengths seem less affected. These mean bond lengths for ligands 1 and 2 are S-C 1.710 (8) Å, C-C 1.516 (23) Å, C=O 1.226 (8) Å; the respective means for ligand 3 are 1.665 (7) Å, 1.603 (16) Å and 1.226 (10) Å. The mean sulphur-carbon bond length is significantly shortened from a paraffinic single bond length (1.82 Å [74,116]); the sum of the Pauling covalent radii[140] for C-S is 1.812 Å and for C=S 1.607 Å. The carbonyl bond length is not significantly different from the average (1.245 (53) Å) found[87] for the poorly refined [Co ox$_3$]$^{3-}$ ion in KNIPHECOOX (Chapter 4); the increased ligand bite of thiox (3.16 Å) compared with ox (2.58 Å)[87] reflects the increased C-S bond length (1.73 Å for a shortened partial double bond[74]) relative to a similarly shortened C-O bond (1.36 Å [74]).

The bond angle errors for [Co ox$_3$]$^{3-}$ are so large, except for angles at the metal, that comparison with CADCOTHIOX is not justified. The ligand angle, O-Co-O, in $Co(ox)_3^{3-}$ was found to be 84.3 (1.5)°; the mean intraligand S-Co-S angle for $Co(thiox)_3^{3-}$ is 89.68 (19)°. However, both complex ions are distorted toward a trigonal-prismatic (D_{3h}) geometry such that the interligand plane dihedral angles (γ) are more nearly *120°* than is the case in octahedral geometry (γ = *90°*). In $Co(thiox)_3^{3-}$ the six atom ligand planes are more closely parallel to the pseudo-C_3 axis (mean γ = 97.7°) than are the Co, S, S planes (mean γ = 93.0 (6)°); for $Co(ox)_3^{3-}$ the dihedral angles between the six atom ligand planes only were calculated but the Co and oxygen donor atoms are only slightly displaced from this mean plane (γ = 92.0°). Geometric distortion of tris-complex ions from an idealized geometry having an orthogonal arrangement of chelate rings is further discussed in sections 8.2 and 8.3.

Although the thio-oxalate ligands are essentially planar (Table 3.4) the displacement of the Co atom from the mean planes induces some torsion in the chelate rings, the magnitude of the torsion angles in general increasing with increasing displacement of the Co atom (Tables 3.5, 3.6). The direction of this torsion is such as to make the C-C bond of each ligand more nearly parallel to the pseudo-C_3 axis of the complex ion and a small relative twist of the two halves of each thiox ligand about its C-C bond is observed (insignificant for ligand 2).

The esd's in the bond lengths and angles for this structure are a significant improvement over those of NADCOMALEN and CRMALTCOPN; this is particularly true of the angles subtended by the ligands at the metal atoms — in NADCOMALEN, σ for these three angles averaged 0.90°, in CRMALTCOPN where the metal atoms occupy special positions the average σ was 0.75°, and here 0.15°. It is this angle (α) and its related angles which are important in the evaluation of the distortion model of optical activity as it applies to chiral trigonal-dihedral transition metal complexes. Although some of the improvement in the average σ can be attributed to the presence of heavier atoms, i.e. sulphur, in the first coordination sphere of $[\text{Co thiox}_3]^{3-}$ it is due largely to having an excess of accurate counter data. It is probable that a more correct representation of the random errors in the data set by the weighting scheme and a more rigorous application of absorption corrections (either through a more realistic description of the crystal morphology or empirically[44b] by making use of the observed differences in the intensities of zero-layer Friedel pairs) would further reduce the estimated standard deviations of the positional and thermal parameters, and hence of the derived bond lengths and angles. In view of this improvement in σ a more complete data set (especially for hkl, $l = 2n + 1$ should be obtained on a diffractometer for the CRMALTCOPN structure.

Some miscellaneous notes on refinement details and data presentation for the three structures NADCOMALEN, CRMALTCOPN and CADCOTHIOX are collected together as Appendix IV.

CHAPTER 4 THE ABSOLUTE CONFIGURATION OF POTASSIUM $(+)_{589}$-TRIS(1,10-PHENANTHROLINE)NICKEL(II)-$(-)_{589}$-TRIS(OXALATO)COBALTATE(III) DIHYDRATE.

$K(+)_{589}[Ni\ phen_3](-)_{589}[Co\ ox_3].2H_2O$, KNIPHECOOX.

4.1 INTRODUCTION

In 1968 the structure of the title salt was solved and refined by full-matrix least-squares using *MoKα/Zrf* integrated precession intensities; $R_1 = 0.126$, $R_2 = 0.108$. However, an attempt to determine the absolute configuration of the structure using *CuKα/Nif* integrated precession data was unsuccessful. The absolute configurations of the complex ions were successfully determined in mid 1969 using non-integrated *CuKα/Nif* Weissenberg data, visually estimated against the calibration strip used for the NADCOMALEN anomalous data. Although the full structure refinement is in print (ref. 87) the derivation of the complex ion configurations was presented as a summary without listing the Friedel pairs; these data are given in full here.

4.2 DETERMINATION OF THE CONFIGURATION

Several well formed crystals of $K(-)[Ni\ phen_3](+)[Co\ ox_3].2H_2O$ were grown by interfacial growth over periods of 24 hours from cooled aqueous acetone solutions of the two components: details concerning the ensuring of the optical purity of these crystals are given elsewhere.[87] One such crystal was used to generate the *hk1* and *hk3* reciprocal layers. The equi-inclination angle, μ, for each layer was offset by ca.

0.5° to minimize possible multiple reflection effects.[141-143] Because the *00l* reflection, where $l = 2n + 1$, is systematically absent the odd level data should be less susceptible to multiple reflection disturbance than the even order layers. An automatic liquid nitrogen cold temperature attachment was developed for use in this work to increase the quality of the anomalous diffraction data consequent on the reduced thermal vibration, but the device has not been tested sufficiently to permit details to be given here.

The visually estimated data were scaled approximately against the *Mo* microdensitometer data before comparison with the calculated structure factors based on the K(+)[Ni phen_3](-)[Co ox_3].$2H_2O$ structure having both complex ions in a Λ absolute configuration. Absorption corrections were not applied. From an inspection of Table 4.1 it can be seen that most reflections designated "unobserved" have appreciable $|F_c|$ values while some having $|F_c| < 100$ occur with measurable intensity. Others, e.g. (2,11,3) and (4,3,3), exhibit insignificant differences between the calculated structure factors of the $\overset{+}{k}$ and $\bar{k}$ reflections.

Three structure factor calculations were made with

(i) Co^{+2} scattering anomalously, $\Delta f''_{Co} = 3.87$;

(ii) Co^{+2} and Ni^{0} scattering anomalously, $\Delta f''_{Ni} = 0.60$;

(iii) Co^{+2}, Ni^{+1}, K^{+1} scattering anomalously, $\Delta f''_{K} = 1.10$.

Details of the scattering factor curves are given in Appendix IV, note 1. All three calculations confirmed the Λ absolute configuration for both (+)[Ni $\text{phen}_3]^{2+}$ and (-)[Co $\text{ox}_3]^{3-}$. Of the 33 unique pairs the number

TABLE 4.1 FRIEDEL PAIRS: K(−)$_{589}$[Ni phen$_3$](+)$_{589}$[Co ox$_3$].2H$_2$O. CALCULATED FOR THE Λ MODEL.

			Calc. (i)		Calc. (ii)		Calc. (iii)	
l = 1	$F_o{}^b : \overset{+}{k}$	$F_o : \bar{k}$	$F_c : \overset{+}{k}$	$F_c : \bar{k}$	$F_c : \overset{+}{k}$	$F_c : \bar{k}$	$F_c : \overset{+}{k}$	$F_c : \bar{k}$
h = 1, k								
13	255	u	221	329	226	326	172	271
15	u	224	233	185	230	188	187	145
h = 2, 3	342	312	146	159	134	171	164	190
4	330	358	330	215	320	221	374	320
h = 3, 2	370	400	619	533	624	532	589	454
4	365	406	539	365	532	375	482	322
h = 4, 2	330	365	237	166	254	150	274	165
3	406	381	417	548	426	538	405	524
4	342	281	181	310	180	311	153	306
5	281	351	302	248	314	235	339	241
6	406	390	557	747	562	744	500	646
h = 5, 4	181	309	243	154	244	151	206	91
7	351	330	187	334	187	331	258	370
11	u	281	241	142	237	141	198	100
h = 6, 5	347	329	616	686	624	679	600	657
h = 7, 5	154	275	201	50	194	60	163	56
h = 8, 4	351	330	289	373	286	377	270	362
h = 10,5	301	281	288	326	290	323	236	279
h = 11,1	235	181	81	105	72	100	105	140
h = 12,3	301	248	333	359	329	366	291	333

(contd.)

TABLE 4.1 (contd.)

			Calc. (i)		Calc. (ii)		Calc. (iii)	
$l = 3$	$F_o{}^b : \overset{+}{k}$	$F_o : \bar{k}$	$F_c : \overset{+}{k}$	$F_c : \bar{k}$	$F_c : \overset{+}{k}$	$F_c : \bar{k}$	$F_c : \overset{+}{k}$	$F_c : \bar{k}$
h = 1, 2[a]	375	330	146	159	134	171	164	190
4[a]	363	347	417	548	426	538	405	524
h = 2, 1[a]	285	308	619	533	624	532	589	454
4[c]	253	u	317	233	306	248	227	224
5	367	336	290	453	285	461	265	440
7	235	330	300	253	295	251	255	170
11[d]	u	218	156	152	149	146	198	214
13	309	235	237	367	241	363	233	357
h = 3, 7	375	351	448	584	458	576	412	531
h = 4, 1[a]	359	381	539	365	532	375	482	322
2	u	260	157	87	169	90	143	40
3[c]	312	289	94	88	96	85	158	140
11	u	275	311	154	312	155	278	123
h = 5, 6	358	330	415	605	424	601	364	531
h = 6, 2	358	390	558	427	555	429	563	439
4	358	400	774	553	774	553	688	460
h = 7, 3	365	351	448	584	458	576	412	531

a. symmetry equivalent to an *hk1* reflection.

b. $|F_o|, |F_c| \times 10$.

c. (2,4,3) and (4,3,3) contradict the Λ assignment in all three calcs.

d. (2,11,3) inverted in relative $|F_c|$ values in calculation (iii).

favouring this assignment were (i) 31, (ii) 31 and (iii) 30. In calculations (i) and (ii) the *Mo* scattering curve was mistakenly used for Ni^{0} rather than the *Cu* curve (for *MoKα*, $\Delta f'_{\mathrm{Ni}} = 0.4$; for *CuKα*, $\Delta f'_{\mathrm{Ni}} = -3.1$) but this error will not affect the relative ordering of the $|F_c|$'s within a Friedel pair; it can affect the magnitude of the difference between the two $|F_c|$ values. Calculations (i) and (ii) were closely similar. Introduction of $\Delta f''_{\mathrm{K}}$ in calculation (iii) together with use of the correct scattering curve for Ni with *CuKα* radiation gave some appreciable changes in F_c (apart from the change in scale of some data), e.g. the pair (2,4,3) became identical in $|F_c|$ and (2,11,3) which had previously calculated the same became unequal for the $\overset{+}{k}$ and $\bar{k}$ reflections.

Thus, even for this inadequately refined structure[87] (no anisotropic refinement, water molecules not located) comparison of Friedel pair intensities gives a quite definite indication of the absolute configuration. It has been noted elsewhere[144] that this method of determining absolute configuration is not limited to accurately refined structures whereas comparison of R_1 values for the two enantiomers may not give a significant indication.

CHAPTER 5 ABSOLUTE CONFIGURATIONS BY CORRELATION

5.1 INTRODUCTION

The powder method of X-ray crystallography can be used to assign the absolute configuration of a molecule or ion of unknown chirality by correlation with a related molecule of known configuration. The success of the technique relies on a qualitative comparison of the spacing and relative intensities of the diffraction lines produced by a microcrystalline specimen having only one hand of the "unknown" molecule in the crystal lattice with the diffraction pattern obtained from the reference powder.

Two approaches have previously been used. In cases where racemization in solution is slow and completely resolved samples of the relevant ions (or molecules) can be readily prepared the method of active racemates[145,146] has been successfully applied, e.g. to the tris-(diamines) of trivalent transition metals.[147] The rationale is as follows: for a molecule with optical antipodes (+)α and (−)α the crystal structure of the racemate (+)α(−)α is necessarily different from that of the pure enantiomers. Similarly for (+)β and (−)β. In certain cases, however, where the heavy atoms dominate the scattering, the diffraction patterns of the enantiomers and the racemate may appear qualitatively similar.[147] If β is stereochemically similar to α (i.e. of the same size, shape and ionic charge, such as $Co(en)_3^{3+}$ and $Cr(en)_3^{3+}$) an active racemate can be formed. If, for example, (+)α and (+)β co-crystallize and the resulting crystals (+)α(+)β give a powder pattern identical with that of (+)α(−)α, then (−)α and (+)β have the same absolute configuration. The absolute configuration of (+)β is thus determined if that of (−)α is known. Co-crystallization of (+)α with (−)β would give crystals isostructural with the pure antipodes but correlation via these latter crystals is unacceptable since the (+)α/(−)β mixture could equally well consist of discrete (+)α and (−)β crystals.

A second approach, which is more generally applicable (i.e. can be used where racemization in solution is too rapid to permit complete resolution of the antipodes) but at the same time less rigorous, is to compare the powder pattern of the less-soluble diastereoisomer formed between the molecule of unknown chirality and its resolving agent with that of the reference molecule resolved in the same way; this method is an extension of Werner's least-soluble diastereoisomer approach.[148,149] It is necessary to have a resolving agent of high purity which precipitates one hand of the resolvable complex to the almost total exclusion of the other. Having established the isomorphism of the unknown and reference diastereoisomers it remains only to identify the precipitated chiral molecule.

There are two potential sources of error in this method. In many cases the less-soluble diastereoisomer is only sparingly soluble in neutral solution and any attempt at further purification of the resolved complex by fractional recrystallization normally results in appreciable racemization. It is therefore more convenient to determine the optical sign of the complex present in the diastereoisomer by measuring the optical rotation of the solution remaining after precipitation. Excess resolving agent must be removed from the filtrate to prevent a false indication of resolution and in the present work this was achieved by ion exchange. The success of this operation can be checked by recording the optical rotatory dispersion (ORD) curve for the filtrate throughout the accessible wavelength range, since for the ionic complexes considered here the ORD curve is a good "fingerprint" of the ML_6 chromophore.

The other source of error lies in the degree of specificity of the resolving agent for one hand of the chiral complex. Where discrimination between the two enantiomers is absolute, i.e. no precipitation of one hand even at very high concentration, there can be no doubt as to the assignment. In many systems, however, a change of conditions[150] (e.g. solvent, concentration, temperature) can induce precipitation of either hand of the chiral molecule, e.g. strychnine + $Cr(ox)_3^{3-}$ (ref. 27); $M(en)_3^{3+}$ with $M(ox)_3^{3-}$ where M = Co, Cr, and $Co(thiox)_3^{3-}$ (this work and refs. 129 and 150).

Consider the system $(\pm)\alpha$ with resolving agent R; if R precipitates both $(+)\alpha$ and $(-)\alpha$ as discrete crystals, i.e. $R(+)\alpha$ and $R(-)\alpha$, in approximately equal proportions then the resulting powder pattern will be a composite of the two diastereoisomer patterns. One set of experimental conditions may precipitate $R(+)\alpha$ in slight excess, say 10%,of $R(-)\alpha$; the filtrate would show a negative residual rotation but the powder pattern would be that of the $R(+)\alpha/R(-)\alpha$ mixture. A slightly different set of conditions could give R(−)α in 10% excess over R(+)α; this time the residual rotation of the filtrate would be positive but again the powder pattern would be that of the mixture. Although the relative line intensities would be slightly different for the two mixtures a qualitative examination of line positions would reveal them to be identical and the non-sensical conclusion could be drawn that (+)α and (−)α have the same absolute configuration. Here the fallacy in the argument is obvious because the resolving agent has been shown to precipitate appreciable proportions of both enantiomers, but where the comparison is being made between two related systems α and β, treated independently with resolving agent R, precautions must be taken to exclude the possibility of erroneous comparison of diastereoisomer mixtures, i.e. R(+)α/R(−)α with R(+)β/R(−)β. This difficulty can be averted if pure samples of the reference enantiomer, (+)β and (−)β, are available since powder patterns of the pure diastereoisomers R(+)β and R(−)β can then be generated for comparison.

This chapter summarizes the preparation and attempted resolution of several complexes related to the four structures reported in Chapters 1-4. In the discussion section the absolute configurations determined during the course of this work, i.e. Chapters 1-5, are compared with the configurations previously assigned on the basis of published CD and ORD curves.

5.2 EXPERIMENTAL

(1) MO_6 Chromophores.

i. oxalates:

$K_3[Co\ ox_3].3H_2O$ [151] and $K_3[Fe\ ox_3].xH_2O$ [152] were prepared by literature methods. Attempted resolution of the ferric complex ion and a student preparation of $K_3[Al\ ox_3].3H_2O$ [151] with $(+)[Ni\ phen_3]^{2+}$ and $(+)[Co\ en_3]^{3+}$ was unsuccessful. Resolution[153] of $K_3[Co\ ox_3].3H_2O$ and $K_3[Cr\ ox_3].3H_2O$ [151] (supplied by Dr. M.R. Snow) with $(+)[Ni\ phen_3]^{2+}$ gave (+)Ni(-)Co and (+)Ni(+)Cr as the less-soluble diastereoisomers; powder photographs showed these to be isomorphous.

Exclusive precipitation of the (+)Ni(-)Co isomer has been demonstrated elsewhere.[87] Thus $(+)[Cr\ ox_3]^{3-}$ has the Λ configuration previously determined for $(-)[Co\ ox_3]^{3-}$, (see Chapter 4). Precipitation of these two anions as salts of $(+)[Co\ en_3]^{3+}$ and $(-)[Co(-)pn_3]^{3+}$ resulted in the formation of both possible diastereoisomers (this work and ref. 150), the one forming to excess depending on the conditions of resolution.

ii. malonates:

a) $K_3[Co\ mal_3].4H_2O$ was prepared by the method of Kneten and Spees;[154] other reported methods[103] require more rigorous control of pH. The emerald green needles of the racemate (turquoise by transmitted light) were characterized by determination of the lattice constants from *MoKα/Zrf* (λ = 0.7107 Å) precession photographs -

$K_3[Co(C_3H_2O_4)_3].4H_2O$; $M = 547.5$; orthorhombic, P_{na2_1} (No. 33); $a = 21.32$, $b = 12.07$, $c = 14.05$ Å, $U = 3617$ Å^3, $D_m = 2.00_7$ gm. cm^{-3}

(by flotation in 1,2-dibromopropane and 1,2-dibromoethane at $23^{\circ}C$), $Z = 8$, $D_c = 2.01$.

The solution absorption spectrum was identical with that of Kneten and Spees.[154] Ion exchange chromatography indicated the presence of two components, a narrow faint green band moving even more slowly than the major emerald green $Co(mal)_3^{3-}$ species. Aqueous solutions become pale pink on standing, the rate of decolouration being accelerated by light; a similar but slower colour change occurs in the solid state and probably indicates decomposition to Co(II) malonate and bis(malonato) species analogous to the solid state deterioration[155] of $K_3[Co\ ox_3].3H_2O$ on prolonged exposure to sunlight.

Resolution as the least soluble $(-)[Co(-)pn_3]^{3+}$ diastereoisomer precipitated the $(-)_{600}$ $Co(mal)_3^{3-}$ enantiomer. The powder pattern was identical with that of $(-)[Co(-)pn_3](+)[Cr\ mal_3].3H_2O$. Extreme insolubility of the $Co(pn)_3.M(mal)_3$ salts and very high solubility of the tris(malonato) ions in water render further purification by fractional crystallization difficult. Optical purity of the precipitated diastereoisomers is suggested by the following points:

— using a slight excess, e.g. 1.1:2, of resolving agent to racemate for the initial precipitation resulted in a residual green filtrate from which no precipitation could be induced by the further addition of a large excess (5x) of $(-)[Co(-)pn_3].Br_3$:

— microscope examination of several batches of diastereoisomer crystals revealed only the trigonal-prismatic morphology and all single crystals of $(-)[Co(-)pn_3](+)[Cr\ mal_3]$ examined gave X-ray diffraction patterns consistent with the space group R_{32} (see Chapter 2). The purity of the less-soluble diastereoisomers could be tested by calculation of the powder pattern corresponding to the known $(-)[Co(-)pn_3](+)[Cr\ mal_3].3H_2O$ structure; a crystalline impurity present at levels exceeding 5% should be distinguishable.

The identical powder patterns suggest that $(-)_{600}[Co\ mal_3]^{3-}$ has a Λ configuration: this enantiomer has a weak negative rotation at 589 nm.

b) Ni(II) malonate[156] and $K[Cr\ mal_2(H_2O)_2]$ [102,157] were prepared by published methods with the intention of determining the conformations of the malonate ligands and the absolute configuration of the chiral forms of the latter complex ion. However, attempts to grow suitable crystals of the former complex were unsuccessful and this work was not pursued when it became apparent (Chapters 1 and 2) that the conformation of the chelated malonate ligand was determined as much by crystal packing and intermolecular hydrogen bonding as by intra-molecular steric interactions.

iii. carbonate and succinates:

The tris(carbonato)Co(III) ion was prepared in aqueous solution[158-160] and resolution of the emerald green complex ion attempted using $(+)Co(en)_3^{3+}$; a green-brown precipitate formed immediately but the residual filtrate was inactive. Attempted resolutions with $(+)Ni(phen)_3^{2+}$, $(-)Co(-)pn_3^{3+}$ and precipitation with $Co(tn)_3^{3+}$ were also unsuccessful.

Attempted preparation of $K_3[Cr\ succ_3]$ by Chang's method[102] for preparing the tris(malonato) complex was not successful; the failure of this method had been previously reported by Lapraik.[101] Attempts to prepare $K_3[Co\ succ_3]$ by oxidation of Co(II) or from the reaction of succinic acid with an aqueous suspension of $Na_3[Co(CO_3)_3]$, methods successfully employed in the synthesis of tris(malonato)- and tris(oxalato)Co(III) complexes, were not successful.

(2) MN_6 Chromophores.

i. 2,4-diaminopentane:[†1]

Dippel and Jaeger[161] successfully synthesized several bis- and tris-transition metal complexes of the *meso* and *racemic* forms of 2,4-diaminopentane: some resolutions were achieved and the conformational specificity of the chelated ligands resulting from the two exocyclic methyl groups indicated. More recent preparations[38,162] follow the original method[163] of reduction of acetylacetonedioxime with ethanolic sodium, but with some modification of the isomer purification and resolution procedures.

Failure of the *racemic* and *meso*-dihydrochlorides to give sharp melting points[38,162,163] necessitated characterization by NMR spectroscopy.[162] We were unable to readily monitor the successive stages of fractional crystallization by this method and it was decided to attempt separation of the isomers by fractional crystallization of the di-nitric acid salts which had reported[163,164] melting points of 165-169°C and 195-196°C for the α- and β- isomers respectively. Dippel[164] separated the *meso* and *racemic* isomers as the diacetyl derivatives claiming resolution of the β-form (therefore *racemic*) with (+)-tartaric acid; he was unable to resolve the α-isomer by any method. On repeating this method of separation it has been concluded[38,162] on the basis of the NMR spectra and resolution properties that the α-form of Dippel corresponds to the pure *racemic* isomer whereas the β-form was an ca. 30:70 mixture of *racemic* and *meso*.

[†1] Preparation of this ligand undertaken with R.J. Geue.

Fractional recrystallization of the dinitric acid salts (from aqueous ethanol) provided a further check of Dippel's assignment. The recrystallization cycle resulted in a low melting (m.pt. 165°C) and a high melting fraction (m.pt. 195-6°C) in good agreement with the literature values. The 60 MHz NMR spectrum of the high melting fraction in D_2O was qualitatively identical with that reported[162] for the *meso*-dihydrochloride; the β-form of Dippel is therefore the *meso*-isomer. The NMR spectrum of the low melting fraction was a composite of the published *meso*- and *racemic*-dihydrochloride spectra. The high melting β fraction was less soluble in aqueous ethanol than the 165°C α fraction: Appleton and Hall[162] found the converse for the *meso*- and *racemic*-dihydrochloride salts.

Inability to purify the racemic ligand[165] and the successively decreasing yields obtained throughout the preparative sequence discouraged further work on this system, especially when it was learnt[39,40] that the structures of the relevant tris-cobalt complexes were already being studied.

ii. 1,3-diaminopropane complexes:

[Co tn_3]Cl_3 was prepared by the method of Jonasson et al,[166] but using a 20% excess of ligand. [Cr tn_3]Cl_3 was synthesized by refluxing a dimethyl sulphoxide solution of anhydrous chromic chloride[67,167] with tn in the presence of a granule of zinc.[168] Both complexes were resolved using (-)K[As cat_3],[37] ($[\alpha]_D^{22} = -527^o$, prepared by M.R. Snow by the published method[169]), added in a molar ratio Co:As = 2:3. Diastereoisomer crystals were obtained from 50% aqueous-acetone solutions after standing for several days; too rapid precipitation gave no apparent resolution.

Solubility of the diastereoisomers in acidified aqueous-acetone with attendant destruction of the resolving agent permits determination of the ORD curve both for the cation present in the crystals and that remaining unprecipitated in the supernatant. For $Co(tn)_3{}^{3+}$ the (+) enantiomer always crystallized to excess; however, with $Cr(tn)_3{}^{3+}$ both possible diastereoisomers were obtained, the precise conditions determining the one forming to excess. Growing the crystals from aqueous-acetone in a desiccator containing anhydrous calcium chloride, conditions favouring more rapid loss of water than acetone, precipitated $(-)_{400}$ Cr(-)As to excess; growth from identical solutions in an open beaker at -5^oC, conditions favouring faster loss of acetone, precipitated $(+)_{400}$ Cr(-)As to excess. Attempted purification of the antipodes of $Cr(tn)_3{}^{3+}$ by fractional crystallization was unsuccessful.

The (+)Co(-)As powder specimen decomposed too rapidly in the X-ray beam to permit the recording of a sufficiently intense powder photograph.

Instead, low angle ($2\theta = 4-25^o$) powder diffractometer traces were run for the three diastereoisomers. The positions and relative intensities of the dominant peaks (set A) were identical in the (+)Co(-)As and $(+)_{400}$ Cr(-)As traces; the $(-)_{400}$ Cr(-)As trace also showed these peaks (A) but at reduced intensity relative to the most dominant peaks (set B). The strongest B peaks were discernible in the (+)Co(-)As and $(+)_{400}$ Cr(-)As traces but with intensities much reduced relative to the A peaks. Although none of the diastereoisomers is optically pure it seems probable that the A lines are characteristic of the (+)Co(-)As and $(+)_{400}$ Cr(-)As diastereoisomers; on this basis $(+)_{400}[\mathrm{Cr\ tn_3}]^{3+}$ is assigned the same absolute configuration as $(+)[\mathrm{Co\ tn_3}]^{3+}$, namely Δ.

A more thorough characterization of this system is desirable.

(3) Phenanthrolines, Dipyridyls.

The tris(phen) and tris(dipy) complexes of Ni(II),[170,171] Fe(II)[172] and Ru(II)[173-175] were prepared by published methods. $\mathrm{Ni(phen)_3}^{2+}$ was resolved as the (+) antimony-tartrate[170,176] and both antipodes purified by fractional recrystallization from aqueous-acetone as the perchlorates ($[\alpha]^{25}_{589} = -1448^o, +1387^o$); precipitation studies confirmed the exclusive precipitation of $(+)\mathrm{Ni(phen)_3}^{2+}$ as the less-soluble antimony(+)tartrate. The three diastereoisomers (+)Ni-, (+)Ru- and (-)Fe(+)antimonytartrate gave identical powder diffraction photographs; thus $(+)[\mathrm{Ru\ phen_3}]^{2+}$ and $(-)[\mathrm{Fe\ phen_3}]^{2+}$ have the Λ absolute configuration determined for $(+)[\mathrm{Ni\ phen_3}]^{2+}$, (Chapter 4).

Attempted resolution of the tris(dipy) complexes using potassium(+)-

antimony tartrate, potassium(+)tartrate, $(-)Co(ox)_3^{3-}$ and $(-)As(cat)_3^{-}$ was not successful.

(4) Technical Details.

Resins used in the ion exchange columns for removal of excess resolving agent were: anion, Bio-Rad AG1-X4; cation, Dowex 50W/X4.

Powder photographs of the diastereoisomers were recorded using $CuK\alpha/Nif$ radiation and a small radius (r = 28.65 mm.) Nonius general purpose camera; background fogging of the films due to fluorescent scatter from Co derivatives was reduced by placing a dummy film in front of the intensity recording film. Diffraction line positions and relative intensities were compared qualitatively without determination of d spacings. Powder diffractometer traces were recorded with monochromatic $CuK\alpha$ radiation in the range $4^{\circ} \leq 2\theta \leq 25^{\circ}$ on a Philips Geiger Counter X-ray Spectrometer at a scan speed of 0.5 deg. min^{-1} with a slit width of 0.5 degrees.

Qualitative solution absorption spectra were determined using a Perkin-Elmer 402 Ultraviolet-Visible Spectrophotometer. The solution ORD curves of Figures 5.1 and 5.2 were measured manually on a Perkin-Elmer Model 141MC Spectropolarimeter having a quartz-iodine cycle tungsten lamp as illuminating source. The detector was an RCA IP28A photomultiplier. The specified spectral range of this machine is 250-650 nm; the spectral range of the lamp is quoted as 350-650 nm (continuous) and the photomultiplier has a specified response range of ca. 300-700 nm. Most solutions, however, gave measurable optical activity at wavelengths greater than 700 nm and it has been suggested[177,178] that the apparent rotation in this region is the result of higher frequency radiation passing the grating monochromator. The glass sample cell is opaque at wavelengths less than ca. 330 nm. Attempts to measure the ORD curves of solids on this machine were unsuccessful.

ORD and CD curves of the microcrystalline solids and CD curves of the optical enantiomers were recorded by Dr. M.R. Snow at Northwestern University, Evanston, using a Cary Model 60 Circular Dichrograph. All chemical samples were forwarded from Adelaide and in the case of the more labile complexes, resolutions were repeated at Evanston to permit recording of the solution CD spectra. The microcrystalline samples were measured as KBr discs (ca. 5% of diastereoisomer); single crystal specimens could not be measured.

The CD and ORD curves which follow are qualitative representations only; the ordinate is arbitrary in all but Figures 5.1 and 5.2; all curves are plotted against wavelength in nanometres.

5.3 DISCUSSION

Some reference to Chapter 6 may be helpful in reading this discussion section.

5.3.1 ORD and CD Curves

Published solution CD curves, or summaries of their characteristic

FIGURE 5.1: AQUEOUS SOLUTION ORD CURVES OF Δ$[M\ ox_3]^{3-}$:

(+) Co(III), ———; (-)Cr(III), ------.

(1) measured to long wavelength, then

(2) to short wavelength, then finally at 589 nm (3).

FIGURE 5.2: AQUEOUS SOLUTION ORD CURVES OF Δ$[M\ mal_3]^{3-}$:

$(+)_{600}$ Co(III), ———; (-)Cr(III), ------.

$Cr(mal)_3^{3-}$ absorption at ca. 600 nm too intense to allow accurate determination.

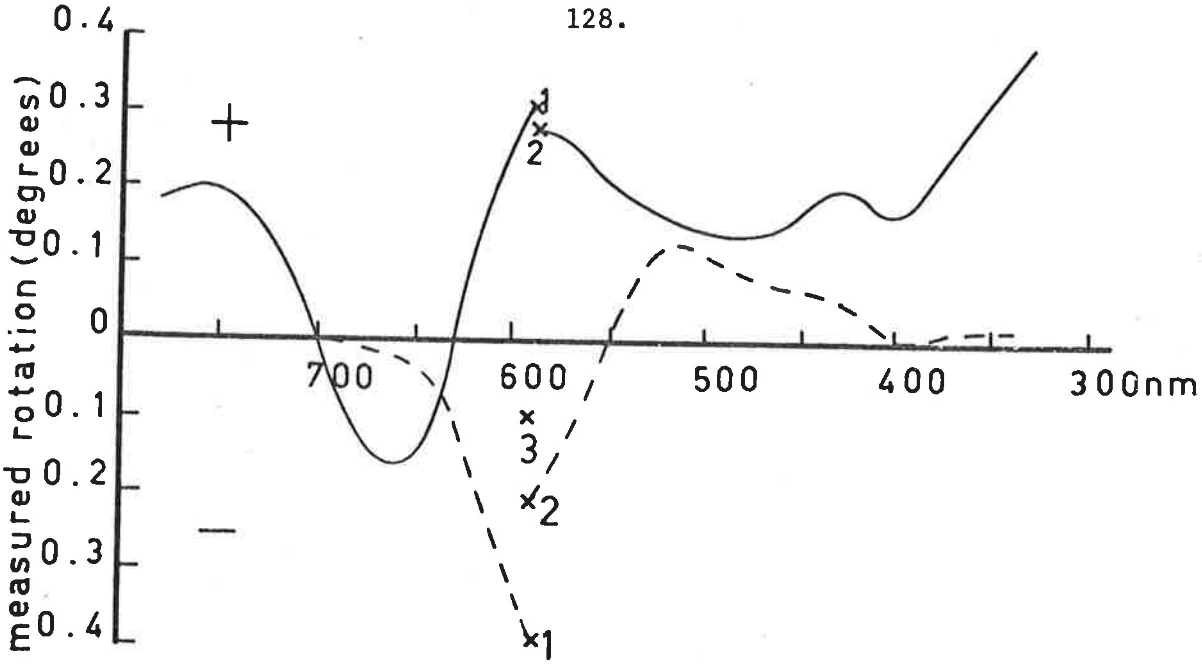

FIGURE 5.1

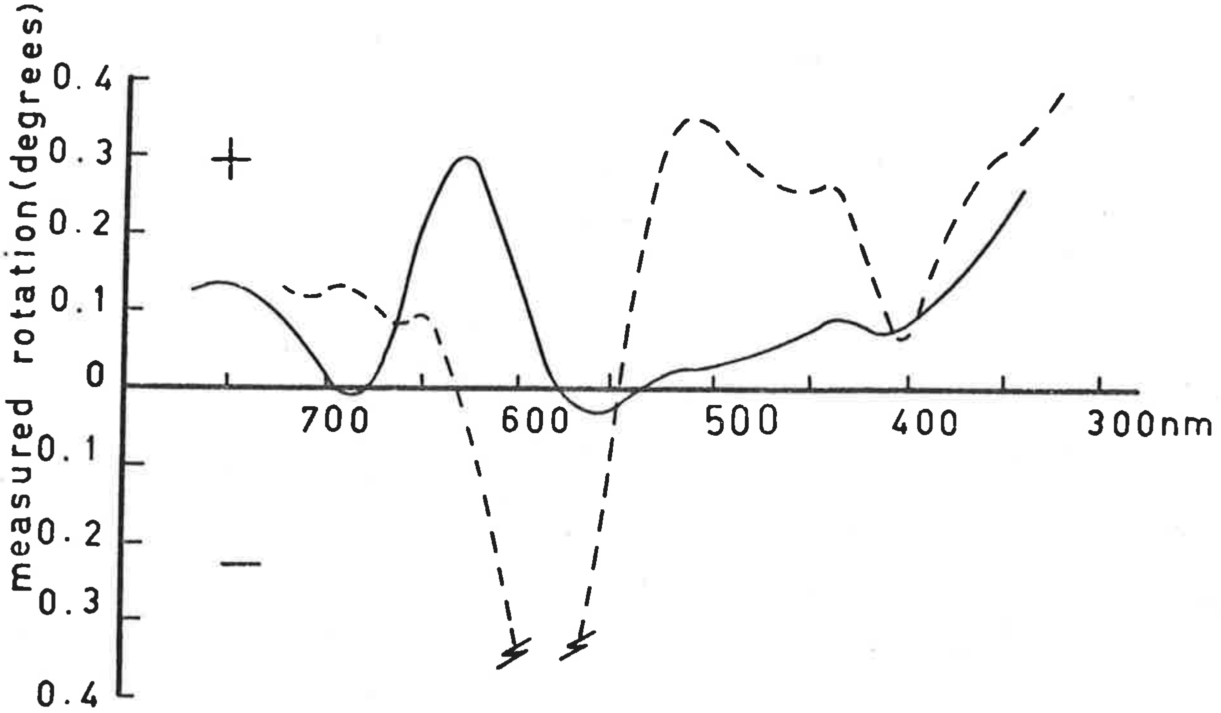

FIGURE 5.2

FIGURE 5.3(a): AQUEOUS SOLUTION VISIBLE ABSORPTION SPECTRUM OF $K_3[Co\ mal_3]$.

FIGURE 5.3(b): ORD CURVES FOR $[Co\ mal_3]^{3-}$.

——— Aqueous solution, $(+)_{600}[Co\ mal_3]^{3-}$

------ KBr disc, $(-)[Co(-)pn_3](-)_{600}[Co\ mal_3]^{3-}$.

FIGURE 5.3(c): CD CURVES FOR $[Co\ mal_3]^{3-}$.

——— Aqueous solution, $(+)_{600}[Co\ mal_3]^{3-}$

------ KBr disc, $(-)[Co(-)pn_3](-)_{600}[Co\ mal_3]^{3-}$.

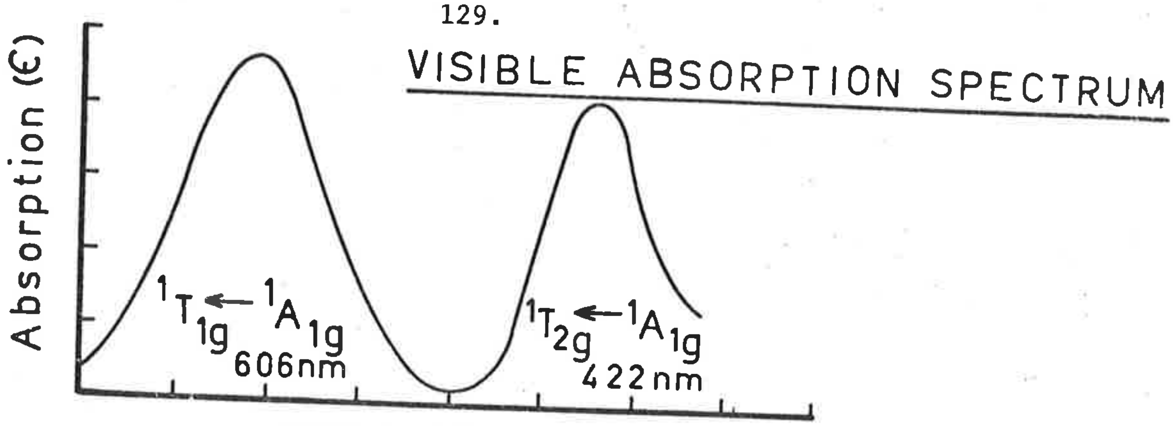

FIGURE 5.3(a)

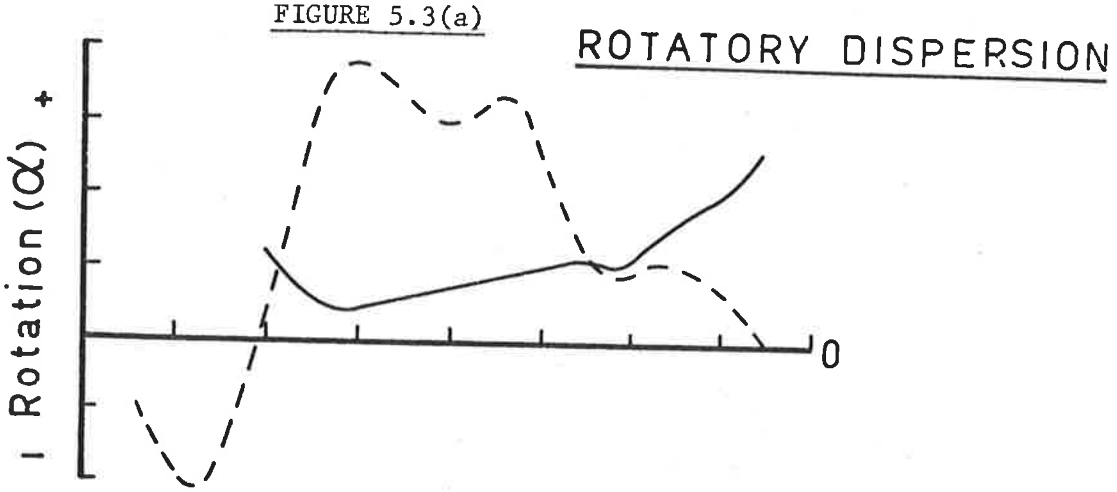

FIGURE 5.3(b)

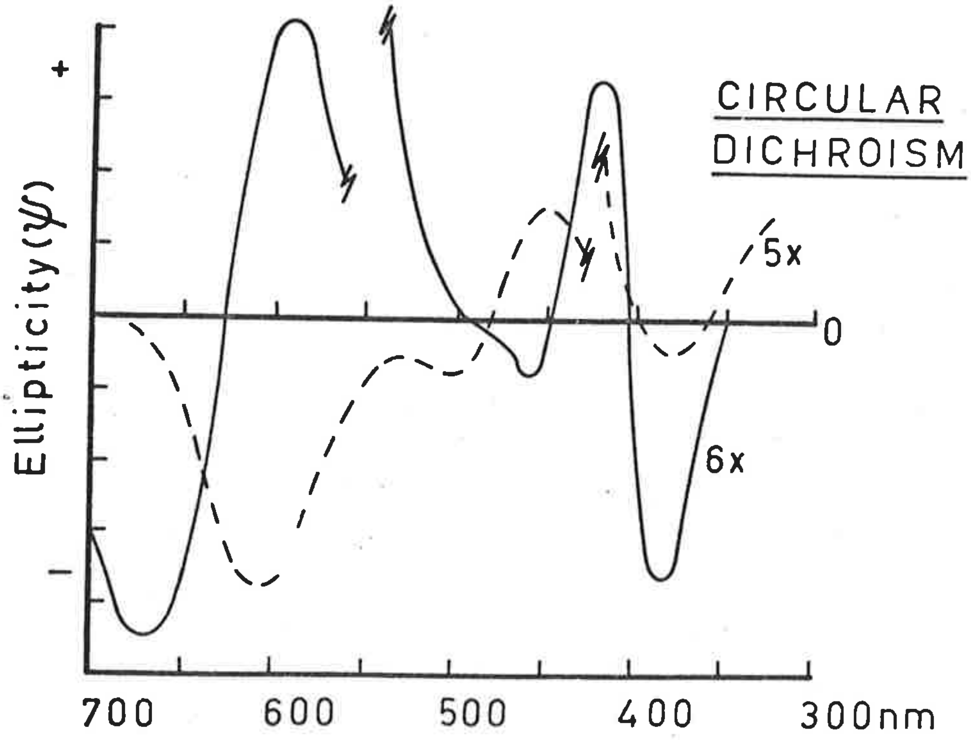

FIGURE 5.3(c)

FIGURE 5.4(a): AQUEOUS SOLUTION VISIBLE ABSORPTION SPECTRUM OF $Na_3[Cr\ mal_3]$.

FIGURE 5.4(b): AQUEOUS SOLUTION ORD CURVE OF $(-)[Cr\ mal_3]^{3-}$.

FIGURE 5.4(c): CD CURVES FOR $[Cr\ mal_3]^{3-}$.

——— Aqueous solution, $(-)[Cr\ mal_3]^{3-}$

------ KBr disc, $(-)[Co(-)pn_3](+)[Cr\ mal_3]^{3-}$.

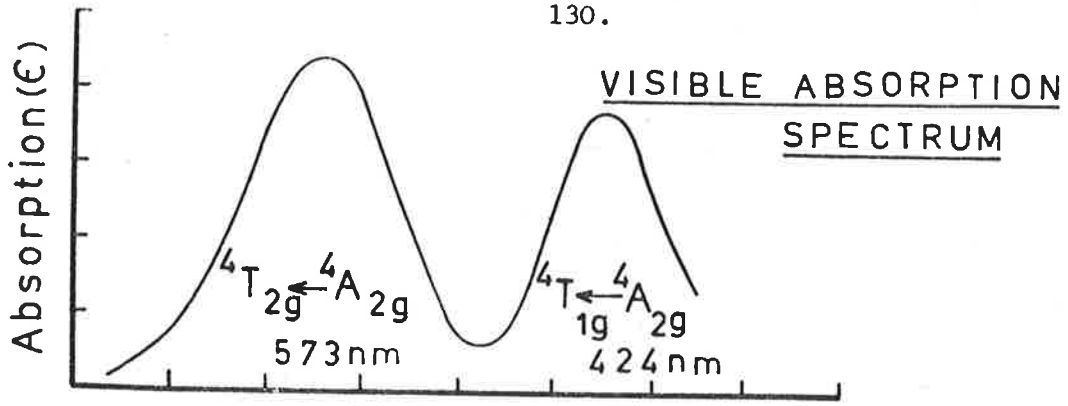
VISIBLE ABSORPTION SPECTRUM

FIGURE 5.4(a)

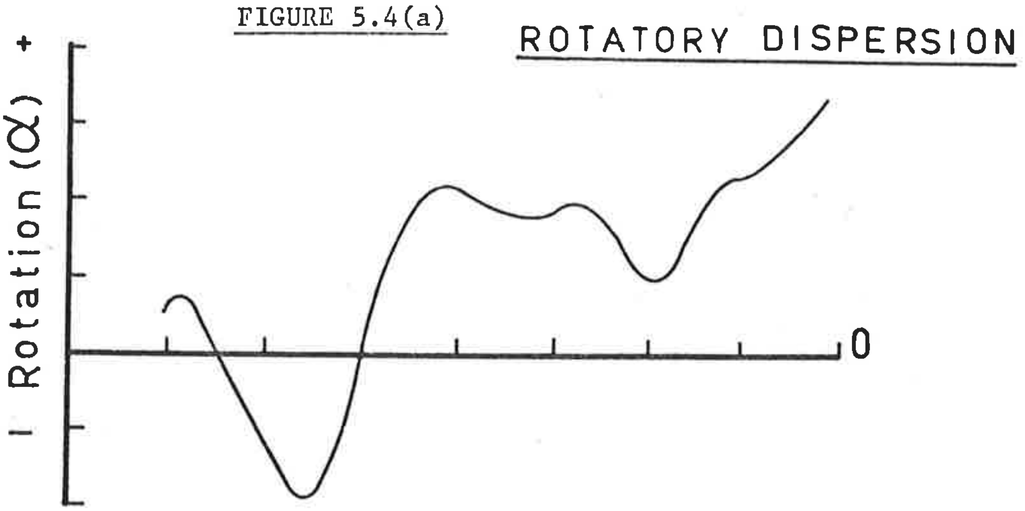
ROTATORY DISPERSION

FIGURE 5.4(b)

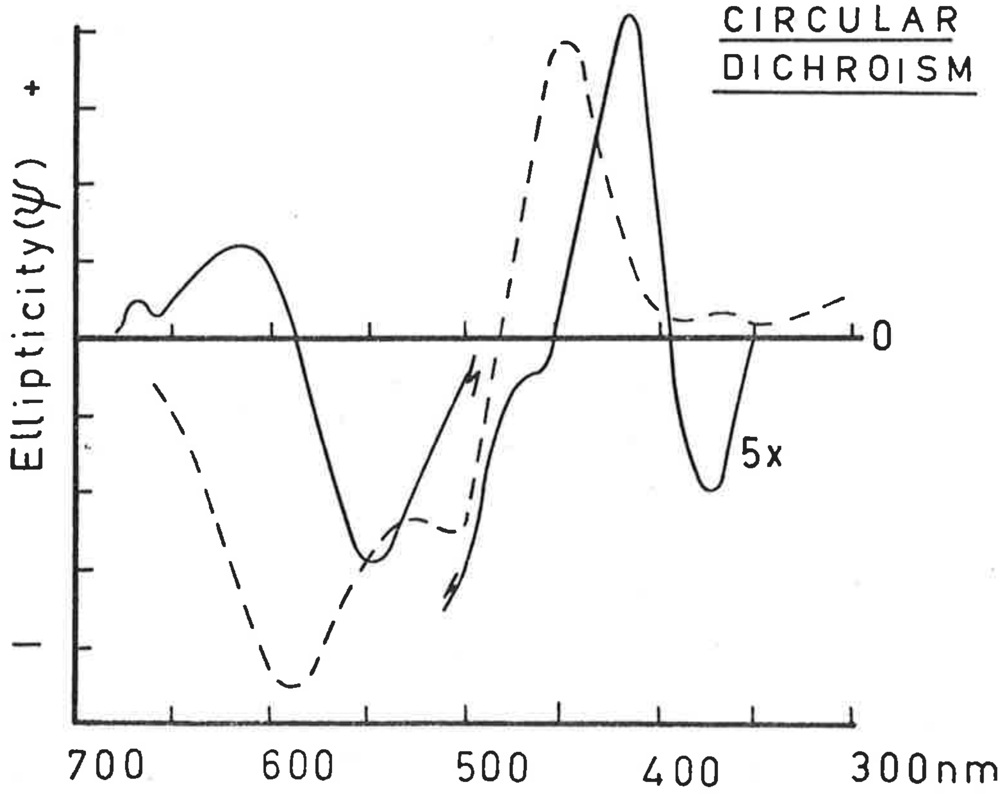
CIRCULAR DICHROISM

FIGURE 5.4(c)

FIGURE 5.5: AQUEOUS SOLUTION CD CURVES OF $(-)[\text{Co ox}_3]^{3-}$ AND $(+)[\text{Co en}_3]^{3+}$.

Separate equimolar solutions of $K_3[\text{Co ox}_3]$ and $[\text{Co en}_3]Cl_3$,

——— $(-)\ \text{Co(ox)}_3{}^{3-}$; ------ $(+)\ \text{Co(en)}_3{}^{3+}$.

FIGURE 5.6: KBr DISC CD CURVES OF $\Lambda(+)[\text{Co en}_3]\Lambda[\text{M ox}_3]$.

——— M = (-)Co; -.-.- M = (+)Cr

------ half the sum of the two curves of Figure 5.5.

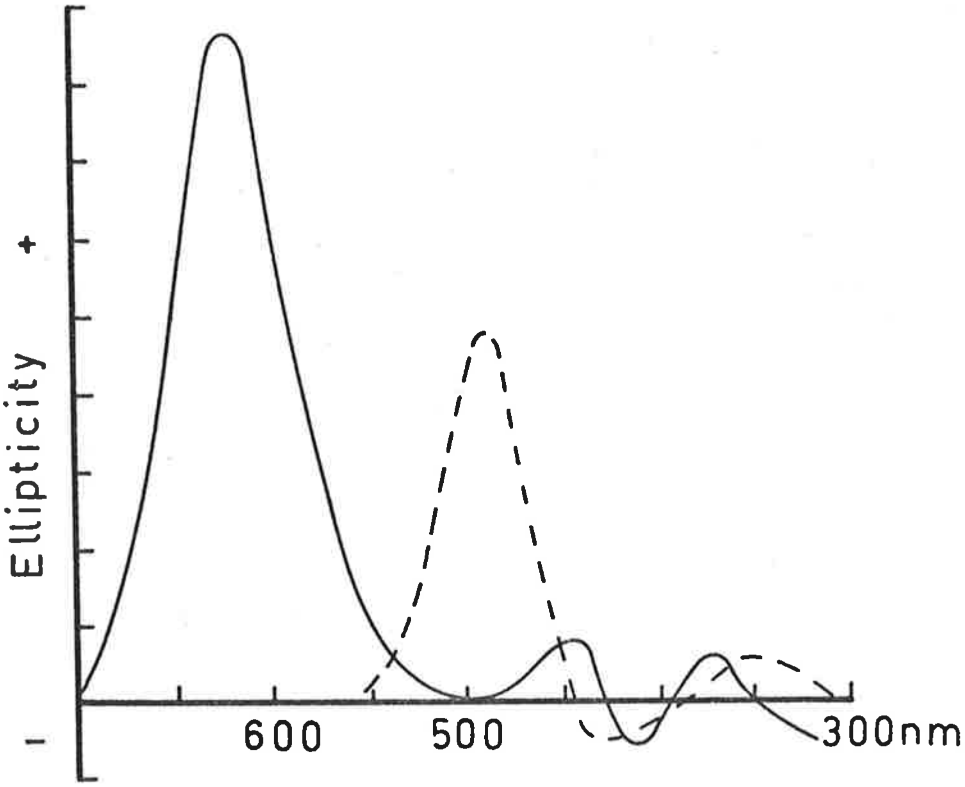

FIGURE 5.5

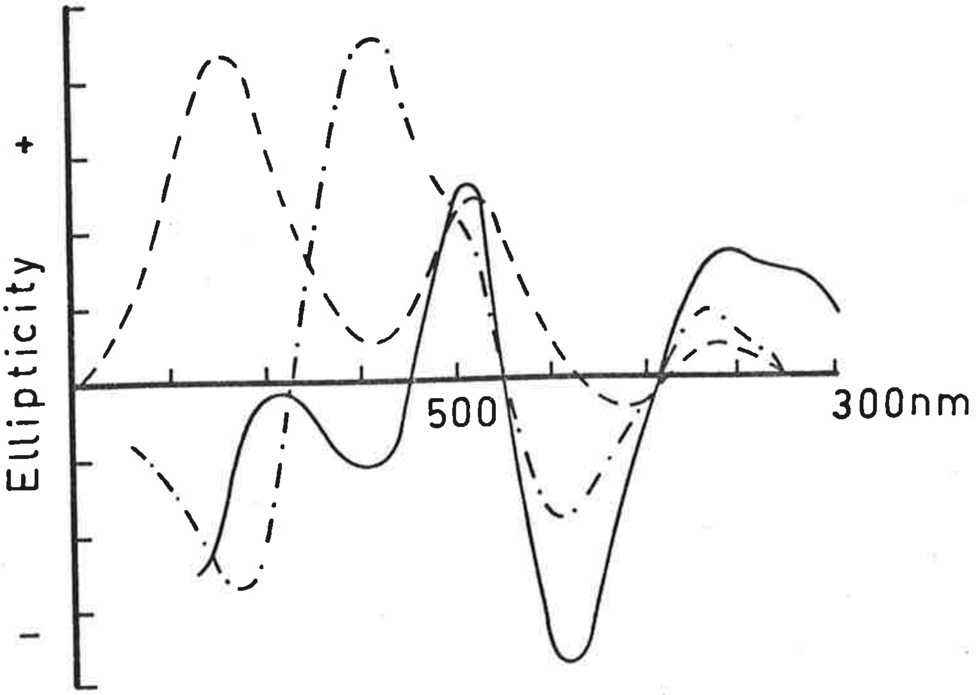

FIGURE 5.6

features, are available for the Co/Cr$(tn)_3^{3+}$, Ni/Ru/Fe$(phen)_3^{2+}$, Co/Cr$(ox)_3^{3-}$, Cr$(mal)_3^{3-}$, Co$(thiox)_3^{3-}$ and Co$(mal)_2(en)^-$ complex ions (see section 5.3.2); solution ORD curves are now rarely published and have been located only for the former five systems.[30,60,99,150,179] Previous attempts[154] to resolve $[Co\ mal_3]^{3-}$ have been unsuccessful and the features of its ORD and CD spectra are here compared with those of related CoO_6 and CrO_6 chromophores; the peak, trough and null positions of the CD spectra of the tris(oxalato)- and tris(malonato)-complexes of Co and Cr are summarised in Table 5.1. $[Co\ mal_3]^{3-}$ was recently resolved[180,181] as the (+) $Co(en)_3^{3+}$ diastereoisomer and the observed solution CD spectrum is in agreement with that of Figure 5.3(c); however, the CD components could not be assigned.

The broad qualitative similarity of the solution ORD curves of Δ-$Co(ox)_3/(mal)_3$ and Δ-$Cr(ox)_3/(mal)_3$ shown in Figures 5.1 and 5.2 suggests that the shape of the rotatory dispersion curve is characteristic of the ML_6-chromophore and the absolute configuration of the complex ion and largely independent of the chelate ring size and possible conformer lability. The published[60] ORD spectra of Λ(+) $Cr(en)_3^{3+}$ and Λ(−) $Cr(tn)_3^{3+}$ are also similar in shape; however, the ORD curve[60] of Λ(−) $Co(tn)_3^{3+}$ exhibits only the short wavelength features of the Λ(+) $Co(en)_3^{3+}$ spectrum. This correspondence between the ORD curves of the five- and six-membered ring complexes confirms the Λ absolute configuration assigned to (−) $Cr(tn)_3^{3+}$, (+) $Cr(mal)_3^{3-}$ and $(-)_{600}$ $Co(mal)_3^{3-}$. A ring size effect[25] [60,182] observed in the $Co(en)_3/(tn)_3$ system, i.e. reduced rotatory strength with increasing chelate ring size, is also found for the

TABLE 5.1 THE CD SPECTRA OF THE Δ tris(oxalato)[a] AND tris(malonato)[b] COMPLEXES OF Co(III) AND Cr(III) IN AQUEOUS SOLUTION.

	λ (nm)	$(\varepsilon_l - \varepsilon_r)$		λ (nm)	$(\varepsilon_l - \varepsilon_r)$
(+) $Co(mal)_3^{3-}$			(−) $Cr(mal)_3^{3-}$		
	385	−0.13		372	−0.04
	405	0		393	0
	423	+0.12		415	+0.09
	447	0		453	0
	460	−0.03		546	−0.29
	491	0		587	0
	593	+1.00		620	+0.12
	625	0			
	670	−1.06			
(+) $Co(ox)_3^{3-}$			(−) $Cr(ox)_3^{3-}$		
	377	−0.21		415	+0.56
	412	+0.26		552	−2.83
	446	−0.26		630	+0.58
	617	−3.30			

a. ref. 27.

b. this work.

$M(ox)_3/(mal)_3$ system. Only $Cr(ox)_3^{3-}$ racemized appreciably during the time taken to manually scan the spectra of Figures 5.1 and 5.2 (see the experimental points 1, 2, 3 on Figure 5.1).

The visible absorption maxima of the $Co(ox)_3/(mal)_3$ and $Cr(ox)_3/(mal)_3$ systems correspond almost exactly: peak positions, with ε_{max} in parentheses are $Co(ox)_3^{3-}$ 602 nm (153), 422 (204),[27] for $Co(mal)_3^{3-}$ 607.5 (148), 423.5 (127),[154] for $Cr(ox)_3^{3-}$ 571 (74), 422 (97)[27] and for $Cr(mal)_3^{3-}$ 575 (30), 428 (24).[27] For the tris(oxalato) complexes the high energy *d-d* transition has the greater electric-dipole strength but this situation is reversed in the tris(malonates). The absorption spectra of Figures 5.3(a) and 5.4(a) were determined qualitatively for the samples used in determining the ORD and CD spectra of those figures.

The ORD and CD spectra of Figures 5.3, 5.4, 5.5 and 5.6 were measured on the Cary Model 60 Circular Dichrograph. The (-) $Cr(mal)_3^{3-}$ solution ORD curve (5.4(b)) is identical with that of Figure 5.2; the (+) $Co(mal)_3^{3-}$ curve (5.3(b)), however, has not been recorded to sufficiently high wavelength since it is still increasing, in violation of the Drude equation.[8] A similar criticism can be made of the (-) $Cr(mal)_3^{3-}$ curve of Figure 5.2 although in that case the effect is most probably due to higher frequency "stray" light — it is not possible on the available evidence to decide the correct long wavelength termination of the manual ORD curves.

ORD spectra of the microcrystalline less-soluble diastereoisomers diluted in pressed KBr discs give no readily interpretable information. However, some features of the CD spectrum of such a matrix are of interest when compared with the CD spectra of the isolated optically active components of the diastereoisomer. Before discussing the curves of Figures 5.3(c) and 5.4(c) some observations on the (+) $Co(en)_3^{3+}$-$Co/Cr(ox)_3^{3-}$ CD spectra represented in Figures 5.5 and 5.6 are warranted.

a) The CD spectra of Λ(−) $Co(ox)_3^{3-}$ and Λ(+) $Co(en)_3^{3+}$ are unaltered by pressing in a potassium bromide disc.

b) The spectra (Figure 5.5) are qualitatively similar; the dominant CD peak is positive in both curves and occurs at 493 nm for (+) $Co(en)_3^{3+}$ and 617 nm for (−) $Co(ox)_3^{3-}$. This relative displacement of the major CD maxima corresponds with a shift of the $^1A_{1g} \rightarrow {}^1T_{1g}$ transition from 469 nm in $Co(en)_3^{3+}$ to 602 nm in $Co(ox)_3^{3-}$.

c) Comparison of the composite curve (Figure 5.6) with the KBr disc spectrum of (+)[Co en_3](−)[Co ox_3] (precipitated from a mixture of the pure optical enantiomers; $[\alpha]^{22}_D$ (+)[Co en_3]$Cl_3 \cdot 3H_2O$ = 148°, (−)K_3[Co ox_3]$\cdot 3H_2O$ = −2300°) indicates that the latter is not simply a 1:1 summation of the component spectra. There is, however, some correspondence of peak and trough positions although there is obviously an additional long wavelength trough (λ ca. 650 nm) in the diastereoisomer CD spectrum.

The crystal structure of Λ(+)[Co en_3]Λ(−)[Co ox_3] is not known (see subsequent comments on the Δ(−)[Co(−)pn_3]Λ[M mal_3] diastereoisomer CD spectrum). The (+)[Co en_3](+)[Cr ox_3] CD spectrum is included in Figure 5.6 for comparison.

The positions and relative magnitudes of the observed maxima and minima in the (-) $Cr(mal)_3^{3-}$ aqueous solution CD spectrum (Table 5.1) correspond closely with those published by McCaffery et al.[27] Further, these CD peaks and troughs occur at wavelengths similar to those of the observed inflexion points in the solution ORD curves. Despite the expected complication of overlapping dispersion curves arising from adjacent optically active transitions, similar close correspondence occurs between the CD and ORD curves of other chiral transition metal complexes, e.g. (+) $Cr(en)_3^{3+}$, (+) $Cr(tn)_3^{3+}$, (ref. 60), and more particularly here for (-) $Co(ox)_3^{3-}$ and $(+)_{600}$ $Co(mal)_3^{3-}$. Mathematical deconvolution of a complex ORD curve into the contributions from the individual transitions is a distinct possibility[71,183] if the frequency interval of the optically active transitions is known.

(-) $Co(-)pn_3^{3+}$ gives absorption peaks at 468 nm (ε_{max} = 96) and 340 nm (90).[27] Its CD curve is similar to the inverse of that shown (Figure 5.5) for (+) $Co(en)_3^{3+}$ with some change in relative peak heights; published[27] $(\varepsilon_l - \varepsilon_r)_{max}$ values for the two complex ions are—

(-) $Co(-)pn_3^{3+}$	493 nm (-1.95),	439 (+0.58),	348 (-0.20)
(+) $Co(en)_3^{3+}$	493 nm (+1.89),	428 (-0.17),	351 (+0.25).

The rotatory strengths of the *d-d* transitions of $Cr(mal)_3^{3-}$ are an order of magnitude less than those of the five-membered ring tris(diamine) and tris(oxalato) complexes in line with the reduced electric-dipole strengths of the electronic transitions. The literature[27] values of $(\varepsilon_l - \varepsilon_r)_{max}$ for the (-) $Cr(mal)_3^{3-}$ ion in aqueous solution are—

620 nm (+0.07), 555 (-0.20), 420 (+0.04);

these values are $\frac{1}{2}$ to $\frac{2}{3}$ of the values given in Table 5.1 but this is of no significance to the following discussion. A further small negative peak, $(\varepsilon_l - \varepsilon_r)_{max}$ ca. −0.02 on the scale of the literature data, was found at 372 nm (Table 5.1).

The major interest lies in the (−)[Co(−)pn_3](+)[Cr mal_3] diastereoisomer curve (Figure 5.4(c)); if this curve were merely a 1:1 superposition of the CD spectra of the component enantiomers then, neglecting probable peak overlap, the succession of peaks (relative heights and assignments from literature) to decreasing wavelength should be

E_a *mal*	A_2 *mal*	E_a *pn*	A_2 *pn*
620 nm (−3.5),	555 (+10),	493 (−97.5),	439 (+29),

E_b *mal*	? *mal*	E_b *pn*
420 (−2),	372 (+1),	348 (−10).

The diastereoisomer KBr disc CD spectrum bears little resemblance to this composite pattern, providing further evidence that the optical activity profile of a solid diastereoisomer is not simply the superposition of its component spectra. Assignment of transitions to the peaks of the (−)[Co(−)pn_3](+)[Cr mal_3] CD spectrum is therefore somewhat tenuous. The structure is known (Chapter 2) and the trigonal R_{32} space group makes this an ideal case for the measurement of single-crystal solid state spectra provided large crystals can be grown.

Regrettably absorption spectra of the diastereoisomers pressed as KBr discs were not recorded; hence it is not known if the *d-d* transitions in the diastereoisomer are appreciably shifted from their positions in the component spectra. However, some comment is possible.

a) In the (-) $Cr(mal)_3^{3-}$ solution spectrum two CD peaks occur under the short wavelength absorption band and for $(+)_{600}$ $Co(mal)_3^{3-}$ there are three. Three weak CD peaks are also observed in this region in the solution CD spectrum of (-) $Co(ox)_3^{3-}$ (Figure 5.5) and have been quoted[27,184] as evidence of lower symmetry species, e.g. $[Co\ ox_2(H_2O)_2]^-$. This interpretation has been questioned[185,186] and in the present work ion exchange chromatography of a sample of $K_3[Co\ ox_3]$ showed only one slow moving band. A similar explanation is possible for the three high energy components in the (+) $Co(mal)_3^{3-}$ CD spectrum but ion exchange showed the concentration of species other than the triply negative tris-(malonato) ion to be negligible[187] — N.B. this does not exclude the possibility of a triply charged dimeric species.

Contributions from different conformers can also be postulated in the six-membered ring systems. Although the structure refinement (Chapter 2) indicates the presence of orientational disorder in the $\Delta(-)[Co(-)pn_3]\Lambda(+)[Cr\ mal_3].3H_2O$ lattice no evidence was found in the difference maps for malonate species other than the particular flattened conformer indicated in Figure 2.1. Even so, the complex ion need not be three-fold symmetric but simply three-fold disordered. The solid state conformation implies nothing about the conformational lability of $Cr(mal)_3^{3-}$ in solution.

b) The CRMALTCOPN structure showed the complex ions to be strongly hydrogen bonded parallel to their C_3 axes (Figure 2.3). This hydrogen bonding scheme seemingly induces appreciable distortion of both the cation and anion (see Tables 8.1, 8.6) in excess of that predicted on the basis of the electrostatic repulsion model outlined in section 8.2. The observed enhancement of the A_2 component rotatory strength relative to that of E_a in the aqueous solution CD spectrum of $Co(en)_3/(pn)_3^{3+}$ on the addition of tetrahedral oxyanions (e.g. phosphate, selenite — see section 8.3) has been rationalized[67,188,189] in terms of hydrogen bonding of the anion to the trigonal nitrogen faces of the cation. On this basis the $(-)[Co(-)pn_3](+)[Cr\ mal_3]$ diastereoisomer peaks at 505 nm (-) and 450 nm (+) can be interpreted as deriving predominantly from the E_a *pn* and A_2 *pn* components.

A similar explanation could be proposed for the dominant negative peak at ca. 590 nm, namely as being due to enhancement of E_a *mal* at the expense of A_2 *mal*, analogous to the situation observed[60,67,189,190] for $Co(tn)_3^{3+}/PO_4^{3-}$ on the most recent assignment[36] of trigonal components. No change was observed in the aqueous solution spectra of (-) $Cr(mal)_3^{3-}$ or $(+)_{600}$ $Co(mal)_3^{3-}$ on the addition of ammonium ions (as NH_4Cl) which it might have been thought would hydrogen bond to the carboxyl-oxygen lone-pairs in an orientation similar to that proposed for the binding of PO_4^{3-} to the trigonal faces of the $Co(en)_3^{3+}$ ion. This experiment was not tried for the tris-oxalate ions.

The (+)$[Co\ en_3]$(−)$[Co\ ox_3]$ diastereoisomer is a $\Lambda\Lambda$ arrangement and the crystal structure will be different from that of CRMALTCOPN which is $\Delta\Lambda$. Even so the diastereoisomer CD spectrum shows increased rotatory strength in the region of the A_2 *en* component relative to that at the wavelength of the E_a *en* component (Figures 5.5 and 5.6). Accurate structure determinations of both this and the $\Delta[Co\ en_3]\Lambda[Co\ ox_3]$ diastereoisomer would be invaluable, as would the KBr disc spectrum of the $\Delta\Lambda$ structure.

c) (+) $Cr(mal)_3^{3-}$ and $(-)_{600}$ $Co(mal)_3^{3-}$ have a Λ absolute configuration. The microcrystalline KBr disc spectra of their (−) $Co(-)pn_3^{3+}$ diastereoisomers are closely similar for $\lambda > 400$ nm (Figures 5.3(c) and 5.4(c)); both exhibit enhancement of the 450 nm (+) component relative to the 505 nm (−) peak of the cation. The diminished rotatory strength in the 540-400 nm region relative to the strong negative peak at ca. 600 nm is more pronounced for the $Co(mal)_3^{3-}$ diastereoisomer reflecting the greater dipole and rotatory strengths of the long wavelength transition of this anion compared with that of $Cr(mal)_3^{3-}$. It seems probable that this dominant negative component in the two diastereoisomer spectra has the same origin and can be assigned E_a *mal* by correlation with the polarized crystal assignment[29] for $Cr(mal)_3^{3-}$ in a $(NH_4)_3[Fe\ mal_3]$ host lattice.

The aqueous solution CD spectra of (−) $Cr(mal)_3^{3-}$ and

$(+)_{600}$ $Co(mal)_3^{3-}$ under the envelope of the short wavelength (ca. 420 nm) absorption band are similar with an additional minor trough in the (+) $Co(mal)_3$ spectrum at 460 nm appearing as a shoulder in the (−) $Cr(mal)_3$ curve. A major difference occurs under the low energy band envelope; apart from the presence of a small maximum at ca. 670 nm in the (−) Cr spectrum, the sign ordering of the two major components is reversed. The literature component assignment for (−) $Cr(mal)_3^{3-}$ gives 620 nm ^4E_a, 555 nm $^4A_1$; CD values have been given above.

Non-observance of the 670 nm $Co(mal)_3^{3-}$ solution peak in the KBr disc spectrum suggests that it is analogous to the ca. 550 peak of $Cr(mal)_3^{3-}$ and can hence be assigned $^1A_2$ symmetry. The observed shifts in wavelength of the E_a component peaks from solution to solid (620 → 590 nm for $Cr(mal)_3^{3-}$; 593 → 605 nm for $Co(mal)_3^{3-}$) are consistent with the postulated enhancement of the E_a component rotatory strength and a concomitant reduction of the A component. The greater shift in the $Cr(mal)_3$ case is understandable in terms of a larger relative contribution from the adjacent negative E_a *pn* component compared with the situation in the $Co(mal)_3$ diastereoisomer (see ref. 187 for an alternative discussion — the long wavelength CD components could equally be interpreted in terms of a conformer equilibrium).

This postulated energy ordering of ^1E_a and $^1A_2$ is identical with that found[36] for $\Delta(+)[\mathrm{Co\ tn_3}]\mathrm{Cl_3.4H_2O}$; the reversal of E_a and A component energies from Cr(III) to Co(III) is in agreement with Burer's correlations.[70,191]

Thus, to summarize, it seems that the broad shape of the ORD curve is characteristic of the ML_6-core and the complex ion absolute configuration and in favourable instances the inflexion points correlate well with the positions of the observed CD peaks. The ion exchange experiments indicate that the multiple CD components commonly observed under the short wavelength absorption band envelope of chiral Co(III)/Cr(III)O_6 species do not result from low symmetry mono- and bis-complexes although triply charged dimeric species and tris-species having one "dangling" bidentate ligand are not excluded; for the tris(malonato) complexes contributions from different conformers offer a possible explanation of the solution spectra. Solid state CD spectra of microcrystalline diastereoisomers can not be regarded simply as a superposition of the spectra of the individual enantiomers; in the present work a rationalization in terms of relative enhancement and diminution of spectral components seems plausible.

Finally, in retrospect, comparison of the recorded curves would have been facilitated by accurate quantitative determination of all spectra although this is difficult for the KBr disc measurements. Replotting the curves against frequency would have permitted identification of non-Gaussian peaks and possibly given some indication of minor spectral components (though there is some question as to whether CD peaks should be symmetrical with respect to frequency or wavelength[191]).

5.3.2 Absolute Configurations: Literature References

This section collates the absolute configuration determinations summarized in this and the preceding four chapters. Except for the tris(phen) and tris(dipy) complexes all literature predictions of absolute configuration referenced here are based on the empirical model[58,192,193] which assigns a Λ absolute configuration to complexes exhibiting a positive E_a CD component, or E_a derivative in cases having symmetry lower than C_3, under the envelope of the long wavelength T_1 symmetric octahedral transition. The varying predictions of other models as they apply to tris-bidentate Co(III) and Cr(III) complexes are summarized in Chapter 7 and the often conflicting predictions of the "E_a sign model" and "trigonal-twist distortion model" discussed more fully in section 8.3.

The Δ absolute configuration determined for $(+)_{546}[\text{Co mal}_2\text{ en}]^-$ has recently been confirmed by the independent[89,90] structure refinement of $\Delta(-)[\text{Co en}_2(\text{NO}_2)_2]\Delta(+)[\text{Co mal}_2\text{ en}]$; there is no sign change in the aqueous solution ORD curve of this complex anion between 546 nm and 589 nm. This assignment is in agreement with an earlier prediction[30] based on a comparison of the CD spectrum of $(-)[\text{Co mal}_2\text{ en}]^-$ with that of $(+)_{589} \equiv (-)_{546}[\text{Co ox}_2\text{en}]^-$; both spectra exhibit a positive low-frequency peak which was assigned A symmetry and considered to derive from the E_a component[3,58] of $(+)[\text{Co en}_3]^{3+}$.

Prolonged discussion of the CD spectra of the oxalate/en and malonate/-en complexes of Co(III) is not warranted but the following correlation of absolute configurations should be noted. (-)$[\mathrm{Co\ en_2(NO_2)_2}]^+$ precipitates[72] (+)$[\mathrm{Co\ mal_2\ en}]^-$ as the less-soluble diastereoisomer, both complex ions having the Δ absolute configuration.[89,93] (-)$[\mathrm{Co\ en_2(NO_2)_2}]^+$ also precipitates[150] (+)$[\mathrm{Co\ ox\ en_2}]^+$, $(+)_{546}[\mathrm{Co\ ox_2en}]^-$ and $(+)_{546}[\mathrm{Co\ EDTA}]^-$, (EDTA = ethylenediaminetetraacetate), although none of these four diastereoisomers can seriously be considered to be isostructural; indeed with a slight change of conditions $(-)_{546}[\mathrm{Co\ ox_2en}]^-$ precipitates to excess.[72,194] $(+)_{546}[\mathrm{Co\ ox_2en}]^-$ and $(+)_{546}[\mathrm{Co\ EDTA}]^-$ have been assigned[179] Δ configurations from the correspondence of their ORD curves with that of the related stereospecifically coordinated[195] $(+)_{546}[\mathrm{Co(-)PDTA}]^-$, (PDTA = propylenediaminetetraacetate). The similarity of the ORD curves[179] in the substitution sequence (+)$[\mathrm{Co\ en_3}]^{3+}$, (+)$[\mathrm{Co\ ox\ en_2}]^+$, $(-)_{546}[\mathrm{Co\ ox_2en}]^-$, (-)$[\mathrm{Co\ ox_3}]^{3-}$ also suggests a Λ configuration for these four ions; the Λ configuration for (+)$[\mathrm{Co\ ox\ en_2}]^+$ has been confirmed[196] by X-ray diffraction. The sequence of Λ absolute configurations is thus (-)$[\mathrm{Co\ ox_3}]^{3-}$, $(-)_{546}[\mathrm{Co\ ox_2en}]^-$, (+)$[\mathrm{Co\ ox\ en_2}]^+$, (+)$[\mathrm{Co\ en_3}]^{3+}$, (?)$[\mathrm{Co\ mal\ en_2}]^+$, (-)$[\mathrm{Co\ mal_2\ en}]^-$, $(-)_{600}[\mathrm{Co\ mal_3}]^{3-}$.

Conflicting assignments[28,197-199] of the absolute configurations of transition metal phenanthroline and dipyridyl complexes have been made, opposing predictions arising from the differences in the models used to explain the observed spectral phenomena (for a concise summary see ref. 3). The CD spectra of these complexes are now generally interpreted on the basis of exciton theory and the Λ configuration determined (Chapter 4) for (+) $\mathrm{Ni(phen)_3}^{2+}$ is in agreement with the more rigorous theoretical treatments (see section 7.1). A structure determination[26] of the less-soluble antimony (+) tartrate diastereoisomer of (−) $Fe(phen)_3^{2+}$ confirmed the Λ configuration for the cation; comparison of the powder photographs of the antimony (+) tartrate salts of (+) Ni(II), (−) Fe(II) and (+) $Ru(II)(phen)_3^{2+}$ confirms the Λ configuration suggested for all three from qualitative comparison of their ORD[150] and CD spectra.[21,24,199] Note that although these crystalline diastereoisomers have different numbers of waters of crystallization per formula unit[176,200] this does not imply a structural difference since the water molecules may be randomly disordered.

Oxidation of the divalent $M(II)(phen)_3/(dipy)_3$ complexes (M = Ru, Os) to the +3 state causes significant changes in the long wavelength region of the CD spectrum with only quite small changes in the ultraviolet region [21,199] and it is questionable whether oxidation to the trivalent state occurs with retention of configuration in the Ni(II), Fe(II), Ru(II) and Os(II) complexes; to date the absolute configuration of a trivalent complex has not been determined X-ray crystallographically. Further points of interest are the relationship of the absolute configurations of the divalent tris(phen) and tris(dipy) complexes and the elucidation of possible structural reasons for the more rapid racemization of the latter complexes relative to the $M(phen)_3^{2+}$ species.[23,171,201]

Use of the exciton theory is formally identical in both the $M(phen)_3^{2+}$ and $M(dipy)_3^{2+}$ complexes but early comparisons[28,202] were confounded by incorrect application of Werner's least-soluble diastereoisomer criterion;[148] the antimony (+) tartrate derivatives have been shown not to be isomorphous.[176,200,203] Although Gillard et al[204] have recently successfully correlated the absolute configurations of the M(II)$(phen)_3$/$(dipy)_3$ series by synthesis of (+) $Ru(dipy)_3^{2+}$ from (+) $Ru(phen)_3^{2+}$ with retention of configuration, the paucity of structural data for these systems is disturbing. An accurate structure determination of a resolved $M(dipy)_3^{2+}$ complex is required and in view of the conflicting theoretical treatments[22,24,205,206] of the spectra of mixed (phen)/(dipy) complexes accurate structure determinations of these resolved species would also be of value.

$[Co\ ox_3]^{3-}$ occupies a place in the CD theory of MO_6 chromophores as important as that of (+) $Co(en)_3^{3+}$ in relation to MN_6 chromophores. The E_a component was assigned from a single-crystal polarized absorption spectrum[207] of the $Co(ox)_3^{3-}$ ion diluted in the trigonal host lattice $Na.Mg[Al\ ox_3].9H_2O$; the oriented single-crystal CD spectrum[27,184] of (-) $Co(ox)_3^{3-}$ in the same lattice showed E_a to have a positive rotatory strength. Although the negative anion was assigned a Λ absolute configuration on this basis the interpretation remained somewhat questionable because of the appearance of three CD components under the envelope of the high energy *d-d* visible absorption band whereas only one component is predicted for D_3 symmetry. This assignment of a Λ configuration to the (-) $Co(ox)_3^{3-}$ ion was confirmed by the solution of the KNIPHECOOX structure (Chapter 4).[87]

(+) $Cr(ox)_3^{3-}$ and (-) $Cr(mal)_3^{3-}$ were likewise predicted[27,28] to have a Λ absolute configuration. The Λ configuration for the former complex ion is confirmed by the present correlation of powder diffraction patterns. However, the crystal structure determination of CRMALTCOPN (Chapter 2)[93] has established a Λ configuration for (+) $Cr(mal)_3^{3-}$; the assignment of the E_a component of this complex anion was based on a single-crystal polarized absorption spectrum[29] of $Cr(mal)_3^{3-}$ diluted in a $(NH_4)_3[Fe\ mal_3]$ lattice of unknown structure (see section 8.3).

$(+)_{546} \equiv (-)\ Co(thiox)_3^{3-}$ has previously been assigned[27,134] a Δ configuration on the basis of an observed high-energy negative E_a component in the aqueous solution CD spectrum. Two independent assignments have been made; in one case[134] the E_a component was fixed assuming enhancement[191] of this degenerate transition due to significant π back-bonding from the thiox ligand to the metal but in the other assignment[27] the basis for the energy ordering of the trigonal components was not indicated. These assignments of a Λ configuration to (+) $Co(thiox)_3^{3-}$ are confirmed by the CADCOTHIOX structure refinement (Chapter 3).

Failure to resolve the labile $Fe(ox)_3^{3-}$ and $Al(ox)_3^{3-}$ complex ions has been reported[208-210] previously although resolution of both has reputedly been achieved.[211-213] $Co(CO_3)_3^{3-}$ has recently[214] been resolved by precipitation as the less soluble (+) $Co(en)_3^{3+}$ diastereoisomer. The potassium bromide disc microcrystalline CD spectrum of the $\Lambda(+)[Co\ en_3](-)[Co(CO_3)_3]$ diastereoisomer exhibits a positive component at ca. 610 nm; two more peaks of similar magnitude are observed in the region of the low energy *d-d* transition of $Co(en)_3^{3+}$, namely at ca.

490 nm (+) and 430 nm (-). The similar peak height of the latter two components compared with the situation observed for (+) $Co(en)_3^{3+}$ in solution[27] (493 nm (+1.89), 428 nm (-0.17)) or pressed as a KBr disc[215] is analogous to the situation observed for both $\Delta(-)[Co(-)pn_3]\Lambda[M\ mal_3]$ diastereoisomers and the $\Delta(+)[Co\ en_3]\Lambda(-)[Co\ ox_3]$ diastereoisomer (section 5.3.1). Although the lone positive peak at 610 nm is more closely similar to the situation in the tris(malonate) diastereoisomer spectra (inverted throughout the wavelength region) suggesting a Δ configuration for the $(-)[Co(CO_3)_3]^{3-}$ ion, the $(+)[Co\ en_3](-)[Co(CO_3)_3]^{3-}$ spectrum is not very different from the superposition of the $\Lambda(+)\ Co(en)_3^{3+}/\Lambda(-)\ Co(ox)_3^{3-}$ solution spectra (Figure 5.6) and the literature assignment of a Λ configuration to (-) $Co(CO_3)_3^{3-}$ may yet prove correct. A structure determination is required.

The absolute configuration of the cation in the $(-)[Co\ tn_3]Br_3.H_2O$ crystal lattice was determined[120] as Λ. Earlier assignments[191,216] based on the sign of the prominent Cotton effect of the long wavelength transition predicted the enantiomeric configuration but more recent correlations[60,189,190] were verified, although it now seems[36,96] (see section 8.3) that these were founded on an erroneous interpretation of the solution CD spectrum. The solution ORD spectrum of (-) $Co(tn)_3^{3+}$ determined in the present work was identical with that of Woldbye;[60] the optical activity of several samples of resolved $Cr(tn)_3^{3+}$ was negligible at 589 nm but the ORD curve obtained for $(-)_{400}\ Cr(tn)_3^{3+}$ was qualitatively identical with that reported by Woldbye[60] for $(-)_{589}\ Cr(tn)_3^{3+}$. Solution CD spectra of the $M(tn)_3^{3+}$ species were not redetermined and rapid deterioration of the

$[\mathrm{M\ tn_3}](-)[\mathrm{As\ cat_3}]$ diastereoisomer crystals on isolation from the mother liquor prevented measurement of the spectra for the microcrystalline samples. Both Woldbye[60] and Beddoe[67,190] resolved the $\mathrm{M(tn)_3}^{3+}$ complex ions as the (+) nitro-camphorates (NCS); the less-soluble diastereoisomers were (−) Cr.NCS and (−) Co.NCS.

Diffraction patterns of the two salts were not compared but Beddoe[67] claimed that the similarity of the $(-)[\mathrm{Cr\ tn_3}](+)$NCS and $\Lambda(+)[\mathrm{Cr\ en_3}](+)$NCS powder patterns argued a Λ configuration for (−) $\mathrm{Cr(tn)_3}^{3+}$. Although this reasoning is extremely tenuous, the observation that both (−) $\mathrm{Co(tn)_3}^{3+}$ and (−) $\mathrm{Cr(tn)_3}^{3+}$ are precipitated as the less-soluble (+) nitro-camphorates offers further support to the tentative assignment based on comparison of the powder diffractometer traces of their (−) $\mathrm{As(cat)_3}^{-}$ derivatives and the qualitative similarity of the (−) $\mathrm{Cr(tn)_3}^{3+}$ and Λ(+) $\mathrm{Cr(en)_3}^{3+}$ aqueous solution ORD spectra.

Spectral implications of the geometric distortion of the $\mathrm{ML_6}$-cores of the tris(ox), tris(mal), tris(thiox) and tris(tn) complex ions, *inter alia*, are discussed in section 8.3.

Summary list of complex ions assigned a Λ absolute configuration on the basis of the crystal structure determinations and powder diffraction pattern correlations in the present work.

(+) $\mathrm{Cr(ox)_3}^{3-}$, (−) $\mathrm{Co(ox)_3}^{3-}$, $(-)_{546}$ $\mathrm{Co(thiox)_3}^{3-} \equiv (+)_{589}$
(+) $\mathrm{Cr(mal)_3}^{3-}$, $(-)_{600}$ $\mathrm{Co(mal)_3}^{3-} \equiv (-)_{589}$
$(-)_{546}$ $\mathrm{Co(mal)_2(en)}^{-} \equiv (-)_{589}$
$(-)_{400}$ $\mathrm{Cr(tn)_3}^{3+} \equiv (-)_{589} \equiv (+)_{546}$
(+) $\mathrm{Ni(phen)_3}^{2+}$, (+) $\mathrm{Ru(phen)_3}^{2+}$.